Bicyclic 6-6 Systems: Pteridines

Sharon Rossiter and Mehrnoosh Ostovar

University of Hertfordshire, College Lane, Hatfield AL10 9AB, United Kingdom

s.rossiter@herts.ac.uk

m.ostovar@herts.ac.uk

Keywords

Biosynthesis, Folic acid, Folate, Gabriel-Isay, Heterocycle, Lumazine, Molybdenum cofactor, Nucleophilic substitution, Photochemistry, Polonovsky-Boon, Pterin, Pyrazinopyrimidine, Synthesis, Tetrahydrobiopterin

Abstract

This chapter describes the literature on pteridines, covering the period from 2008 to 2020. The physical properties and reactions include photochemistry, substitution at ring nitrogens, nucleophilic substitution at ring carbons, organometallic couplings and methods for side chain elaboration and extension. Synthesis of pteridines is mainly from the pyrimidine, but there are examples from the pyrazine. Pteridine biological pigments and enzyme cofactors are widespread, and aspects of biosynthetic pathways are reviewed. Compounds of special interest and applications include metal complexes, nucleic acid analogues, natural products and increasingly the use of the pteridine scaffold in medicinal chemistry.

Glossary

ABC transporter, ATP-binding cassette transporter. Membrane-bound protein for import or export of substrates across a cell membrane.

AP (apurinic/apyrimidinic) / abasic site. Location in a DNA chain with a missing base, which can be detected by a probe that will bind with the corresponding unpaired base partner in a duplex chain.

BODIPY. Class of fluorescent dyes with high quantum yields, based upon the 4,4-difluoro-4-bora-3a,4a-diaza-s-indacene structure and used in biological probes.

Bredereck's reagent, *tert*-butoxy bis(dimethylamino)methane. A 1-carbon building block reagent used in enamination reactions under mild conditions.

BRET, bioluminescence resonance energy transfer. A form of measurement of the effieciency of Förster resonance energy transfer (FRET) between two chromophores, using a bioluminescent chromophore to generate the initial photon emission.

Bromodomain. A protein domain that recognizes acetylated lysine and plays a key role in regulating gene transcription.

Circular dichroism. Spectroscopic technique for measurement of differential absorption of circularly polarized light, which is often applied in structural studies of small molecules, proteins and DNA.

Density functional theory (DFT). Method for computational quantum mechanical modelling of electronic structures of molecules.

Dihydropteroate synthase, DHPS. Enzyme in the folate synthesis pathway of bacteria and some parasites that is a useful drug target as the enzyme is not expressed in humans.

Kinase. Protein that catalyzes phosphorylation of molecules by transfer of phosphate from ATP.

Interleukin 6. Member of a family of proteins produced by involved in inflammatory response.

Linear dichroism. Spectroscopic technique for measurement of differential absorption of plane polarized light by a material.

mTOR, mammalian target of rapamycin. Kinase involved in regulation of cellular processes.

Polo-like kinase. Member of a family of serine/threonine kinases involved in cell cycle regulation.

Single nucleotide polymorphism. Difference in a single nucleotide position in a genome that is found in a significant minority of a population.

Stark spectroscopy. A technique for measurement of emission/absorption in an electric field (electrocromism / Stark effect).

Surface enhanced Raman scattering (SERS). A spectroscopic technique to detect adsorption onto a metallic or nanoparticulate surface.

Theranostic. Combined diagnostic and therapeutic functions.

Toll-like receptor. Member of a family of receptors that recognize molecules specific to pathogens and play a key part in the immune reponse.

Xantphos - 4,5-bis(diphenylphosphino)-9,9-dimethylxanthene. A wide-angle bite bidentate bis-phosphine ligand used in Buchwald-Hartwig C-N cross-coupling reactions.

Xenograft. Transplantation of tissue from another species, for example, implantation of human cancer cells in an animal tumor model.

10.18.1 Introduction

10.18.1.1 Overview and history

The pteridine ring system is the fused pyrazino[2,3-*d*]pyrimidine **1** (Figure 1). The chemistry of pteridines has a long and rich history, summarized in the previous edition of this chapter.[1] Pteridines have continued to be of great interest, particularly due to their widespread occurrence in nature, as biological pigments as well as essential enzyme cofactors. There are longstanding applications of folate derivatives in medicine, and increasingly, use of pteridines as nucleic acid analogues in biological applications, as well as an accelerating interest in their photochemical properties and as a scaffold in medicinal chemistry. The recent literature is increasingly focused on these areas.

10.18.1.2 Nomenclature and Literature

The pteridine ring has the IUPAC numbering as in structure **1** (Figure 1). A number of naturally-occurring pteridine derivatives are known by common names, namely pterin **2** (2-amino-4(3*H*)-pteridinone), and lumazine **3**, (2,4(1*H*,3*H*)-pteridinedione). Other pterin derivatives include xanthopterin **4** and isoxanthopterin **5**, the latter coming to prominence as the core for fluorescent nucleic acid base analogue probes. The benzo-fused lumazine derivatives, alloxazine **6** and flavin **7**, are key compounds, as is the pterin analogue, folic acid **8**.

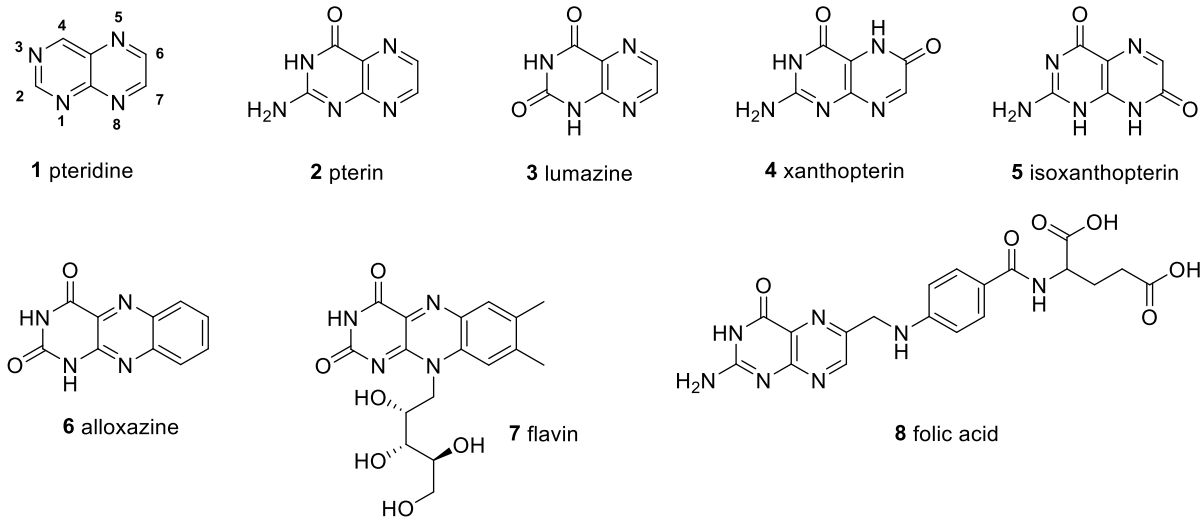

<Figure 1>

A number of reviews of pteridine synthesis and applications have been published in this period.[2-4] The International Society of Heterocyclic Chemistry (ISHC) publishes an annual review, wherein the chemistry of pteridines can be found in the chapter on pyrazines and their derivatives.[5-9]

Pteridines are involved in a wide range of biological and clinical functions. The dedicated journal of that name includes some reviews of compound classes of interest to the non-clinical reader, including pterin function in bacteria[10] and the applications of pterins in molecular sensors.[11] Biological roles of pteridines have been briefly reviewed.[12]

10.18.2 Theoretical methods

Theoretical methods have been widely employed for stability and redox determination of pteridines. Quantum theory of atoms in molecules (QT-AIM) studied neutral, cationic and anionic pterin.[13] Density functional theory (DFT) calculation is the most commonly used technique in recent studies. DFT calculations determined pterin radical stability[14] and the relative energies of neutral[15], anionic[16] and cationic[17] pterin tautomers. DFT calculations determined the possible peroxyl radical photogeneration pathways of acid and base pterin forms.[18] DFT of one electron reduction/oxidation of pterins and lumazines provide a rationale for the mechanistic pathways of the tetrahydrobiopterin cofactor.[19] DFT calculations determined optimized structures and hydrogen bond energies of pterin monomers, dimers and tetramers in the absence and presence of metal anions and metal clusters.[20] Simulations were compared to X-ray data in modelling the structure of a pteridine-2,4(1*H*,3*H*)-dithione – DMF cluster.[21] DFT elucidated the structure of the Mo(V) EPR-active species in the molybdenum cofactor of nitrate reductases.[22]

Time dependent density functional theory (TDDFT) studies are commonly used in combination with experimental spectroscopic techniques for elucidation of structural and energetic features of pteridines. Some combined studies are described in the following section.

10.18.3 Experimental Structural Methods

Spectroscopic and DFT methods were combined in an analysis of L-sodium folinate.[23] Results of FT-IR, FT-Raman and NMR spectroscopy of the folic acid analogue and antimetabolite drug methotrexate (MTX) were in good agreement with DFT molecular orbital calculations of the geometry, vibrational energies, HOMO and LUMO.[24] DFT and HOMO-LUMO analysis were used in conjunction with FT-IR, Raman, UV and NMR spectroscopy of lumazine to gain insight into structural, vibrational and electronic characteristics.[25]

X-Ray crystallography and absorption spectroscopy investigated 6,7-dicyanolumazine, which forms charge-transfer complexes with electron donors and readily loses a proton. The tetrabutylammonium salt was studied and absorption spectra indicated dimeric anions linked by H-bonding are responsible for the observed energy shift in fluorescence.[26] The X-ray structure of a zinc-phenanthroline-aqua complex of 2-amino-7-methyl-4-oxidopteridine-6-carboxylate, in which the pteridine is tridentate through O^-, O-4 and N-5, elucidated that the pteridine and phenanthroline are almost perpendicular.[27]

Surface enhanced Raman scattering (SERS) detected 5,6,7,8-tetrahydropterin and 6-acetyl-7,7-dimethyl-7,8-dihydropterin at sub-nanomolar concentrations. The latter was also detectable in the serum of treated rats.[28]

The excited state electronic structures of two tetrahydrofolate analogues, 5,10-methenyltetrahydrofolate and photodegradation product, 5,10-methylenetetrahydrofolate were determined by Stark spectroscopy.[29] The 6-methylisoxanthopterin excited state structure used Stark spectroscopy and TDDFT calculations.[30]

Inclusion complexes of folic acid with β-cyclodextrin are reported to increase folic acid thermal stability.[31] The structures of complexes of folic acid with α-, β-, and γ-cyclodextrins were

elucidated by ion mobility mass spectrometry, theoretical calculations and docking studies. The stability was in the order γ > β-> α. The proposed structures of the folic-acid complexes were an exclusion complex with α-cyclodextrin, a rotaxane-type complex with β-cyclodextrin and two possible complexes for the γ-cyclodextrin, a rotaxane structure and an additionally-stabilized structure with the pteridine ring within the cavity and additional interactions of the glutamate with the exterior of the cyclodextrin.[32]

10.18.4 Thermodynamic properties

Redox activity of pterins occurs through proton-coupled electron transfer (PCET) involving the pyrazine moiety. In order to understand this further, the ruthenium complex **10** from pterin **9** was studied. The one-electron reduction of the protonated ruthenium-pterin complex **11**/**12** was observed to involve a proton shift from position 1 to position 8, with formation of a pyrazine delocalized radical **13** (Scheme 1). DFT calculations of the energies of the atoms in the complex were used to confirm this mechanism and shed light on the redox mechanisms of pterins.[33]

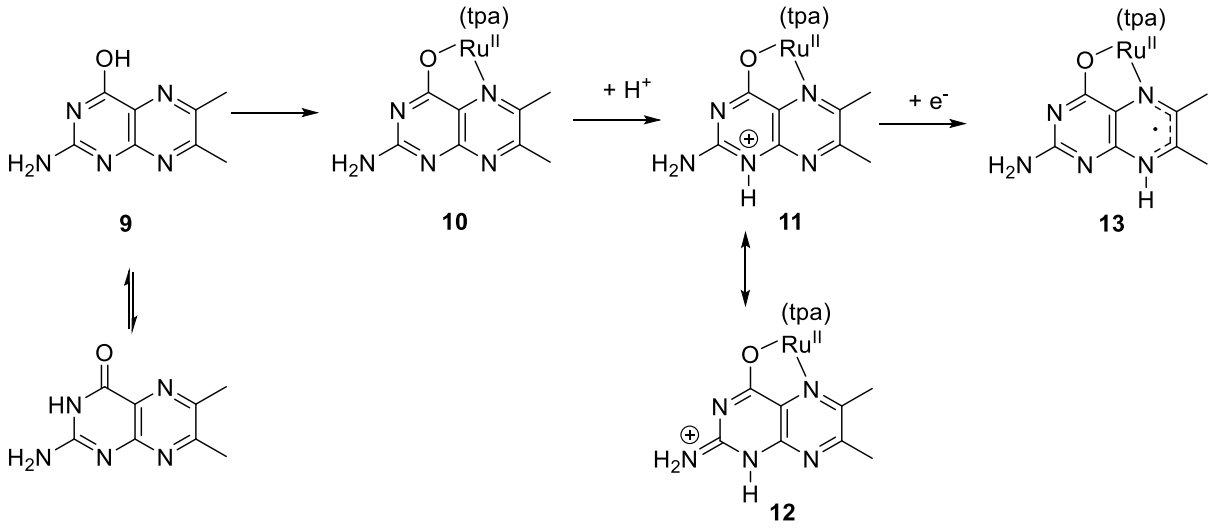

Scheme 1

Ultrafast excited-state dynamics of pterin have been determined using broadband transient absorption spectroscopy and TDDFT calculations.[34]

There was some controversy over the possibility of thiopteridine **14** acting as a catalytic redox mediator for the reduction of carbon dioxide to methanol (Figure 2). Since an initial 2014 report[35] and a 2016 rebuttal[36], theoretical studies have indicated that the activation energies for the reductive steps are 29.0 and 29.7 kcal mol^{-1} and that this is therefore unlikely to be a viable process.[37]

Cyclic voltammetry and voltabsorptometry of the redox mechanism of lumazine identified two reactive intermediates during a regenerative cycle.[38] A study of the electrochemistry of tetrahydrobiopterin in solution demonstrated that reversibility of electron transfer was dependent on the electrodes used and that it was difficult to replicate the one-electron transfer processes undergone in the nitric oxide synthase (NOS) enzyme in an electrochemical cell, due to the instability of the one-electron oxidation product.[39]

Pterin and a tetrahydro analogue, ADT **15** were used as complex ionization examples for a pK_a prediction test set. High-throughput automated spectral gradient analysis method measurement of pK_a employed the optimization of a predictive tool for analogue libraries in drug discovery. The predicted pK_a values for N1 and N3 of pterin and ADT were in good agreement with experimental values.[40]

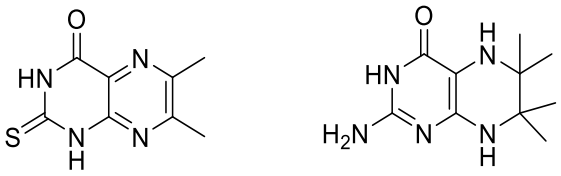

14 **15**

<Figure 2>

10.18.5 Reactivity of Fully Conjugated Rings

10.18.5.1 Introduction

The reactivity of the pteridine scaffold has continued to be of great interest, in order to develop novel compounds for a wide variety of applications. Reactivity varies with the substitution pattern. It is not always possible to find general methods that work for all pteridine derivatives and the chemistry of pteridines can be challenging. The photochemical reactivity of pteridines continues to be a focus for biological applications in particular.

The nitrogen atoms present in the pteridine structure considerably decrease the electron density of the conjugated rings in comparison with typical carbocyclic aromatic compounds. Therefore, pteridines are electron deficient heterocycles with the main mechanism of substitution on the ring, nucleophilic aromatic substitution (S_NAr).

Depending on the substrate, the carbons are all potential sites for nucleophilic attack. Replacement of substituents, such as oxo- or amino-, by a more reactive moiety (for example, a halogen or sulfur) activates for further substitution reactions. Introduction of a halogen or triflate opens up the scope for organometallic coupling reactions. The continued interest in analogues of natural pteridines such as folates, neopterin and biopterin, has led to a focus on methods for the introduction of side chains at C6.

Due to the electron deficiency of pteridines, electrophilic reactions at carbon are rare, but nitrogens can undergo electrophilic attack, for example, in *N*-alkylation. Radical substitution, especially at C6 and C7, is another feature of this ring system. An excellent review article has been published on the methods available for diversification of the pteridine scaffold.[41]

10.18.5.2 Photochemical Reactions

Latest findings were reviewed on the electron transfer-initiated reactions which are photoinduced by the triplet excited state of pterins. This review relates these reactions in the context of photosensitized biological procedures.[42] The excited-state proton transfer (ESPT) from pterin to acetate showed the acid form transfers its proton via a barrierless excited-state transfer. Experimental measurements of fluorescence quenching and theoretical methods determined that the transfer is from the external NH_2. In the base form (**9**), ESPT does not take place and the pterin fluorescence is more long-lived (Figure 3). The difference in fluorescence quenching is due to the changes in hydrogen bonding at different pH values.[43]

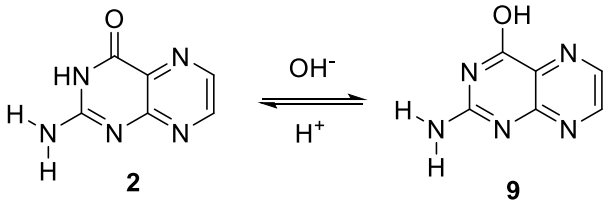

<Figure 3>

Photochemical and photophysical properties of lumazine in aqueous solution have been determined. Lumazine is reported to be an effective singlet oxygen ($^1O_2$) photosensitizer at different pH values under UV-A irradiation in aqueous solution. The dominant, neutral form of lumazine at physiological pH produces $^1O_2$ at high quantum yield (Φ_Δ, 0.44 at pH 5.5) while the monoanionic form is not as efficient (Φ_Δ, 0.080 at pH 10.5). Quenching rate constant experiments determined that lumazine is a poor $^1O_2$ quencher. Lumazine is photostable under UV-A irradiation at 350 nm both in air and in air-free conditions at pH 5.0-5.5. (neutral lumazine) and pH 10.2-10.7 (anionic lumazine).[44] The photooxidative sensitizing ability of lumazine was further assessed in the presence of 2'-deoxyguanosine 5'-monophosphate (dGMP) and HeLa cells as targets. dGMP can be oxidized by both electron transfer from excited state lumazine and by singlet oxygen.[45] The photoprotolytic processes of lumazine were investigated by steady-state and time-resolved UV spectroscopy. An excited-state proton transfer (EPTS) (70 ps) occurs in competition with a non-radiative process with a similarly fast rate. The neutral form of lumazine acts as an irreversible photoacid; that is, transforming from a weak acid ($pK_a \approx 8.0$) in the ground state to a strong acid in the excited state.[46]

UVA exposure of folic acid and photodegradation products, 6-formylpterin and pterin-6-carobxylic acid, leads to the production of reactive oxygen species in skin cells and a reduction of up to 50% of the UVA LD_{50} in the presence of 10 μM of pterin.[47] In the self-sensitized photodegradation of methotrexate, the rate is increased by the formation of photoexcited singlet oxygen, triplet methotrexate and a triplet excited state pteridine degradation product.[48]

10.18.5.3 Electrophilic Attack at Carbon

No notable new examples reported on electrophilic substitution reaction of pteridines during the period covered by this chapter.

10.18.5.4 Electrophilic Attack at Nitrogen

Pteridine nucleosides can be synthesized by various approaches. Structural analogues of adenosine and 2-deoxyadenosine were prepared following a previously reported N-8 glycosylation procedure. For the deoxyribonucleosides, a pteridine anion, formed by DBU (1,8-diazabicyclo[5.4.0]undec-7-ene) deprotonation of the corresponding 4-amino-7(8*H*)pteridinone **16** was reacted with an O-protected α-halodeoxyribofuranose in acetonitrile giving the desired β-anomer, **17,** and the α-anomer **18**, as a byproduct. (Scheme 2). For synthesis of ribosyl analogues, treatment with DBU and the benzoyl-protected α-bromo sugar led to the desired β-product in good yields, for both the 4N-unprotected amine and imido-analogues.[49]

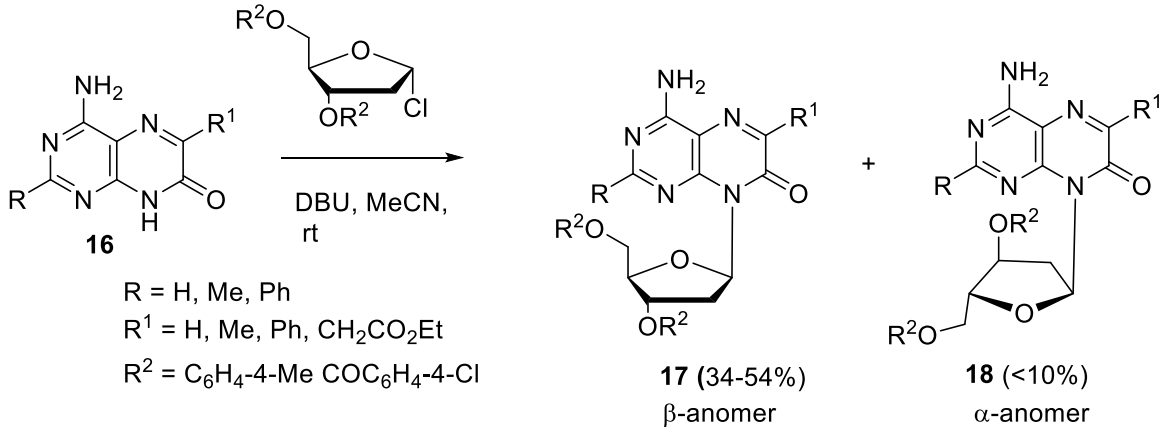

Scheme 2

N8 glycosylated products were similarly obtained when reacting the N4-silyl-protected pteridinones, using BF_3:OEt_2 as catalyst. However, for the 6-phenyl analogue **19**, an unexpected N-1 glycosylated product **20** was obtained (Scheme 3).[49]

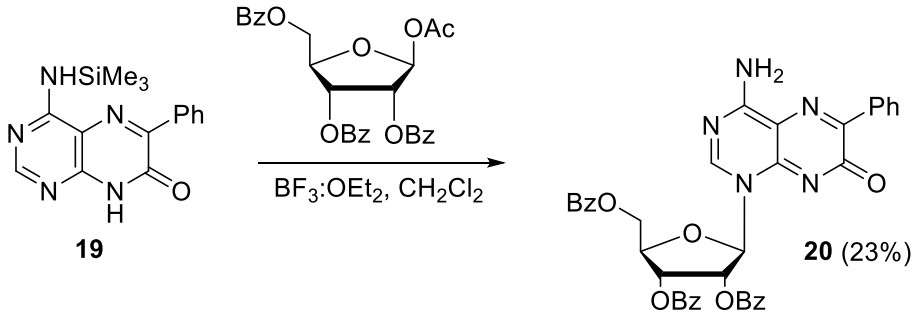

Scheme 3

Compounds **22** and **23,** produced by *S*-alkylation of pteridine **21,** cyclized to the thiazolo-pteridine derivatives in the presence of polyphosphoric acid (Scheme 4). The regioselectivity of this step could be due to the higher electron density at N3 compared to the N1 of 2-thiopteridine, which afforded the absolute cyclization at this nitrogen to give adducts **24** and **25**.[50]

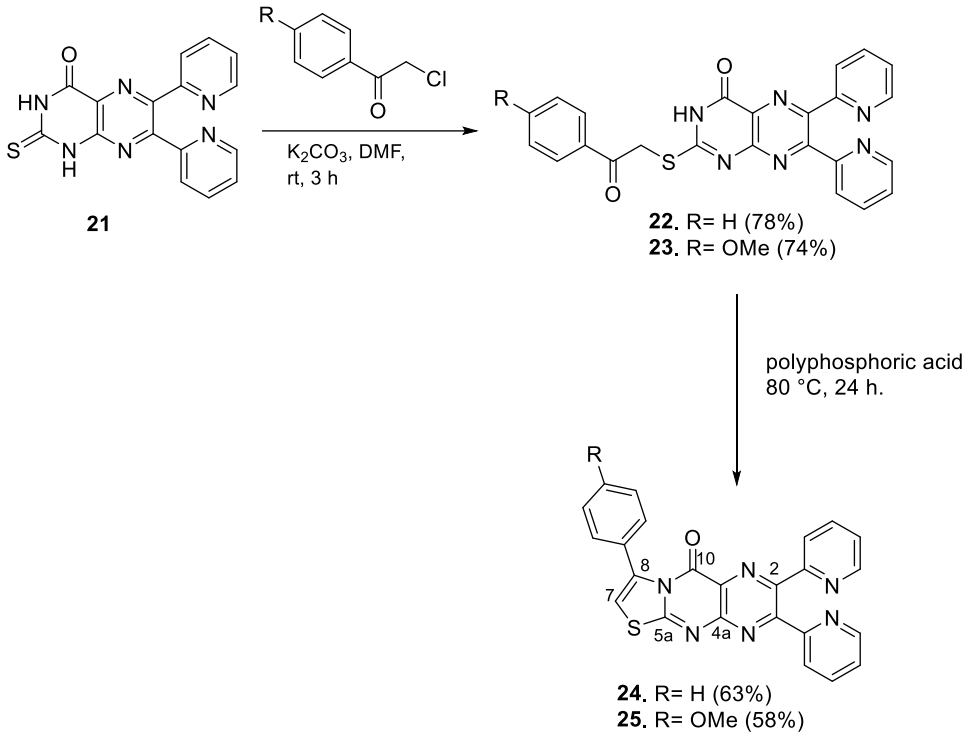

Scheme 4

10.18.5.5. Nucleophilic Attack at Carbon

All carbon atoms within the pteridine ring are activated for nucleophilic attack by the electron-deficiency of the multi-heteroatom structure. However, the majority of synthetic applications are for substituted pteridines with a good leaving group. These reactions, involving nucleophilic displacement of the C-substituent, as discussed in Section 10.18.7.2.

An effective, simple and direct method was developed for preparation of a series of methoxy or ethoxy pterins **27** and **28**, as well as 1,4-dioxanopterin **29,** in a single step from pterins and related alcohols or ethylene glycol, respectively, using Ceric(IV) ammonium nitrate (CAN), (Scheme 5).[51] It was found that this reaction is unique only with pterins or deazapterins and failed with quinoxaline. This could be because of the presence of the 4-oxopyrimidine, which aids the reaction. The proposed mechanism, for this reaction was that in presence of CAN, the pterin creates a cationic radical intermediate, which undergoes nucleophilic substitution by an alcohol to form the desired alkoxypterin. This reaction is only usable for a pterin scaffold with no substituent at either the 6 or 7 positions.

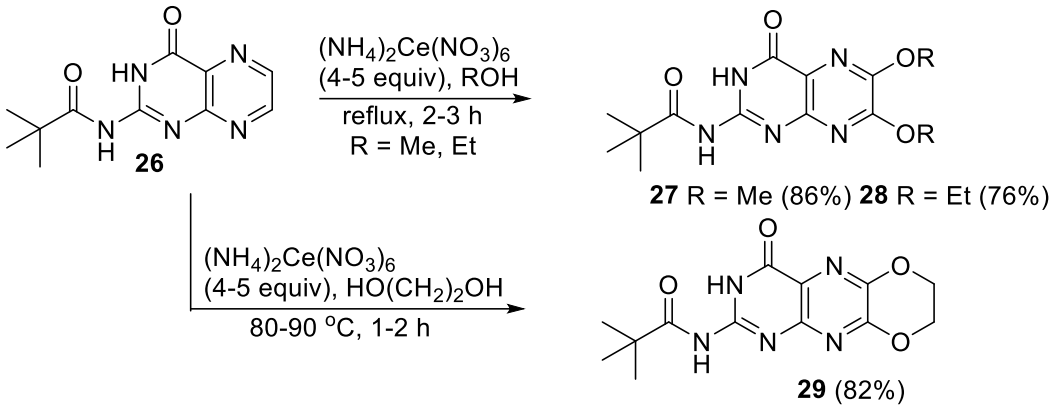

Scheme 5

A novel synthetic methodology was established for nucleophilic substitution of hydrogen in pteridinones by 5,7-dihydroxycoumarins.[52] This chemo- and regioselective C–C coupling reaction occurs smoothly under mild conditions. The key advantages of this metal free and environmentally friendly procedure are short reaction times, good yield and moderate temperatures. Compound **30** reacted smoothly with coumarins in trifluoroacetic acid (TFA) solution giving yield to the dihydro adducts **32** (Scheme 6). Pteridin-4-one **33** gave the rearomatized pteridine products directly.

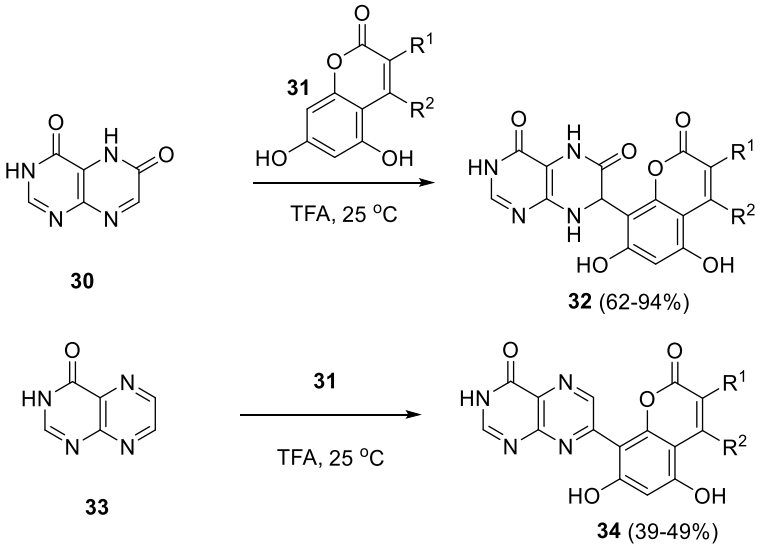

Scheme 6

Novel N^1,N^{10}-ethylene bridged flavinium salts **35**, which are chiral and non-racemic, were synthesized utilizing enantiomerically pure 2-substituted 2-aminoethanols obtained from chiral amino acids. The diastereoselectivity of nucleophilic addition to C10 depended on the type of substituent on the ethylene bridge of the flavinium salt. This addition was monitored by reaction with urea-hydrogen peroxide complex or deuterated methanol in an NMR tube,to give 10a-hydroperoxy- (Nu = OOH) and 10a-methoxy-adducts (Nu = OCD_3) as a mixture of diastereomers **36a** and **36b** in moderate to high diastereoselectivity (**36a** being the major diastereomer), as determined by NMR (Scheme 7). The flavinium salts with benzyl substituents on the ethylene bridge show high diastereoselectivities. Based on the NMR

studies, the benzyl group preferred the face-to-face (*syn*) position compared to the flavinium structure, which is blocking nucleophilic addition from one side. DFT calculations supported this conformation as the most stable one.[53]

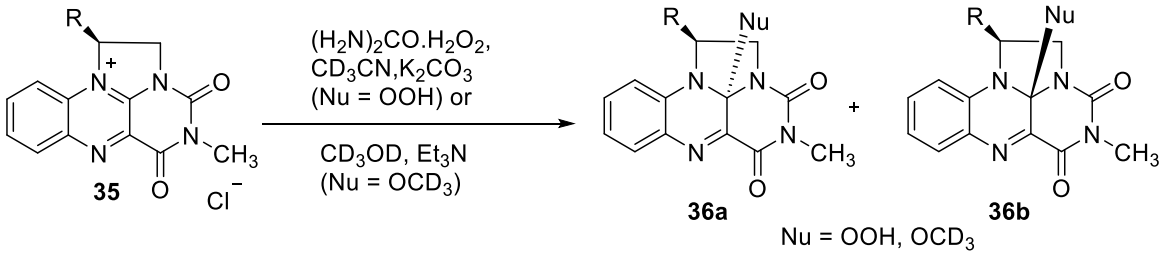

R	Ratio of diastereoisomers a:b	
	4-OOH	4-OCD_3
Pr^i	75:25	75:25
Ph	60:40	60:40
Bn	80:20	90:10
$CH_2C_6H_4$-4-OMe	90:10	95:5
$CH_2C_6H_4$-4-($OCH_2C_6H_4$)	>95:5	>95:5

reactions performed on 30-60 μmol scale in NMR tube

Scheme 7

10.18.5.6. Radical Attack on Carbon

An acyl radical reaction undergoes fast, direct and C-7 regiospecific acylation of pterin. This reaction previously applied on molecules containing the general pteridine substructure, which often required post-reaction substituent conversions to reach the pterin. In this method, *tert*-butylhydroperoxide and iron sulfate gave direct one-step formation of a variety of 7-acylpterins **37**, simply starting from pterin **2** (Scheme 8). Aldehydes afforded ketones, formamide was used to give the 7-carboxamide and α-keto esters for pterin esters.[54]

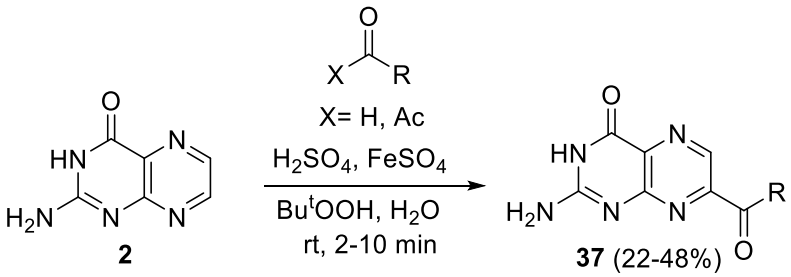

X = H, R = Me, Et, NH_2, C_6H_4-4-OMe
X = Ac, R = OMe, OEt

Scheme 8

10.18.5.7 Other Reactions of Fully Conjugated Pteridines

Reduction of the pyrazine ring of the pteridine scaffold has been reported with isobutyroyl-5,6,7,8-tetrahydropterin **39** obtained *via* PtO_2-catalyzed hydrogenation of *N*2-isobutyroylpterin **38**, in good yield (Scheme 9).[55]

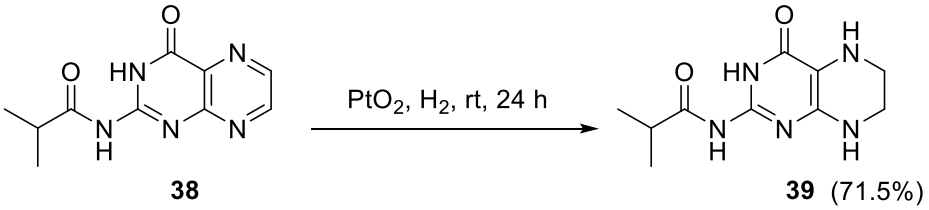

38 **39** (71.5%)

Scheme 9

Pteridine-2,4-diamine **40** was reduced at the pyrazine ring using 9 mole equivalents sodium triacetoxyborohydride in glacial acetic acid to give 5-ethyl-5,6,7,8-tetrahydropteridine **41** after column chromatography. Nonetheless, when only one mole equivalent of triacetoxyborohydride was applied to **40**, the 5,8-diethyl-5,6,7,8-tetrahydropteridine **42** was produced following column chromatography (Scheme 10).[56]

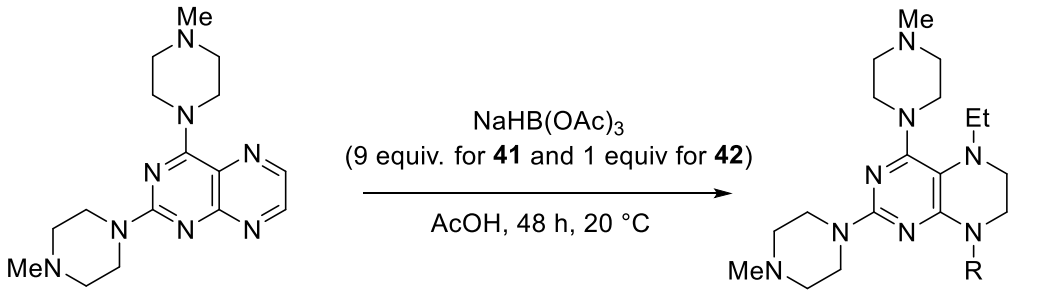

40

41 R =H (29%)
42 R =Et (46%)

Scheme 10

10.18.6. Reactivity of Nonconjugated Rings

10.18.6.1 Introduction

Dihydropterins **44**, **47**, **48** and **49** and tetrahydropterins **45** and **50** are important oxidation states of biopterin **43** and neopterin **46** due to their importance in biology (Figure 4). Dihydropterin – tetrahydropterin redox cycling is important in enzymatic processes such as nitric oxide synthase (where tetrahydrobiopterin **45** is the cofactor) and DNA synthesis pathways, where tetrahydrofolate **50** is the cofactor. Folate **8** → dihydrofolate **49** → tetrahydrofolate **50** pathways are key drug targets in oncology and anti-infective therapies.

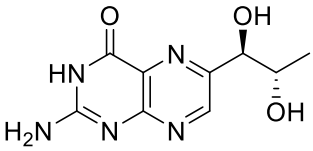

biopterin
43

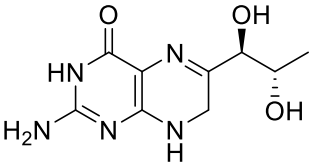

7,8-dihydrobiopterin
44

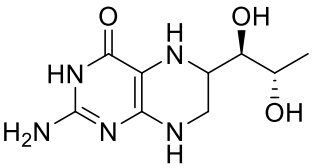

tetrahydrobiopterin, BH_4
45

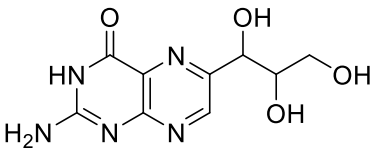

neopterin
46

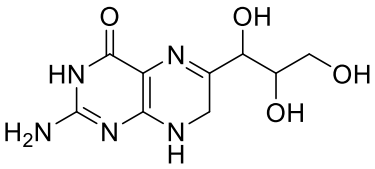

dihydroneopterin
47

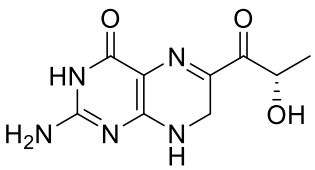

sepiapterin
48

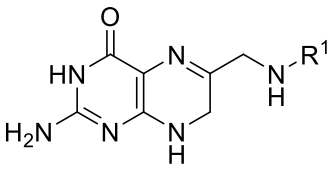

dihydrofolate
49

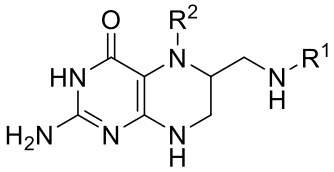

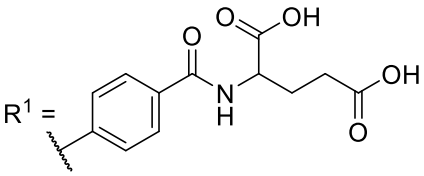

tetrahydrofolate, FH_4

50 R^2 = H tetrahydrofolate

50a R^2 = Me, 5-methyltetrahydrofolate

50b R^2 = CHO, 5-formyltetrahydrofolate

<Figure 4>

As expected, the stability and reactivity of these oxidation states are dependent on the substituents on the ring system and generally, the fully conjugated pteridines show much higher stability. Relevant examples are illustrated in the following section.

10.18.6.2 Reactivity of Dihydropteridines

The natural dihydropteridines undergo a varierty of photochemical and radical reactions. Dihydrofolate **49** and dihydrobiopterin **44** can act as radical scavengers in the same manner as the fully oxidized and reduced analogues. Dihydrofolate **49** is more reactive than folate, with greatest radical scavenging ability at acidic pH values.[57] Dihydroneopterin **47** produced by macrophages, undergoes oxidation by superoxide radicals to give neopterin **46**, and suggested as a mechanism for the raised **46** levels observed in inflammatory disease.[58] Dihydrobiopterin **44** and dihydroneopterin **47** form photodimers under UVA irradiation. Two isomeric dimers observed in spectral data indicate *anti*-R*trans* and *syn*-R*syn* isomers. The dimers are unstable and can undergo a thermal retro [2 + 2] cycloaddition to reform the dihydropterins plus an H_2O addition product.[59]

Aside from the important biological redox roles of dihydropterins, 7,8-dihydropteridines **47** can be synthetically useful . The stability and successful isolation of these products, rather than the fully oxidized pteridines, depends upon the other ring substituents. The 6-oxo substituent

confers suitable stability for these compounds used as scaffolds in medicinal chemistry, as discussed further in Section 10.18.10.8.

As a new class of heterocyclic compounds, synthesis of [1,2,4]triazolo[3,4-*b*]pteridines was reported. In this approach 2,4-dichloro-6-methyl-5-nitro pyrimidine was coupled with different amino acid esters followed by the reductive intramolecular cyclization to give dihydropteridine scaffold **51**. Heating chlorides **51** under reflux with hydrazine hydrate in ethanol gave 2-hydrazinyl derivatives **52**. Treatment with triethylorthoesters, resulted in cyclization and formation of the corresponding [1,2,4]triazolo[3,4-*b*]pteridine derivatives **53** in moderately good yields (Scheme 11).[60]

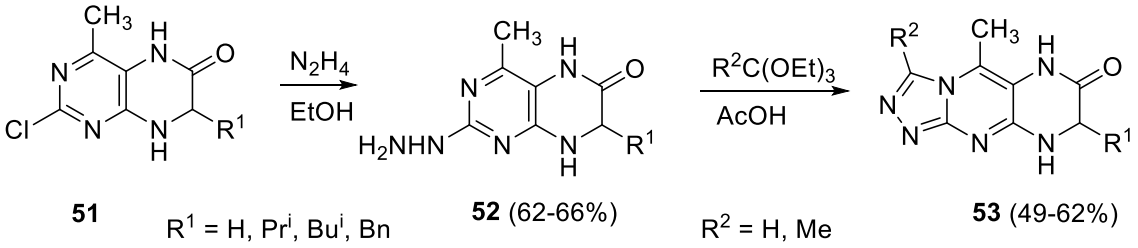

Scheme 11

4,5-Dihydro-[1,2,4]triazolo[4,3-*f*]pteridines **56** were synthesized from 7,8-dihydropteridin-6(5H)-ones **54** using potassium *tert*-butoxide, diethylchlorophosphate and hydrazine hydrate successively at low temperature and finally cyclized in boiling trimethyl orthoacetate or trimethyl orthoformate to give the fused triazole **55**. Eventually, nucleophilic substitution of the chloride of **55** with different amines afforded the desired compounds **56** (Scheme 12).[61]

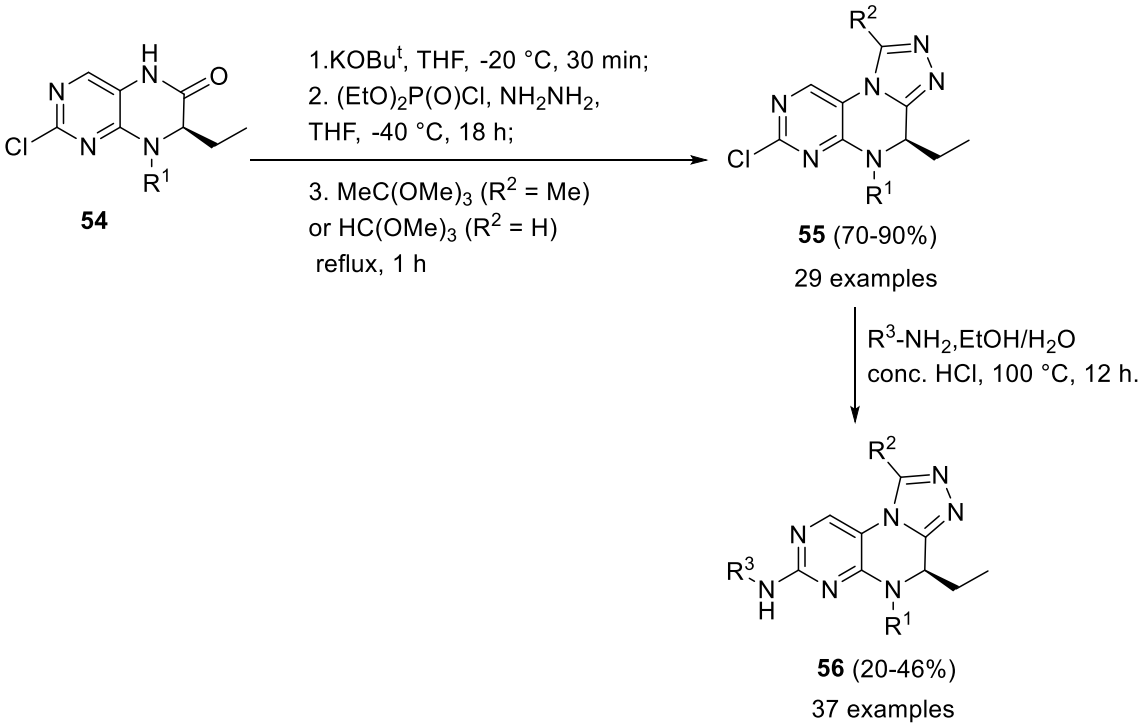

Scheme 12

The 6,7-diphenyl-7,8-dihydropteridine **57** (Figure 5) was isolated as a stable synthetic intermediate in 22% yield from the reaction of 4,5-diamino-2-mercapto-4-hydroxypyrimidine with benzil or two equivalents of benzaldehyde, and oxidation to the fully aromatic system was achieved with nitrobenzene.[62]

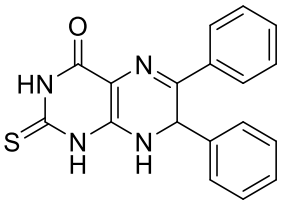

57

<Figure 5>

In a synthetic approach to construct analogues of pteridine-6,7-dione analogues, straightforward oxidation of C-7 of the 8-substituted dihydropteridin-6[5*H*]-one **58** with manganese dioxide gave the pteridine-dione **59** as shown in Scheme 13.[63]

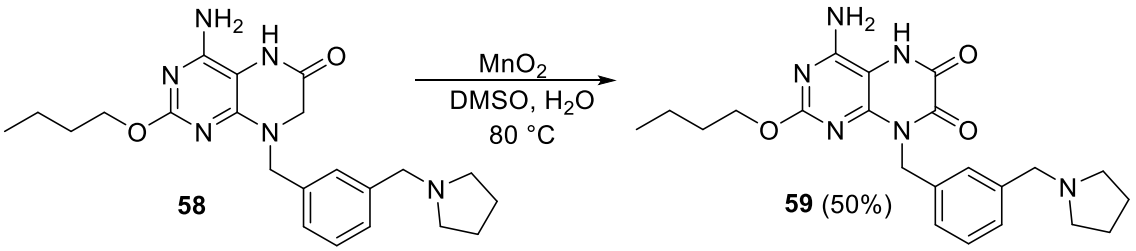

58 **59** (50%)

Scheme 13

The importance of neighbouring electron-withdrawing groups in stabilizing 7,8-dihydropteridines is exemplified by the reaction of coumarins with pteridines described in Section 10.18.5.5, Scheme 6. The 7,8-dihydro adducts obtained from the nucleophilic addition of coumarins to pteridine-4,6(3*H*,5*H*)dione were isolated in good yield. Pteridine-4,6(3*H*,5*H*)diones **32** were oxidized with chloranil to give the aromatic pteridines **60** (Scheme 14). However, in the reaction of pteridin-4(3*H*)-one **33**, the dihydro intermediates **61** could not be isolated, undergoing spontaneous oxidation to the pteridine products.[52]

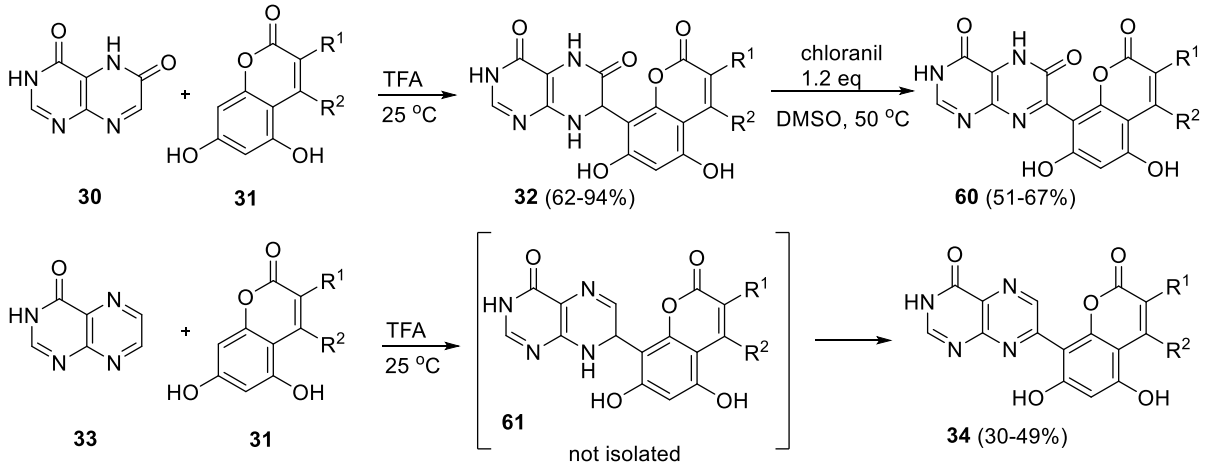

Scheme 14

10.18.6.3 Tetrahydro-derivatives

The radical scavenging activity of folate, biopterin and their tetrahydro-reduced forms over a range of pH values were determined. Both tetrahydrofolate **50** and tetrahydrobiopterin **45** have much higher radical-scavenging activity than both biopterin **43** (which has minimal scavenging activity) and folate due to the lower bond dissociation energies and ionization potentials in the reduced forms with implications for the depletion of folates in oxidative stress.[64] 5-Formyltetrahydrofolate **50b** shows an increase in radical-scavenging activity with increasing pH, which is in contrast to dihydrofolate **49**, tetrahydrofolate **50**, and 5-methyltetrahydrofolate **50a**, which are better radical scavengers at acidic pH values.[57] Tetrahydrobiopterin **45** usually undergoes 2-electron oxidation in solution with stabilization of the radical cation, when bound to NOS due to a radical cation – π interaction with tryptophan.[65] Tetrahydrobiopterin was subjected to UV irradiation in aqueous conditions and the autooxidation products analysed. The pterin-based oxidation products, namely dihydroxanthopterin, dihydropterin **44** and pterin **2** were formed in greater quantities than dihydrobiopterin **44** and biopterin **43**. Dihydrobiopterin and dihydropterin dimers were also detected.[66]

10.18.7 Reactivity of Substituents Attached to Ring Carbon Atoms

10.18.7.1 General Survey of Substituents on Carbon

Substituents on pteridine carbons exhibit reactivity analogous to pyridine or other N-heterocyclic substituents. However, because of the multiple heteroatoms and correspondingly similarly reactive positions in pteridines, selectivity cannot always be achieved and may involve protecting group strategies. Replacement of oxo- or amino- groups leads to increased synthetic utility.

10.18.7.2 Nucleophilic Displacement

Alkylthiopteridines undergo nucleophilic substitution more readily than pyrido[2,3-*d*]pyrimidines and pyrrolo[2,3-*d*]pyrimidines due to greater electron deficiency.[51] A strategy to introduce C2 and C4 substiuents on 6,7-disubstituted 2-benzylthiopteridine-4(3*H*)one **62a** and **62b** to give **63**, **64** and **65** (Scheme 15), involved oxidation of the 2-alkylthio functionality followed by nucleophilic substitution with an amine. In lots of cases, an oxidation step was not needed before nucleophilic substitution of the 2-alkylthio moiety. The 4-position oxo-moiety was substituted by (benzotriazol-1-yloxy)tris(dimethylamino)phosphonium hexafluorophosphate (BOP) activation, followed by amine substitution. The sequence of substitution at C2 and C4 was not crucial and could be carried out in either order, since good yields were obtained by applying oxidation/substitution or BOP activation/substitution chemistry as the first step (Scheme 15).[67]

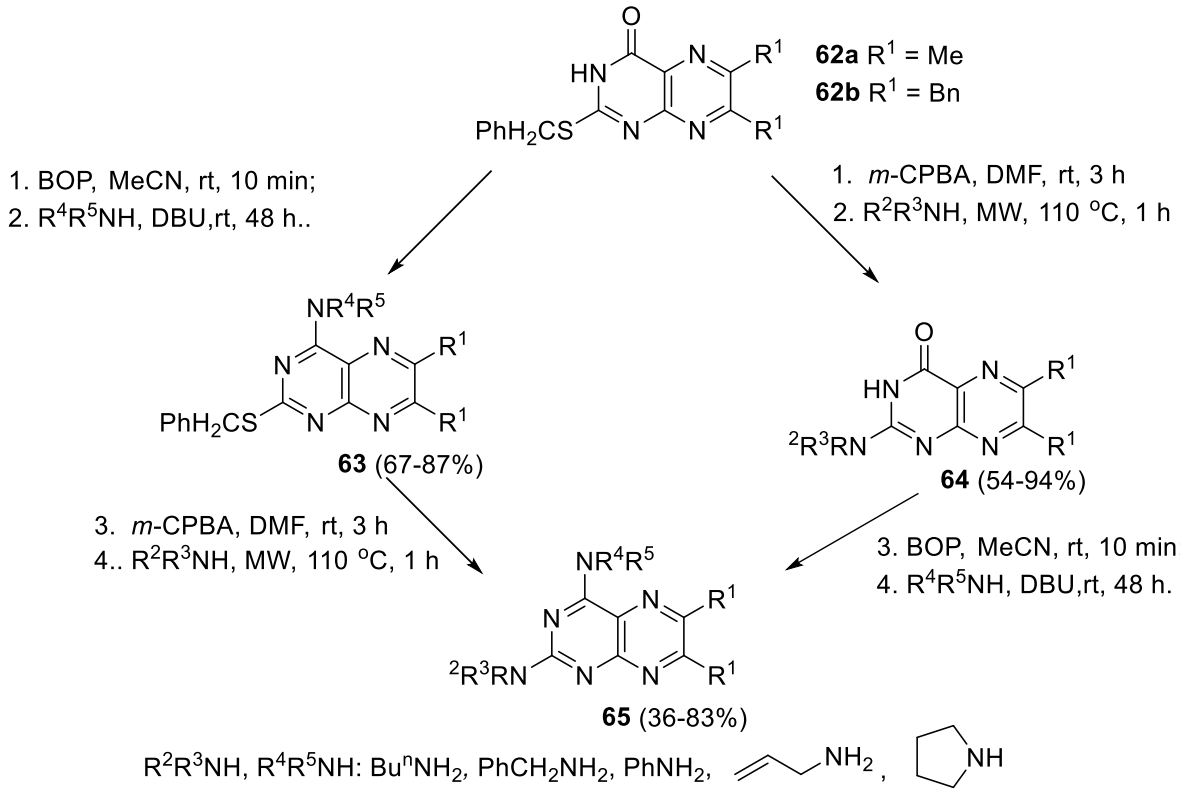

Scheme 15

Pteridines **66** and **67** can undergo thiation with P_4S_{10} to give the 4-thiopteridine analogues **68** and **69** in good yield (Scheme 16). Introduction of amino functionality at C-4 on the pyrimidine ring is possible by treatment with methanolic ammonia, which resulted in formation of isopterin analogues **70** and **71** in moderate yield.[50]

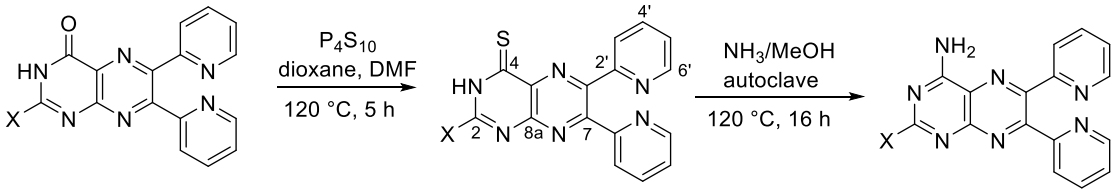

66.X = H
67 X = NH_2

68. X = H (71%)
69. X = NH_2 (79%)

70. X = H (50%)
71. X = NH_2 (54%)

Scheme 16

The 5,8-dihydropteridine-6,7-diones **72** prepared via Gabriel's methodology, were derivatized at C-4 via nucleophilic aromatic substitution with the corresponding alcohols in the presence of sodium hydroxide and KI as promoter, to obtain alkoxyl/phenoxy analogues **73**. The anilino-compounds **74** were prepared in acetic acid with KI as promoter. Cyclic amino-analogues **75** were made by reacting **72** with a variety of cyclic amines in the presence of potassium carbonate and potassium iodide (Scheme 17).[68]

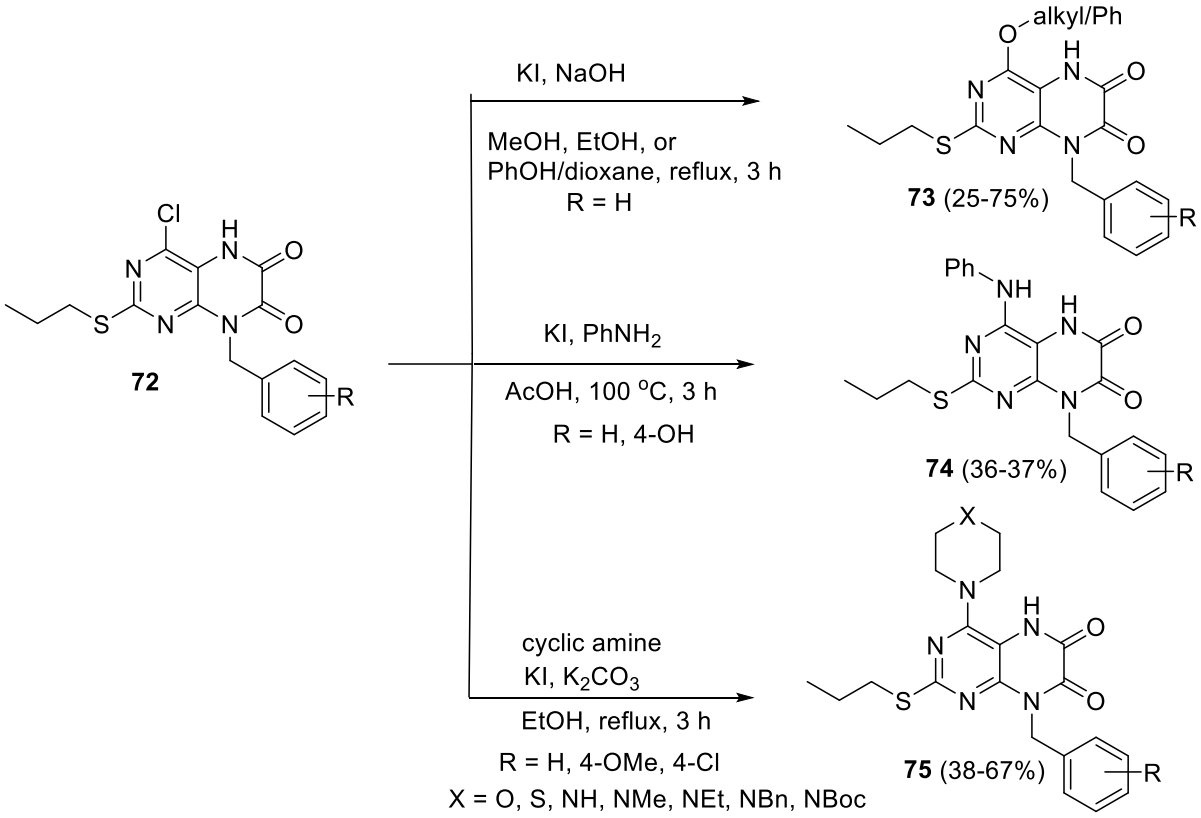

Scheme 17

The 2-chloro-5,8-dihydropteridine-6,7-dione **76** undergoes hydrazinolysis in EtOH to form intermediate hydrazine **77**, which reacts with suitable aromatic aldehydes to produce pteridinones **78** possessing a hydrazone moiety in reasonable yields (Scheme 18).[69]

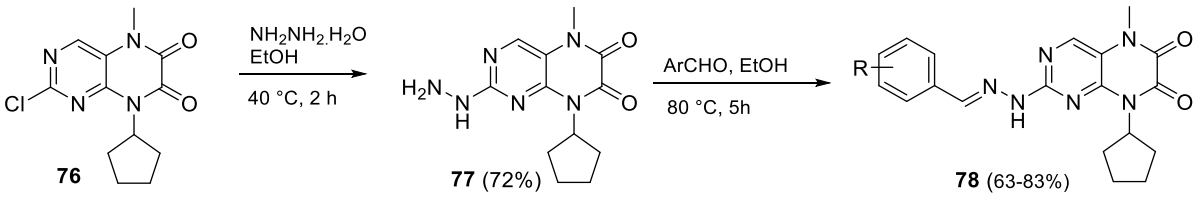

Scheme 18.

The relative reactivities of chloro-substituents to nucleophilic substitution were explored using pteridinone **79** prepared in 4 steps from 2,4-dichloro-5-nitropyrimidine. Upon reaction with sodium azide, in theory both sites can react and as a result the tetrazole products **80** or **81**, as well as 6- or 2-position azide substitution products **82** or **83** can form (Scheme 19). Based on verification by X-ray single crystal diffraction analysis, a single 6-cyclization product **80** was obtained. In addition, for preparing the triazole product by reaction with hydrazine followed by trimethyl orthoformate, in theory compounds of 6-substitution **84** or 2-substitution **85** could form. The 6-cyclization product **61** was the sole product, as confirmed by X-ray single crystal diffraction.[70]

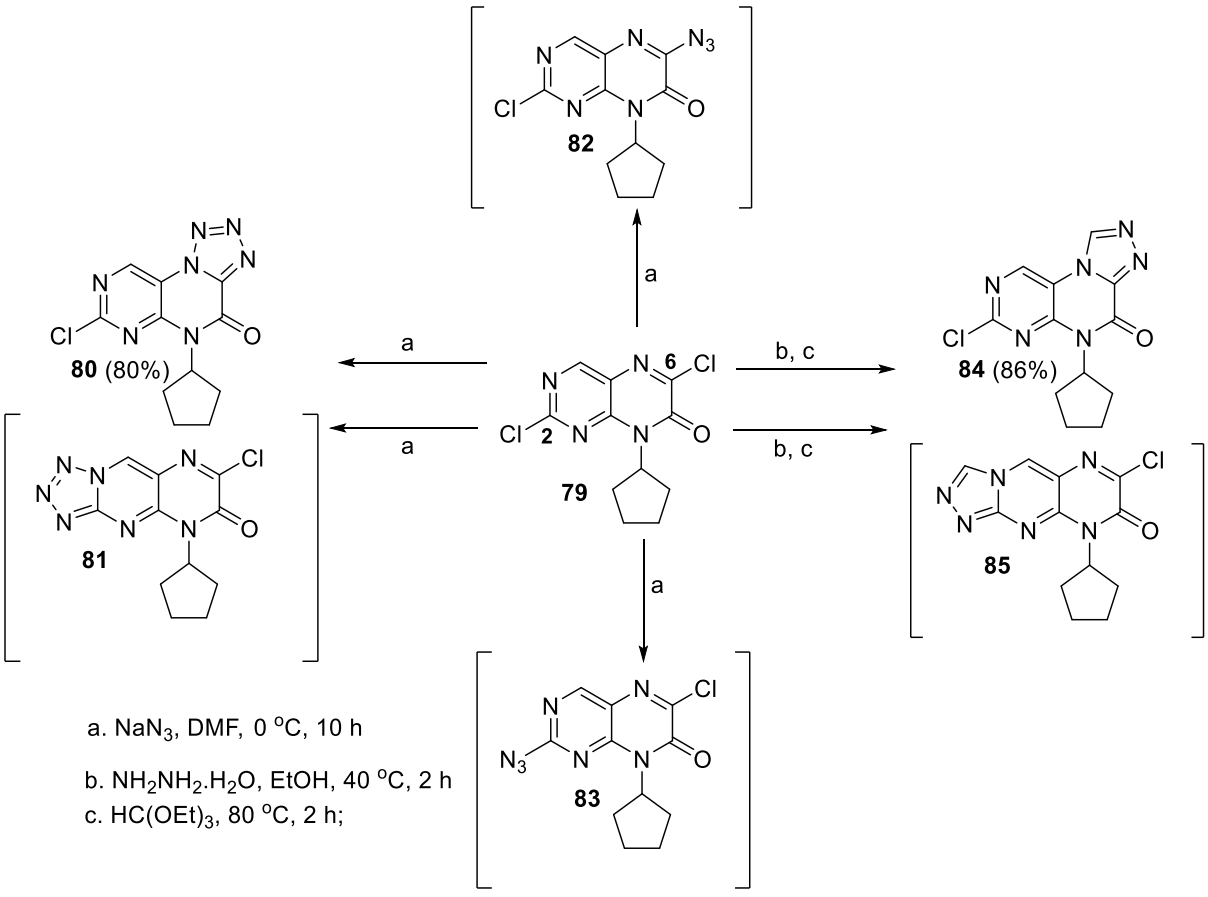

Scheme 19

10.18.7.3 Electrophilic Attack

There have been no significant new reports regarding electrophilic attack on substituents attached to carbons on the electron-deficient heterocycle.

10.18.7.7. Metal-Catalyzed Substitution

The utility of organometallic coupling in reactions with pteridines is growing. Tetrahydropteridine derivatives **88** and **89** were synthesized via metal-catalyzed Buchwald-Hartwig coupling of 2-chlorodihydropteridinone **86** and **87** with a variety of 4-amino-benzenesulfonamides and 5-substituted indoles respectively (Scheme 20).[71] Further Buchwald-Hartwig couplings of tetrahydropteridine derivatives, with the same core scaffold, are reported by the same group.[72]

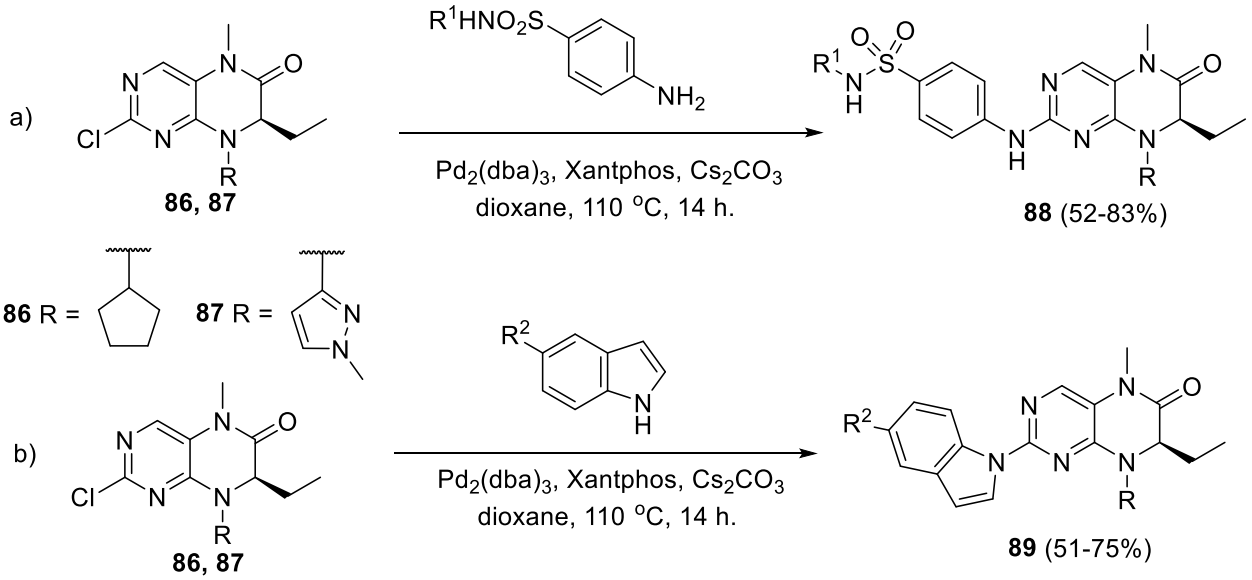

Scheme 20.

Pd-catalyzed cyanation of pteridine-2,4-dione-6-triflate **90** followed by nitrile hydrolysis gave carboxylic acid **91**, which could couple with various amines to give amide analogues. Alternatively, alkynyl side chains were introduced at the 6-position into **90** *via* Sonogashira coupling. (Scheme 21).[73]

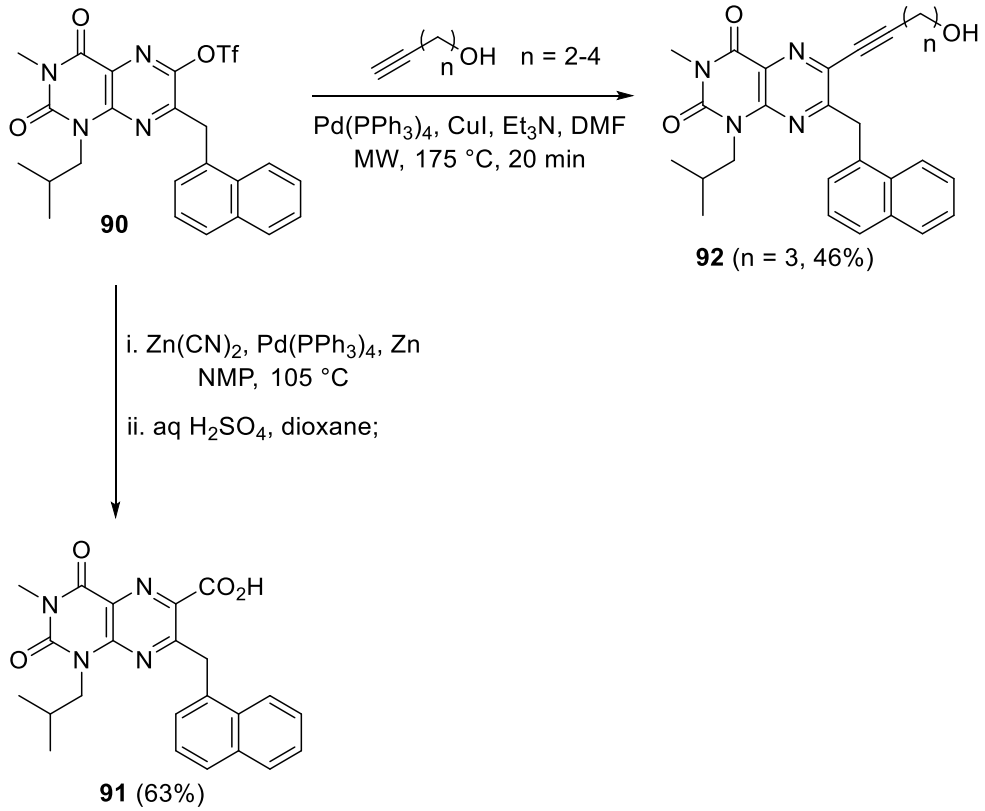

Scheme 21

6,7-Dialkynyllumazines **95** was prepared by the Sonogashira coupling reaction of 6,7-dichlorolumazine derivative **93** with terminal alkynes. The chloride substituents have different reactivity, which permits a stepwise addition of alkynyl moieties. Therefore, reaction of **93** with one equivalent of phenylacetylene in presence of Pd_2dba_3/CuI/K_2CO_3 in DMF at 25–30 °C produced the 6-chloro-7-(phenylethynyl)lumazine **94**. If two equivalents of phenylacetylene were applied at 90–100 °C, the 6,7-dialkynyl derivative was obtained. Coupling of compound **94** with the appropriate 1-alkynes at 90–100 °C gave the corresponding 6,7-dialkynyllumazines **95** in moderate yields (Scheme 22).[74]

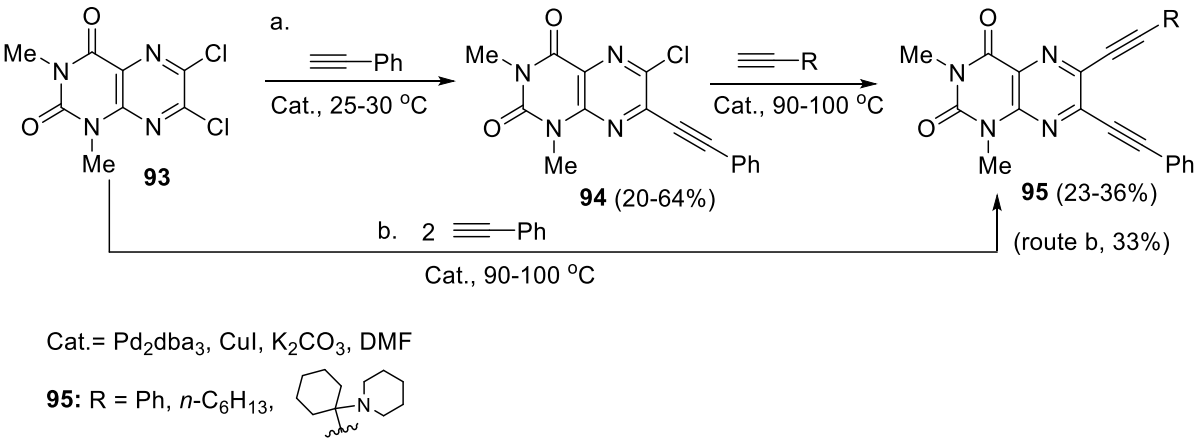

Scheme 22

10.18.7.5 Oxidation Reactions

Methyl groups attached to pteridine ring carbons are benzylic in nature and subject to oxidation. Heating 6,7,7-trimethyl-7,8-dihydropterin **96** with bromine or *N*-bromosuccinimide in ethanol furnished the ester **97** [84]. 6-Aldehyde **98** was obtained from **96** using oxidation of the methyl group with SeO_2. Having these two intermediates in hand enables straightforward extension of the side chain at position 6 of 7,7-dimethyl-7,8-dihydropterin (Scheme 23).[75]

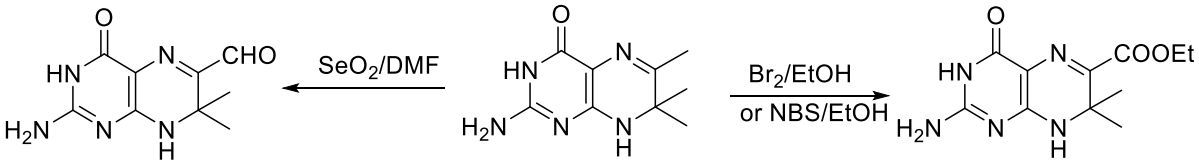

Scheme 23

10.18.7.6 Reduction Reactions

No significant new reactions involving reduction of substituents have been reported.

10.18.7.7 Side-Chain reactions

Introducing substituents particularly at carbon 6 is important in pteridine chemistry. This is achieved by the previously discussed substitution of halide at this carbon or by functional group modifications at C-6. Lumazine and pterin 6-acetyl and 7-methyl derivatives **99** and **100** can be converted to 6-[1-(arylamino)ethyl]pteridine derivatives **101** and **102** respectively, in a one-step reductive amination in the presence of 2-picolineborane complex (*pic*-BH_3) (Scheme 24).[76] The authors report that deprotection of **102** to give the pteridine-4-one should be facile.

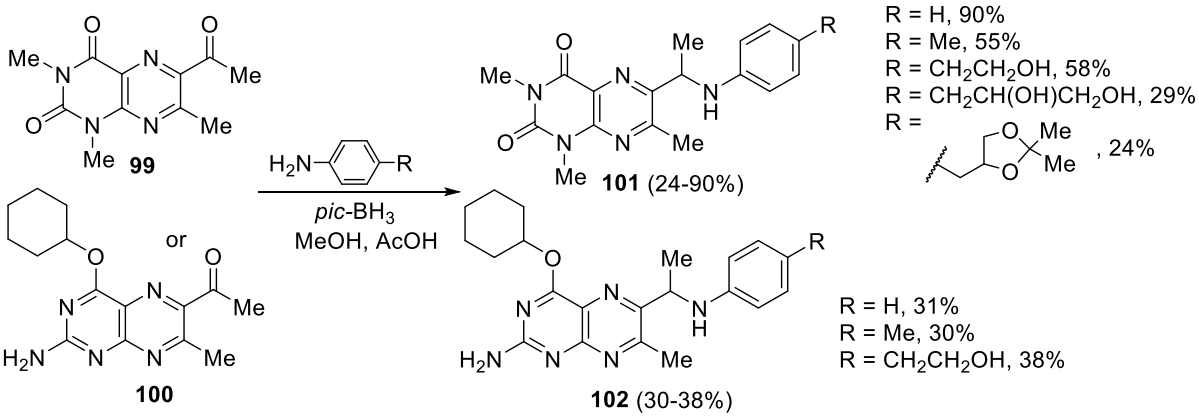

Scheme 24

Synthesis of the natural product sepiapterin-C **104** is reported through hydrolysis of 6-ethynylpteridine **103** using mercury oxide in sulfuric acid at 80 ˚C to produce 6-acetyl-2-amino-

3,4-dihydropteridin-4-one, followed by mild imine reduction using dissolved alumninium turnings in 1 M aqueous ammonia (Scheme 25).[77]

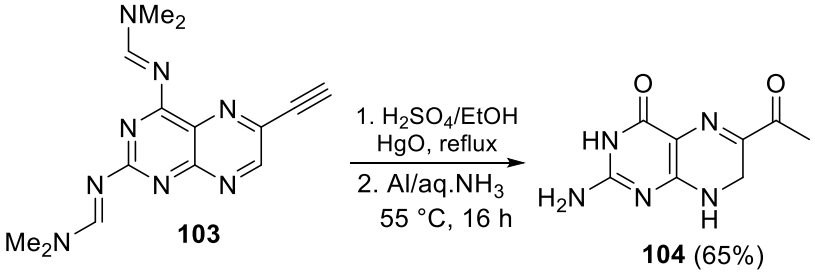

Scheme 25

A refined microwave-assisted procedure for the preparation of methotrexate diester **107** and a series of related 2,4-diaminopteridines is reported.[78] The time and yield issues previously reported for the S_N2 reaction between halogenated pteridine **105** and amine **106** (Scheme 26) were resolved in this process. By applying microwave irradiation and including 3 equivalents of potassium carbonate with catalytic KI, the yield and purity of the products were improved. Interestingly, starting materials were recovered easily due to a less complex reaction mixture.

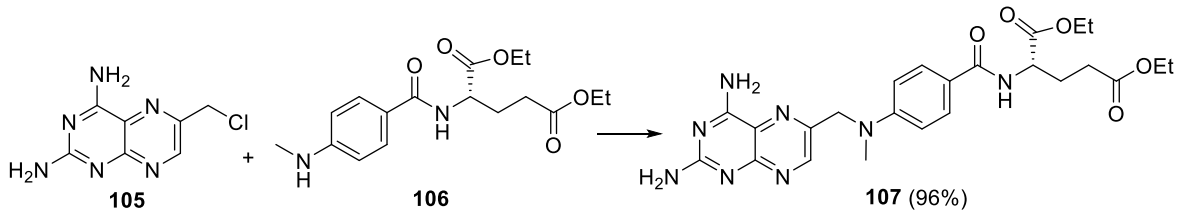

Reaction conditions: **105** (1.2 equiv.), **106** (1.0 equiv.), K_2CO_3 (3 equiv.), KI (0.1 eq.), DMA, MW, 60 °C, 20 min.

Scheme 26

The key 6-formyl intermediate **108** was coupled to different 4-aminobenzenesulfonamides to give the corresponding Schiff base, which was reduced with borane *tert*-butylamine complex and deprotected to afford the sulfonamides **109**, with a variety of alkyl, aryl and heteroaryl substituents (Scheme 27).[79]

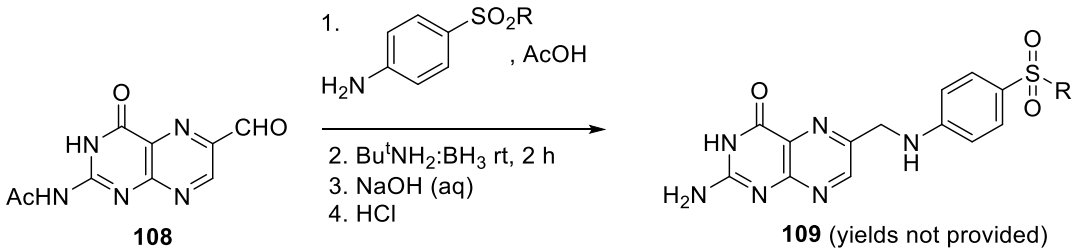

Scheme 27

Other examples of side chain reaction include nucleophilic substitution reactions of pteridine **110** with primary amines in isopropylamine, which resulted in unexpected products.[80] Surprisingly, the isopropoxy group on C-4 was substituted by the amine, and the Cl-atom in the side chain of C-6 was replaced by the isopropoxy residue, giving products **112–114**. When EtOH was used as solvent in the reaction between compound **110** and neopentylamine, this again resulted in alcohol substitution of the side chain to furnish 6-(1-ethoxyethyl)-7-methyl-*N*4-neopentylpteridine-2,4-diamine (**115**). Replacing alcoholic solvents with aprotic solvents such as DMF or MeCN and replacing chloro- with bromo- was to some extent a solution to this problem and now primary aromatic amines e.g. aniline, *p*-toluidine and ethyl 4-aminobenzoate reacted with **111** in the expected way replacing the bromine to give the corresponding 6-[1-(arylamino)ethyl] derivatives **116–118** (Scheme 28). Attempting this substitution reaction between **110** and *p*-toluidine using excess of amine and extended reaction time as illustrated resulted in a disubstitution product **119**. Under basic hydrolysis of compounds **116–118**, the pterin derivatives **120–122** were obtained. In addition, treatment of pteridine **110** with suitable alcohols in the presence of Et_3N afforded **123–125**. Hydrolysis of these compounds in 1N NaOH gave the corresponding pterin derivatives.

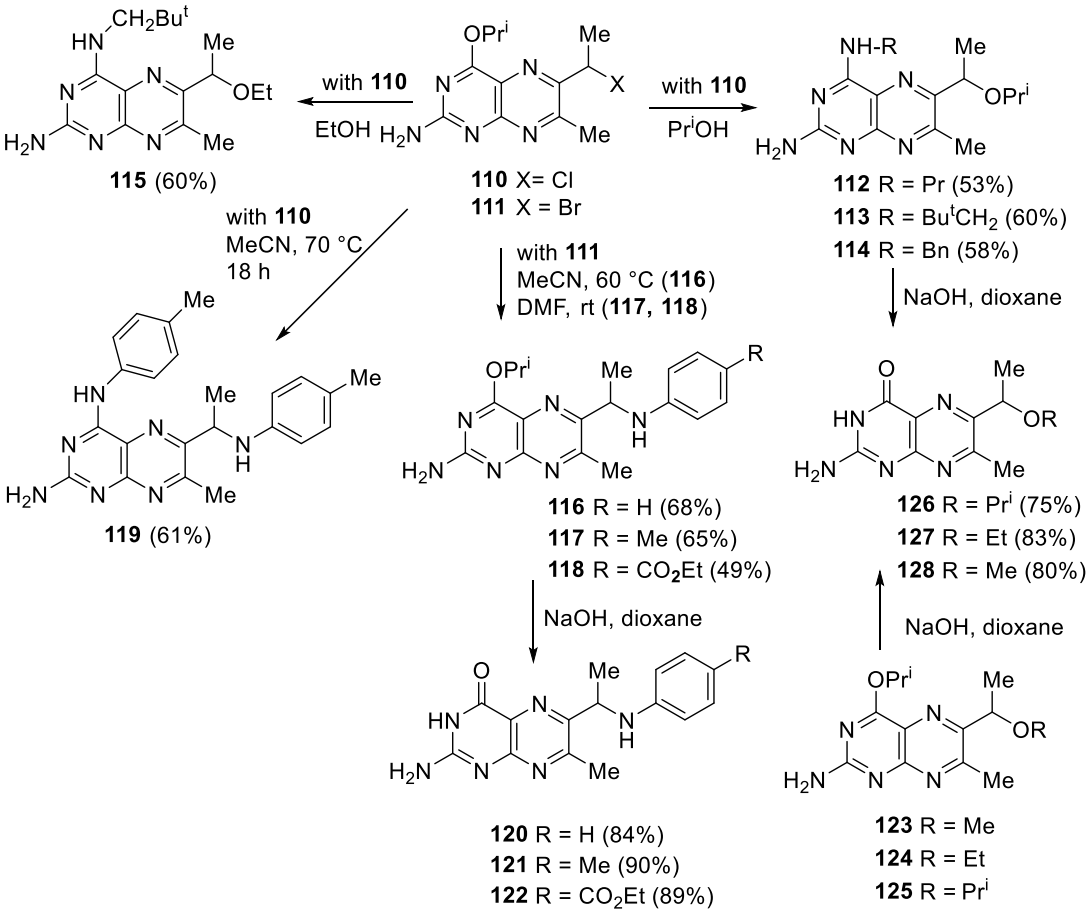

Scheme 28

Solubility issues limit synthetic applications of pterin. A useful methodology has been recently developed using DBU-promoted amidation of 7-methoxycarbonylpterin **129** for quick preparation of new pterin derivatives **130** (Scheme 29).[81] In this strategy, 7-carboxymethylpterin **129** is converted into the soluble DBU salt, along with DBU aiding the amide formation. The reactions were typically complete within 5-10 minutes at 60-80 °C and products isolated by acidification. Steric effects were evidenced by lower reactivity for secondary amines and lower yields for more hindered amines with a substituent on the α-carbon. However, this could be widely overcome in amines with additional hydrogen-bonding substituents such as a β-hydroxy functional group, as evidenced by the good yield achievable for serine (88%).

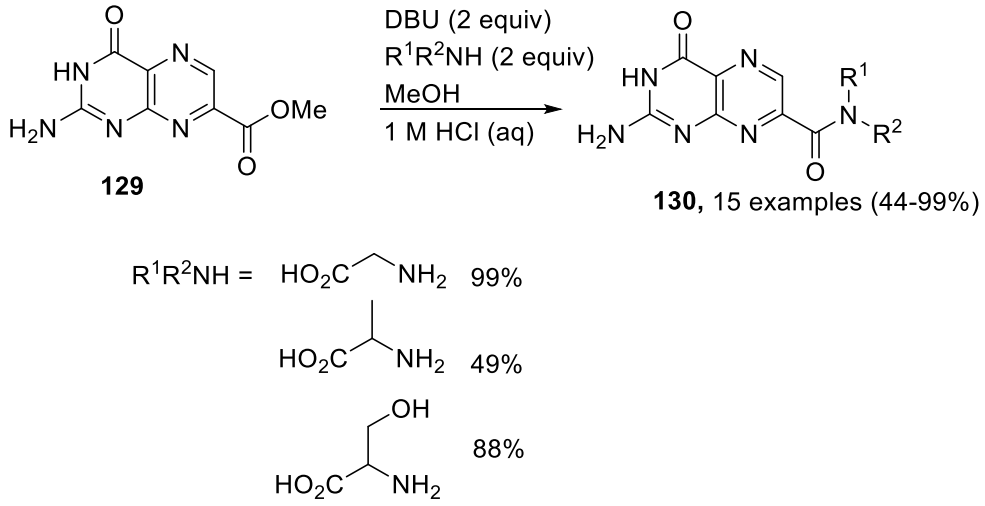

Scheme 29

Tandem cyclization of 6,7-dialkynylpteridines **95** into [1,2,3]triazolo-[1',5';1,2]pyrido[4,3-*g*]pteridines **130** and **131** is promoted by sodium azide. The mechanism for this transformation is 1,3-dipolar cycloaddition of an azide ion to the C≡C bond to form the 1,2,3-triazole *N*-anion intermediate, which undergoes intramolecular nucleophilic addition to the other triple bond in the molecule (Scheme 30).[82]

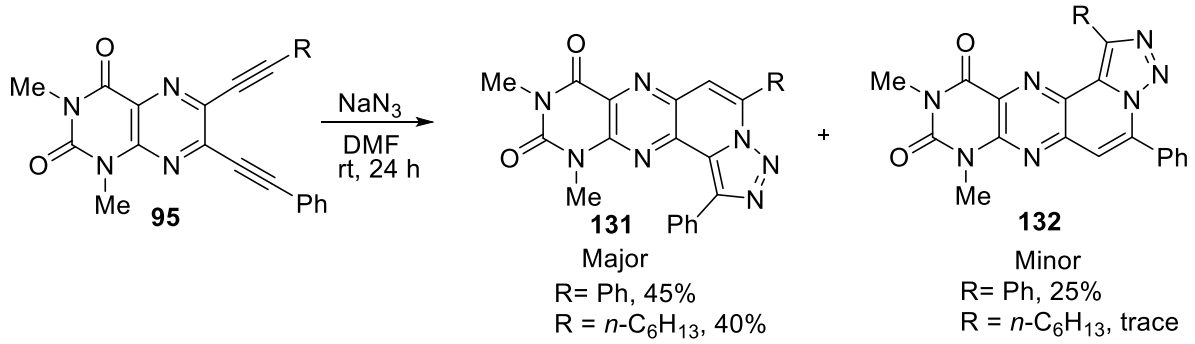

Scheme 30

Further studies demonstrated that alkynyl azines and alkynyl carboarenes show different reactivity with nucleophiles.[83] Because the azine ring is highly electron deficient, *ortho*-dialkynylpteridines **133** react quickly even with neutral nucleophiles. Therefore, the addition product **134** undergoes base-induced or spontaneous heterocyclization with direct involvement of the nucleophile used to give **135** (Scheme 31a). Reaction of pteridine **136** with a carbanion formed from the treatment of diethyl malonate with base, resulted in formation of the cyclopentadiene ring attached to the parent heterocyclic ring system in **137** (Scheme 31b). The structure of **137** confirmed by X-ray single-crystal analysis. Two possible mechanistic pathways for this tandem carboannulation were proposed. Substitution of the chlorine atom by the nucleophilic carbanion followed by annulations to form the cyclopentadiene ring or the addition of the nucleophile to the C≡C bond followed by the intramolecular replacement of the chlorine atom. The latter was more likely, because formation of the vinylic intermediate favors the cyclization geometry. The scope of annulation reactions was further investigated and studies showed that in most cases the reaction of 3-alkynyl-2-chloro- and 2,3-dialkynyl derivatives of pyrazines with carbanion intermediates begin with the addition of a nucleophile to the more electrophilic alkyne. Nearly all of the reactions progressed via tandem or cascade cyclizations forming polynuclear heterocyclic compounds. Further methods for synthesis of pteridines fused onto a heterocyclic ring, an important class of compounds in natural products, were reviewed. [84]

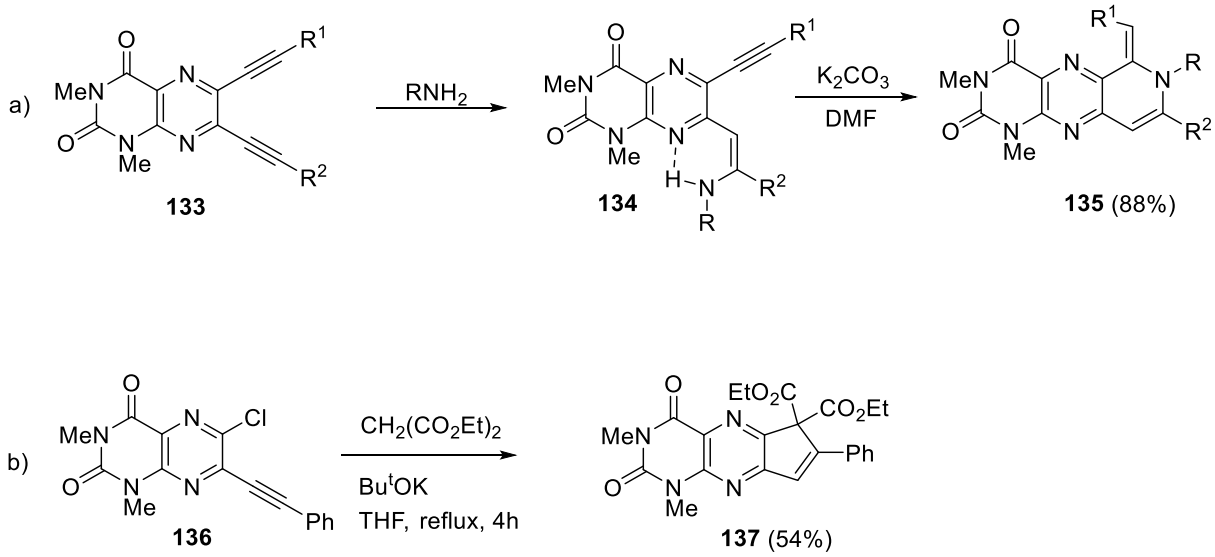

Scheme 31

The alteration to the C-6 side chain of pteridinetrione derivatives **138** containing a highly-reactive carbonyl functionality at C-6 can be achieved *via* reduction.[85] Using an excess of sodium borohydride in the presence of sodium hydroxide, ketones **138** were converted to the secondary alcohols in good yields. Reaction with hydrogen halides resulted in an elimination to produce the corresponding (*E*)-1-methyl-6-(2-aryl(heteryl)ethenyl)pteridine 2,4,7(*1H,3H,8H*)-triones **139** (Scheme 32).

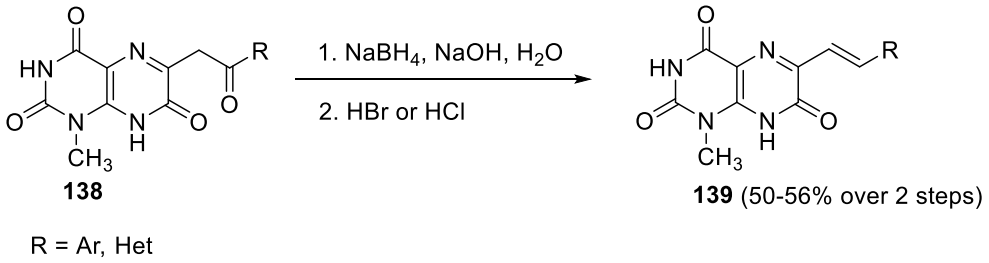

Scheme 32

10.18.8 Reactivity of Substituents Attached to Nitrogen

10.18.8.1 *N*-Oxides

The 4-protected 5-*N*-oxide of isoxanthopterin **140** undergoes a 1,3-dipolar cycloaddition with a number of dipolarophiles. The oxazoline intermediate **141** is not isolated, undergoing ring opening via cleavage of the N-O bond to give the 6-alkyl product **142** bearing an alcohol (Scheme 33).[86] 2-Deoxo-2-methylthioflavin-5-oxides substituted at position 2 by amines underwent concomitant N-deoxygenation for some analogues.[87]

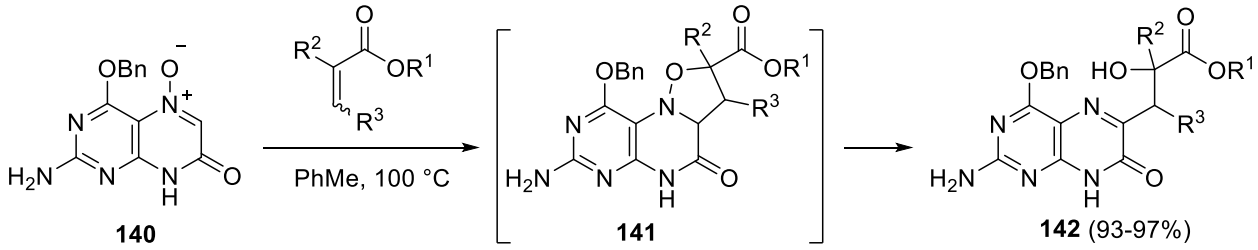

Scheme 33

10.18.8.2 Metal Complexes

Pteridines are important ligands, particularly in nature, including Mo-dithiolene-complexed ligand in the molybdenum cofactor. Lumazines are used in transition metal complexes as monodentate or bidentate ligands, often coordinating through O4 and N5. Derivatized lumazines, such as the benzoylhydrazone are used as tri- or tetradentate ligands, for example, the rhodium complex of the benzylhydrazone-lumazine derivative **143** [$RhCl_2$(BZLM)(CH_3CN)], which coordinates through pyrazine N5 and the side chain.[88] There are corresponding O4/N5 bound flavin/alloxazine complexes, as exemplified by **144,** which forms a multinuclear complex with further coordination to pyrimidine nitrogens.[89] The effects of different metal cations in metal-pterin complexes on the pterin reactivity were analyzed using density functional approximation calculations. The effects on the ability of the pterins to act as electron acceptors or donors was determined. Complexes with Au, Ag and Cu were the best electron acceptors, whereas complexes with Zn, Cd and Hg were better electron donors. Electron donation to the hydroxyl radical was exergonic for these complexes indicating

antioxidant activity.[90] The synthesis and applications of metal complexes are discussed in Section 10.18.10.3.

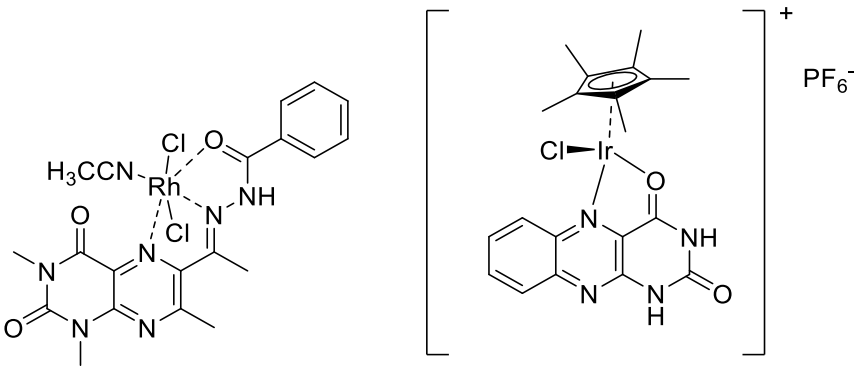

<Figure 6>

10.18.9 Ring Syntheses

The synthesis of pteridine ring systems has a long history. The two heterocycles in pteridine, pyrimidine and pyrazine can be synthesized in any order, *i.e.* starting with a pyrazine and constructing the pyrimidine ring or from a pyrimidine and building on the pyrazine ring. A review of pteridine synthesis provides an overview of the most common methods for contruction of the heterocyclic rings.[91] Pteridines show a variety of biological activities and are incorporated in the backbones of several marketed drugs, and have attracted increasing attention from the medicinal chemistry community.

10.18.9.1 Ring Syntheses from Pyrimidines

Classical but popular methodologies for synthesizing pteridines were developed by Gabriel–Isay, Timmis, Polonovsky-Boon, and Taylor many years ago and are reviewed in earlier editions.[1, 92] Gabriel and Isay's method requires condensation of 5,6- pyrimidinediamines with compounds having a 1,2-dicarbonyl functionality. Because the pyrimidine ring is unsymmetrical, reactions with unsymmetrical diketones result in the formation of regioisomers. When this condensation reaction is with α-oxo oximes, it provides regioselective products.[93]

6- and 7-Aryl pteridines **146** and **147** were prepared from condensation of substituted 5,6-diaminopyrimidines **145** with substituted phenylglyoxals or benzils.[94] The synthetic strategy was based on a conventional approach, starting with prefunctionalized intermediates with up to 14 positions available for structural developments. In reactions using phenylglyoxals, regioselective syntheses of 6- and 7-substituted pteridines **146** and **147** were under pH-

controlled conditions (Scheme 34). The 6- substitution is achieved by *in situ* generation of the glyoxal monoxime and cyclization under acid conditions, whereas direct condensation under neutral or basic conditions yields the 7-substituted products.

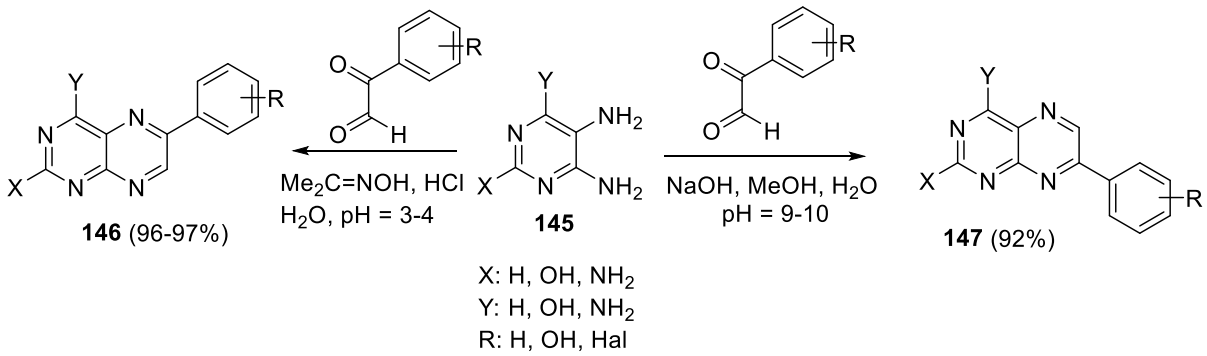

Scheme 34

Synthesis of 2-phenyl-4-amino(hydroxyl)pteridines from 4-amino and 4-chloro substituted 5,6-diamino-2-phenylpyrimidines cyclization with glyoxal using classic Gabriel-Isay was descrobed. Various amino and ureido substituents were placed on C-4 of the pyrimidine ring by replacement of the hydroxyl group on the ring with suitable amines or by reacting the amino function with suitable isocyanates respectively.[95] 1,3-Dimethyl-2,4-dioxo-6-substituted-1,2,3,4-tetrahydropteridines **149b-149f** were achieved using cyclization of 6-amino-1,3-dimethyl-5-(substituted methylidene)aminouracils **148b-148f** with triethyl orthoformate as a one-carbon source.[96] Using the same conditions, compound **148a** yielded a mixture of 6-substituted pteridine **149a** and 8-substituted xanthine **150a**. Alternatively, by applying another one-carbon sources such as triethyl orthoacetate and triethyl orthobenzoate to cyclize derivatives, 5-benzylideneamino **148b** or 5-(2-furylidene)amino **148g**, the corresponding xanthine derivatives were also obtained and not the pteridines. This is due to the higher reactivity of triethyl orthoformate as a one-carbon source compared to triethyl orthoacetate or triethyl orthobenzoate (Scheme 35).

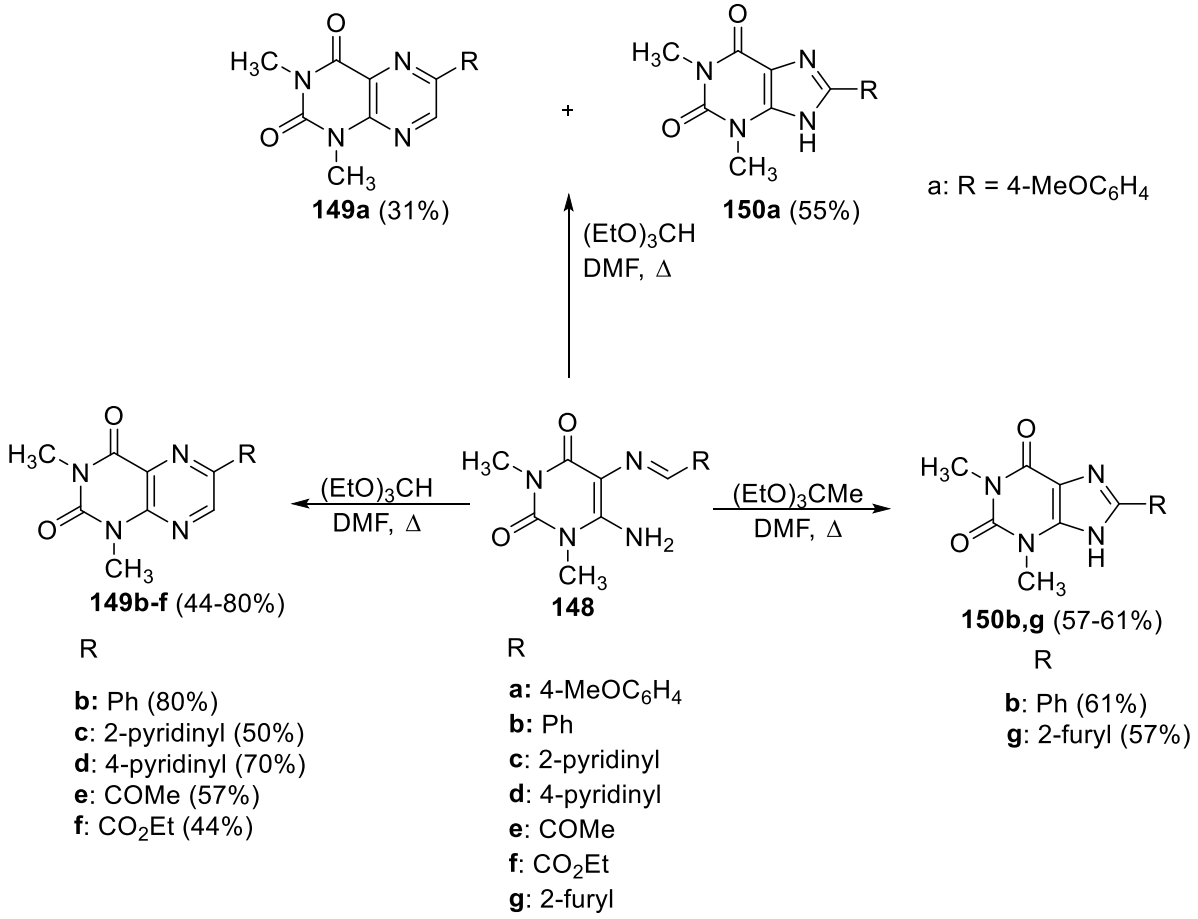

Scheme 35

The first synthesis of a natural product tepidopterin, 2'-*O*-(2-acetamido-2-deoxy-β-D-glucopyranosyl)-L-*threo*-biopterin **158** was reported (Scheme 36).[97] In this synthesis, L-*threo*-pentos-2-ulose derivative **151**, which was prepared from L-xylose in 6 steps, and condensed with the sulfate of 2,5,6-triamino-4-hydroxypyrimidine **152** using aqueous sodium bicarbonate solution. The preferential formation of the desired **153** and the 7-substituted isomer **154** occurred in a ratio of 75:25. Under neutral conditions, the same condensation reaction gave a mixture of the **153** and **154** in a less favorable 35:65 ratio with separated products characterized after conversion to the fully protected derivatives **155** and **156**. Methanolysis of **155** afforded the 10-*O*-PMB derivative **157**, which is a versatile precursor for the 2'-*O*-monoglycosylation. Synthesis of tepidopterin **158** was completed by reaction with 3,4,6-tri-*O*-acetyl-2-deoxy-2-phthalimido-β-D-glucopyranosyl bromide, followed by removal of the protecting groups.

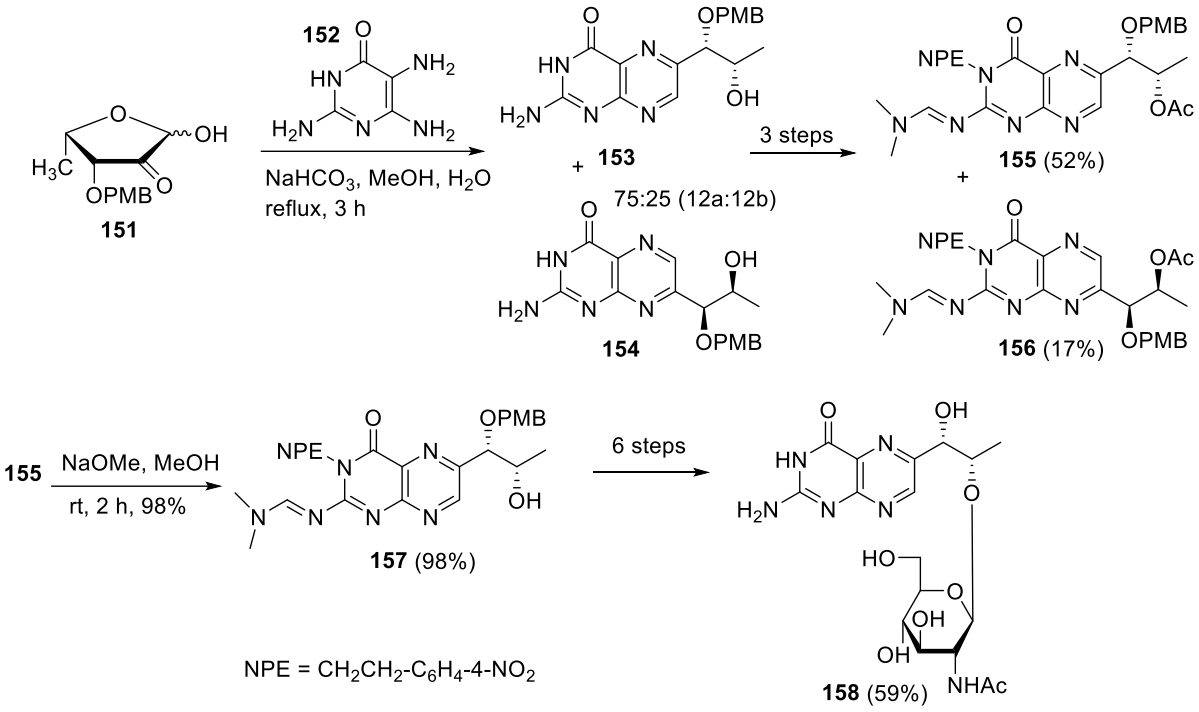

Scheme 36

Pterin 2'-*O*-glycosides were prepared from N^2-(*N,N*-dimethylaminomethylene)-1'-*O*-(4-methoxybenzyl)-3-[2-(4-nitrophenyl)-ethyl]biopterin and its ciliapterin analogue, respectively, from D-xylose (in 14 steps) and L-xylose (in 11 steps). These key intermediates subsequently underwent glycosylation with 3,4,6-tri-*O*-acetyl-2-deoxy-2-phthalimido-β-D-glucopyranosyl bromide followed by removal of the protecting groups, providing the first efficient selective syntheses of natural products limipterin and tepidopterin, respectively.[98]

There are several examples of the use of the nitroso-ene reaction to form pteridines. The most applicable use of the nitroso-ene reaction involves electron-deficient nitroso compounds. A regioselective preparation of pteridines substituted with branched and linear alkenyl moeties at C(6) was reported using the intramolecular nitroso-ene reaction of *N*-(alk-2-enoyl)-4-amino-5-nitrosopyrimidines **162** and **163** (Scheme 37).[99] The structure of the alkenyl substituents depends on the starting material as well as the regioselectivity of the nitroso-ene reaction. 5-Nitrosopyrimidines **162** and **163** were synthesized in good yield by acylation of compound **159** with (*E*)-pent-2-enoyl chloride (**160**) and (*E*)-dec-2-enoyl chloride (**161**) respectively. Pyrimidine intermediates **162** and **163** were suspended in toluene followed by heating to 100 °C, which resulted in progressive transformation into a yellow precipitate in about 3 hours. Pteridin-7(8H)-ones **164** and **165** were obtained in high yields with approximately 8:2 (*E)-*:(*Z)*-mixtures. Isomerization of (*E/Z*)-**164** and **165** resulted in pure (*E*)-isomers. Debenzylation of (*E*)-**164** to the poorly soluble C(6)-(*E*)-prop-1-enyl-isoxanthopterin **166** was achieved using chlorotrimethylsilane.The amidine **167** was also obtained by treatment of (*E*)-**164** with Bredereck's reagent (*tert*-butoxy bis(dimethylamino)methane).[99] Synthesis of 4-amino-pteridines was also studied using the nitroso-ene reaction of amides derived from 2,4,6-triamino-5-nitrosopyrimidine, however due to a lower reactivity of the less electrophilic NO group, the reaction time was considerably longer.

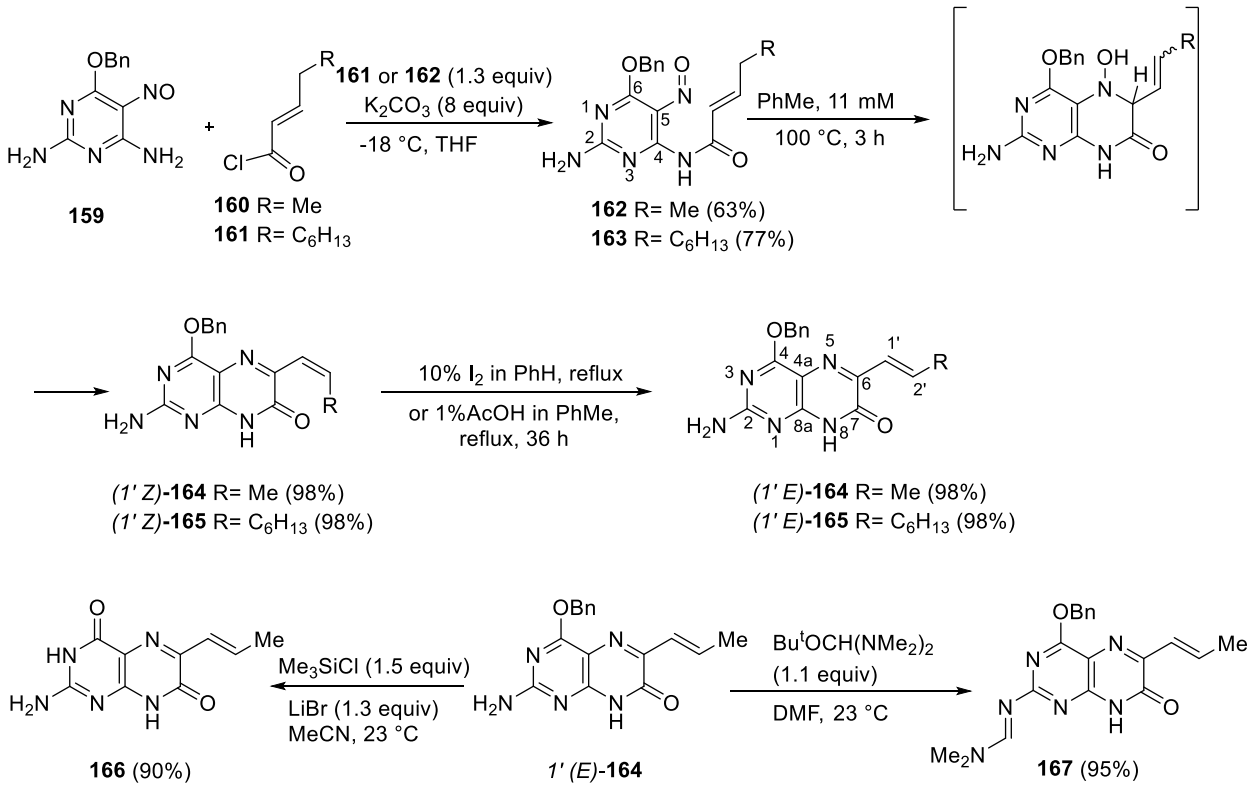

Scheme 37

2-Deoxo-2-phenylflavin-5-oxides **169** were synthesized as a new class of antitumor agents by nitrosative cyclization of 6-*N*-monoalkylanilino-2-phenylpyrimidin-4(3*H*)-ones **168** using an excess of sodium nitrite in acetic acid (Scheme 38).[100] Similarly, 2-deoxo-2-methylthioflavin-5-oxides were prepared by nitrosative cyclization of 6-(*N*-alkylanilino)-2-methylthiopyrimidin-4(3*H*)-ones and used as versatile intermediates, for the synthesis of various antitumor 2-alkylamino-2-deoxoflavin-5-oxides.[87]

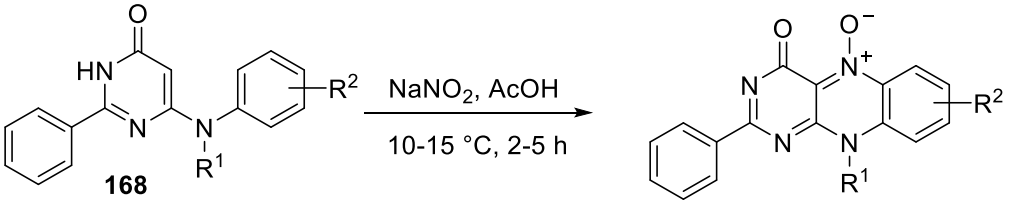

Scheme 38

A successful scaffold-hopping study afforded a novel series of pteridine analogues with variant 2-, 4- and 8-positions, as inhibitors of bacterial glutamate racemase (MurI, Scheme 39). The synthesis of the 2-position variants was carried out with reaction of 2-thio-4,6-diamino pyrimidine **170** with an alkyl bromide under basic conditions to give the 2-alkylthio-4,6-diamino pyrimidine **171**. Nitrosation of the pyrimidine ring via electrophilic aromatic substitution gave **172**, which was followed by hydrogenation of the nitroso moiety to give 2-alkylthio-4,5,6-

triamino pyrimidine **173**. Cyclization to the pteridinedione **174** used the classic Gabriel-Isay approach using ethyl chlorooxalate. Alkylation gave the 8-substituted analogues **175** using alkyl halide and triethyl amine. To prepare the 4-position analogues, 6-amino-4-hydroxy-2-thiopyrimidine **176** alkylated under basic conditions gave **177**. Introduction of the triflate at C-4 gave **178** by treatment with triflic anhydride, which provided a good leaving group for displacement with various amines. The same sequence of subsequent steps allowed construction of the pteridine scaffold **180** from **179**. (Scheme 39).[101]

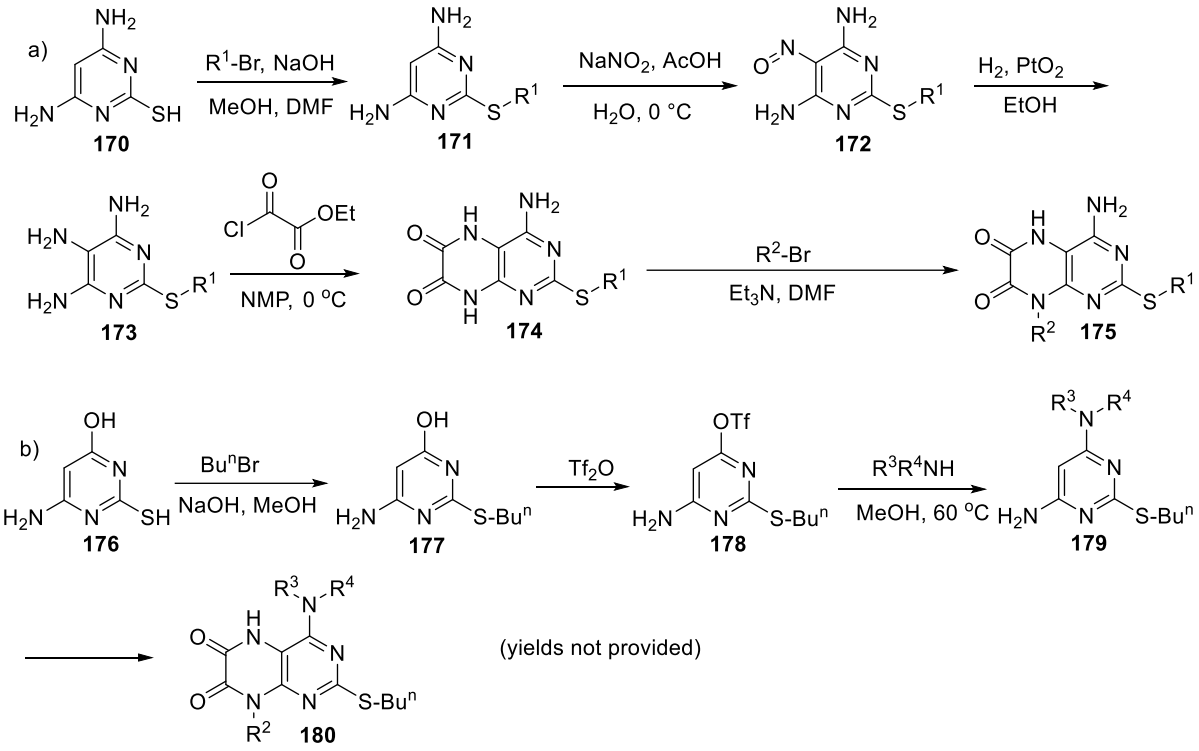

Scheme 39

6-Acetyl-1,3,7-trimethyllumazine **182** was synthesized as a proligand for transition metal complexes from 6-amino-1,3-dimethyl-5-nitrosouracil **181** in 2,4-pentanedione using standard Timmis conditions (Scheme 40). The 6-acetyl group on the pyrazine ring allowed for further condensation to obtain new multifunctional ligands containing the azomethinic C=N bond. In one example, the proligand **182** was reacted with thiosemicarbazide under reflux in absolute ethanol using acetic acid as catalyst to give the thiosemicarbazone-lumazine ligand **183**.[102]

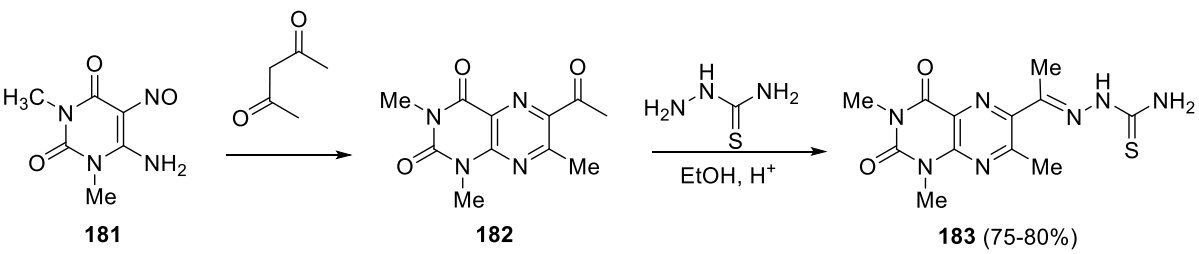

Scheme 40

The synthesis of 2-amino-4-arylamino and isopropylamino-6-arylpteridines was carried out by regioselective condensation of 2,5,6-triamino-4-arylamino and isopropylaminopyrimidine derivatives **188** with different substituted phenylglyoxal monoximes following the Viscontini method. (Scheme 41). *p*-Chloroaniline **184** was diazotized to **185**, followed by coupling with 2,6-diamino-4-chloropyrimidine to give **186** in 81% yield. The Cl-atom at C-4 on the pyrimidine ring is activated enough to undergo nucleophilic displacement by acyclic or aryl amines to provide **187**, which upon reduction with Zn powder gave **188**. Finally, condensation with monoximes resulted in the corresponding 2,4-diaminopteridine derivatives (Scheme 41).[103, 104]

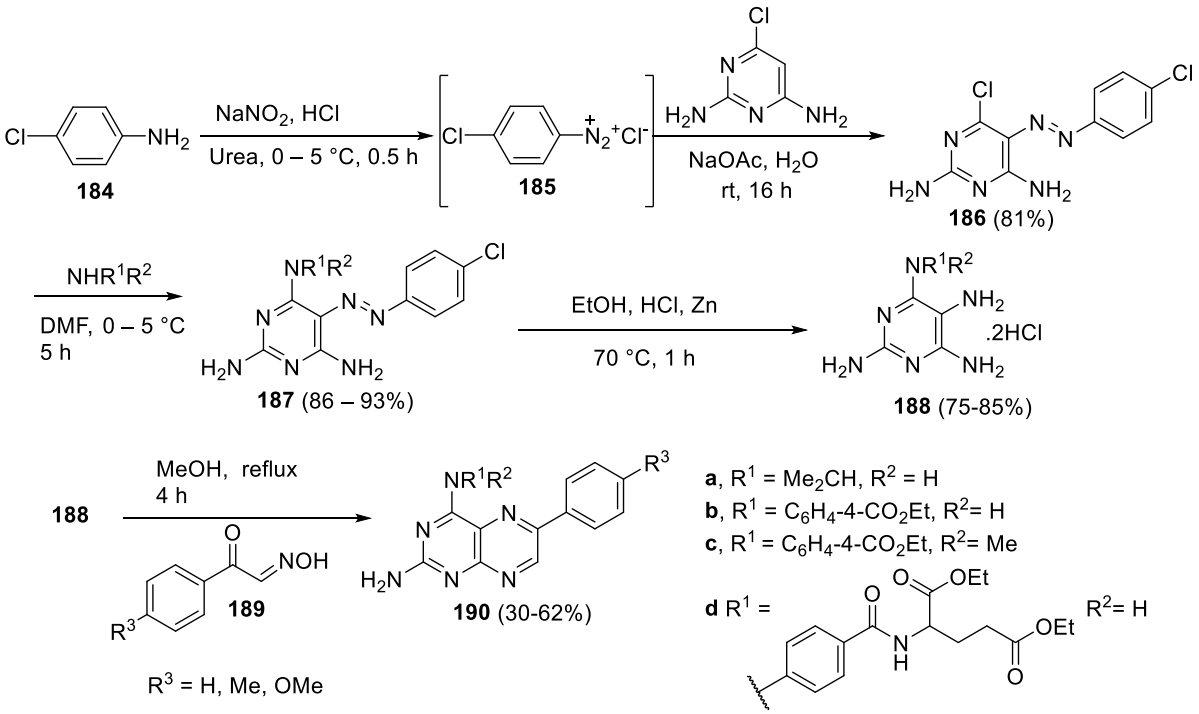

Scheme 41

A series of 2-amino-4-*N*-piperazinyl-6-(3,4-dimethoxyphenyl)pteridines **194** were prepared by introducing nitrogen nucleophiles at C-4 position of the pteridine scaffold (Scheme 42). 6-(3,4-Dimethoxyphenyl)pteridine **193** was built by a regioselective condensation reaction using Viscontini methodology between pyrimidine **191** and ketoaldoxime **192**. The piperazine moiety was introduced at position 4 in the pterin scaffold using a one-step silylation–amination approach affording the target 2-amino-4-*N*-piperazinyl-6-(3,4-dimethoxyphenyl)pteridine analogues **194**.[105]

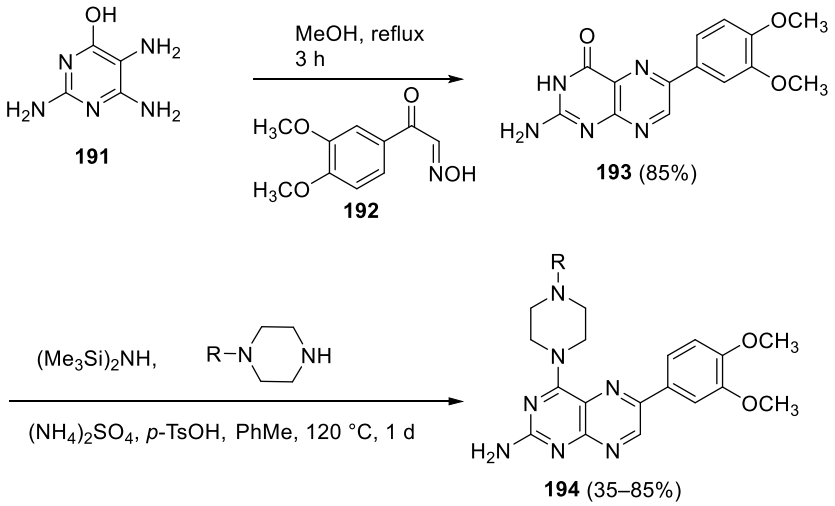

Scheme 42

Often the 4,6-dihydropteridinone scaffold is constructed in a two-step sequence from a 4-chloro-5-nitropyrimidine and an amino ester via S_NAr reaction between the aryl chloride and the amine followed by reduction of the nitro functionality and subsequent intramolecular cyclization. Sun and co-workers reported that both steps could be done in a single procedure by heating 4,6-dichloropyrimidine-2,5-diamine **195** with *N*-substituted glycine ethyl ester **196** in *n*-butanol with triethylamine as base, giving 4,6-dihydropteridinone **197** (Scheme 43).[106] Analogues of pteridines with 7-carbonyl, 6,7-dicarbonyl or no substitution at either 6- or 7-position were synthesized, as Hsp90 inhibitors. The Gabriel-Isay and related intramolecular cyclization strategies were deployed; reacting 4,6-dichloropyrimidine-2,5-diamine **195** and various amines and aminoesters respectively in the construction of the pteridines **197**.[107] Intramolecular cyclization of aminopyrimidines, after the reduction of a nitro functionality to amino was used to access analogues of pteridinone-based Toll-like receptor 7 agonists.[63]

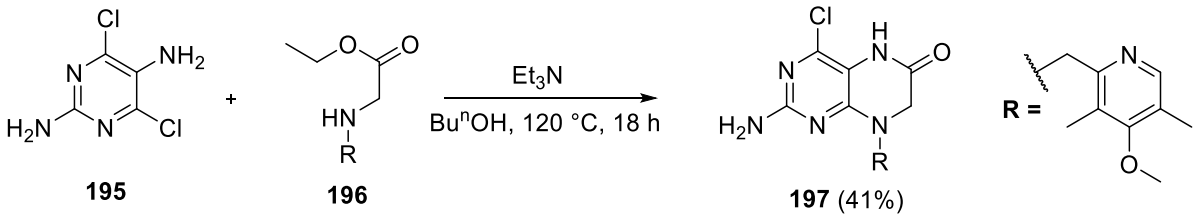

Scheme 43

The Gabriel-Isay methodology was employed in the synthesis of several pteridin-7(8*H*)-one derivatives, with a variety of potential medicinal chemistry applications, which are discussed in Section 10.18.10.8.[108-111] A novel 6,7-dioxo-6,7-dihydropteridine scaffold was also prepared by the Gabriel-Isay method, condensing 2,6-diaryl substituted 2,5,6-triaminopyrmidines with diethyl oxalate.[112] A new series of radical-scavenging, anti-inflammatory *N*-substituted 2,4-

diaminopteridines were prepared using the traditional Gabriel–Isay approach by condensing with glyoxal, butan-1,3-dione and benzil.[56]

Under microwave irradiation, rapid synthesis of 2-mercapto-6,7-disubstitutedpteridin-4-one derivatives **199** was performed without solvent in 12-22 minutes and the yield was high, 90-97%, compared to yields of 34-60% using conventional heating of **198** in acetic acid/sodium acetate for 3-5 hours (Scheme 44).[113]

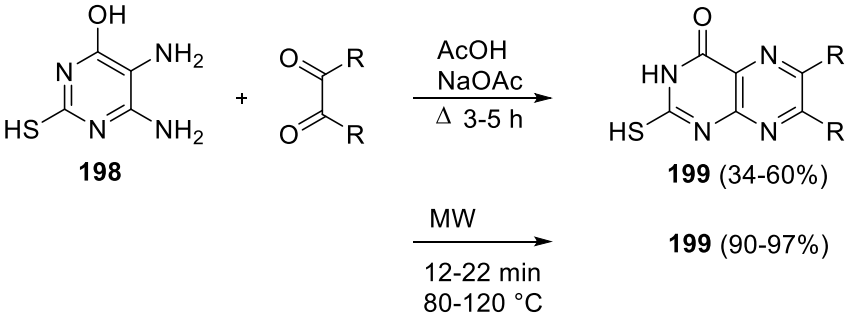

198

199 (34-60%)

199 (90-97%)

Scheme 44

Biosynthetic Intermediate **202** is cyclic pyranopterin monophosphate (cPMP), a molybdenum cofactor (MoCo, Scheme 45). The synthesis of **202** employed the Viscontini reaction of 2,5,6-triamino-3,4-dihydropyrimidin-4-one dihydrochloride **152** with D-galactose phenylhydrazone **201**, which is in equilibrium with tautomer **200**.[114] Any ambiguity in the structure of compound **202** (not **203**) was resolved by X-ray crystallography, which confirmed relative and absolute stereochemistry. Compound **202** gave cyclic pyranopterin monophosphate over four steps.

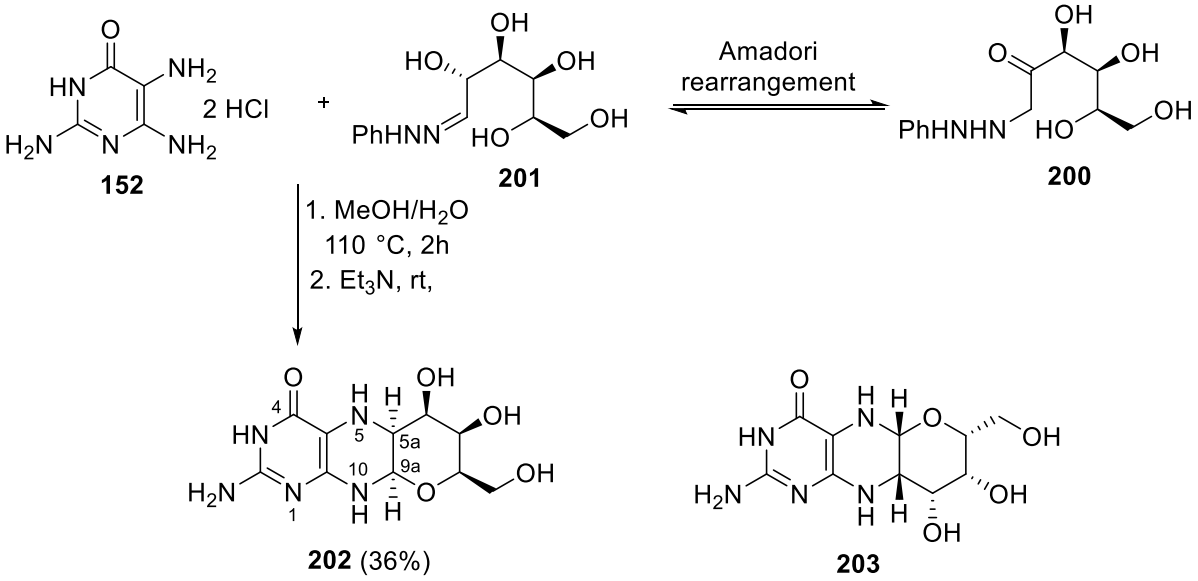

152

201

200

202 (36%)

203

Scheme 45

A series of fluorescing 8-(6-hydroxyhexyl)isoalloxazine derivatives was constructed from **204** by nucleophilic chloride displacement and reaction of 6-[(6-hydroxyhexyl)amino]uracil **205** with 1-chloro-4-nitrosobenzene to afford 8-chloro-10-(6-hydroxyhexyl)isoalloxazine, which could be substituted by a range of amines to furnish **206** (Scheme 46). Applying the same synthetic method, 8-substituted 10-{3-[(2,2-dimethyl-1,3-dioxolan-4-yl)methoxy]propyl}isoalloxazines **207** were built which in turn, over 3 steps, were transformed into the corresponding 2'-(2-cyanoethyl *N,N*-diisopropylphosphoramidites) **208** as building blocks for the synthesis of oligonucleotides.[115]

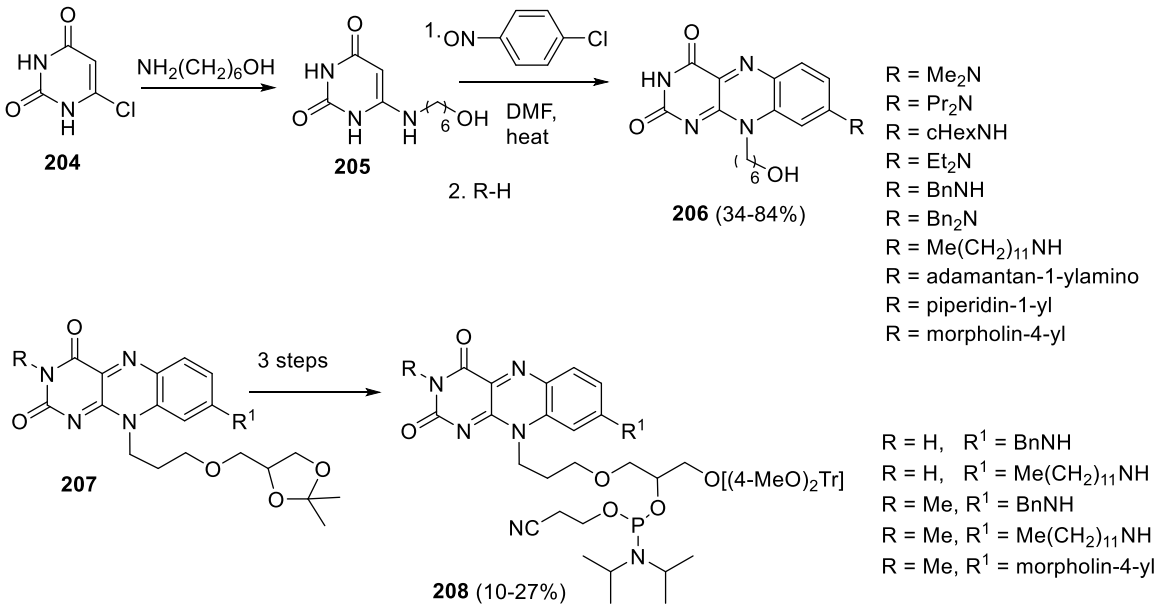

Scheme 46

The first synthesis of naturally occurring isoxanthopterin glycoside, asperopterin A **215** involved key intermediate **211** prepared by direct condensation of **209** with **210** (Scheme 47). Glycosylation of **212** with 1-*O*-acetyl-2,3,5-tri-*O*-benzoyl-β-D-ribofuranose **213** using tin(IV) chloride gave the corresponding β-D-ribofuranoside **214**, which was deprotected to afford **215**.[116]

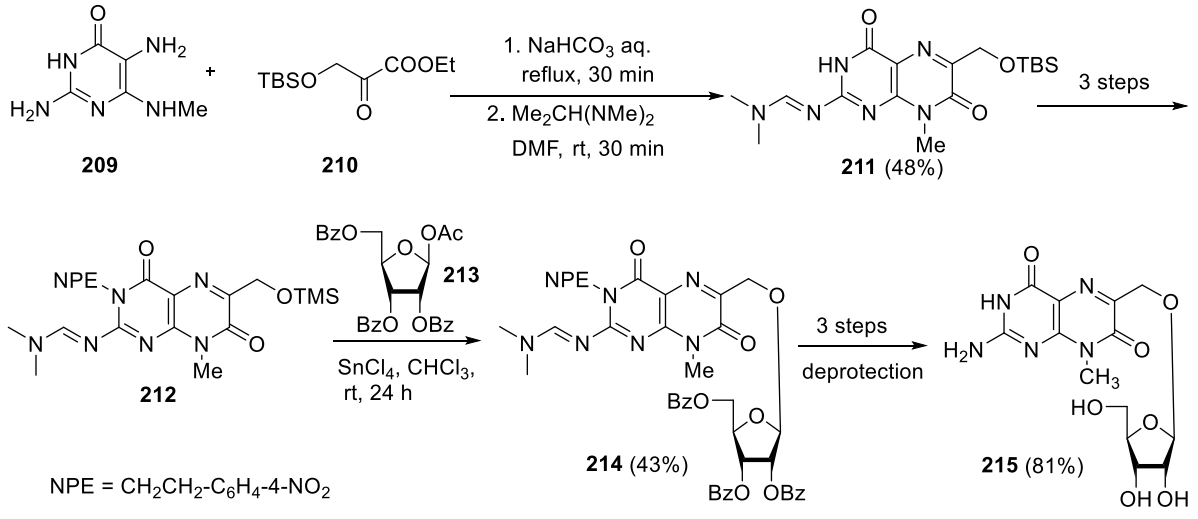

Scheme 47

A diamagnetic synthon, 1-methoxy-2,2,5,5-tetramethylpyrrolidine-3,4-dione **216** was prepared over two steps, which was condensed with 5,6-diaminopyrimidine and 5,6-diaminouracil and the adducts **217** and **219** *O*-deprotected to give the paramagnetic pteridines **218** and **220** (spin-labeled lumazine) respectively (Scheme 48).[117]

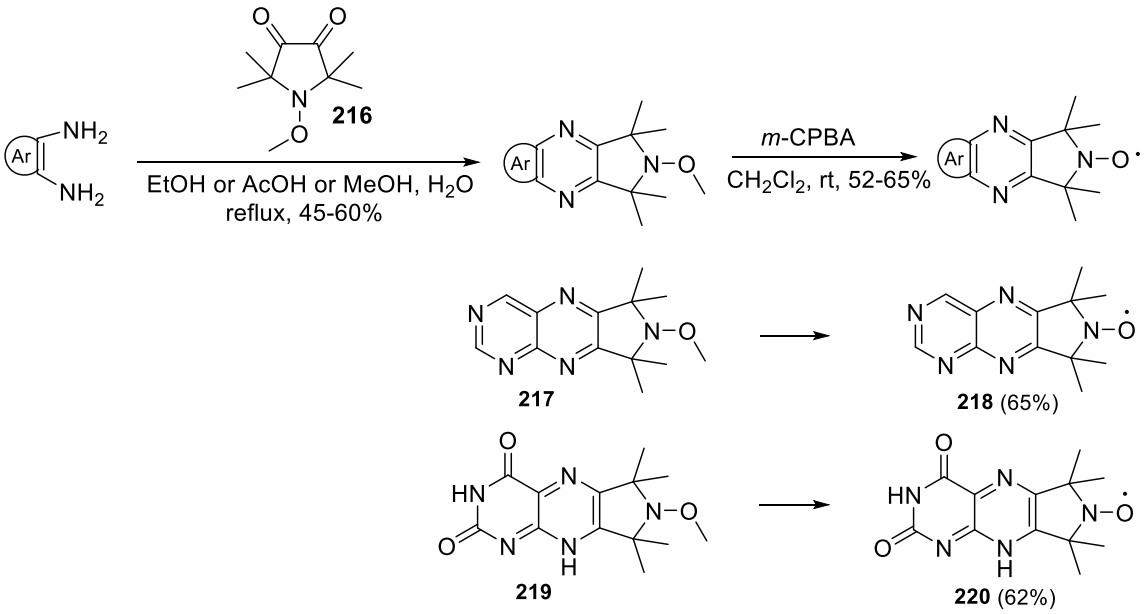

Scheme 48

Synthesis of 6,7-diaryl-2-thioxopteridine-4-one **221a-221b** and 6,7-diaryl-2-thioxo-7,8-dihydropteridine-4-one **222a-222b** scaffolds is reported by reaction of 4,5-diamino-6-hydroxy-2-mercaptopyrimidine with 2 equivalents of aromatic aldehydes (Scheme 49).[62]

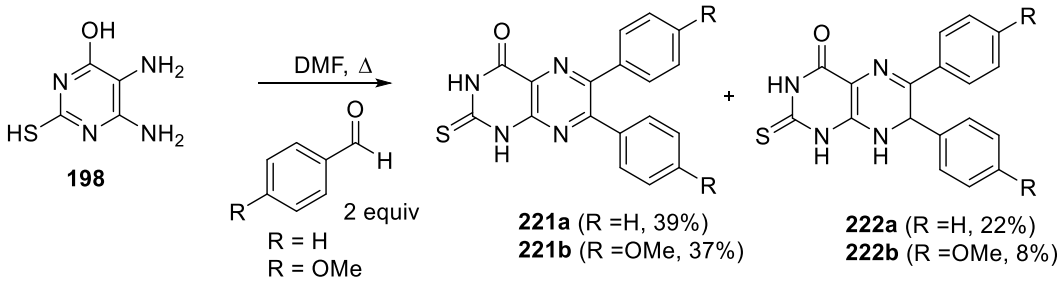

Scheme 49

The 2-amino-7,8-dihydropteridin-6(5*H*)-ones **227** were synthesized from 2,4-dichloro-5-nitropyrimidine **223** and hydrochloride **224** via the Polonovsky-Boon ring-closing strategy to give **225** (Scheme 50). The key intermediate 2,4-disubstituted aminopyrimidine derivatives **226** was prepared in two-step via nucleophilic substitution reaction at C-4 and C-2 of the pyrimidine ring. Reduction of the nitro group of **226** using iron and glacial acetic acid led to an *in situ* intramolecular cyclization affording the target **227** in yields ranging from 60% to 94%.[118]

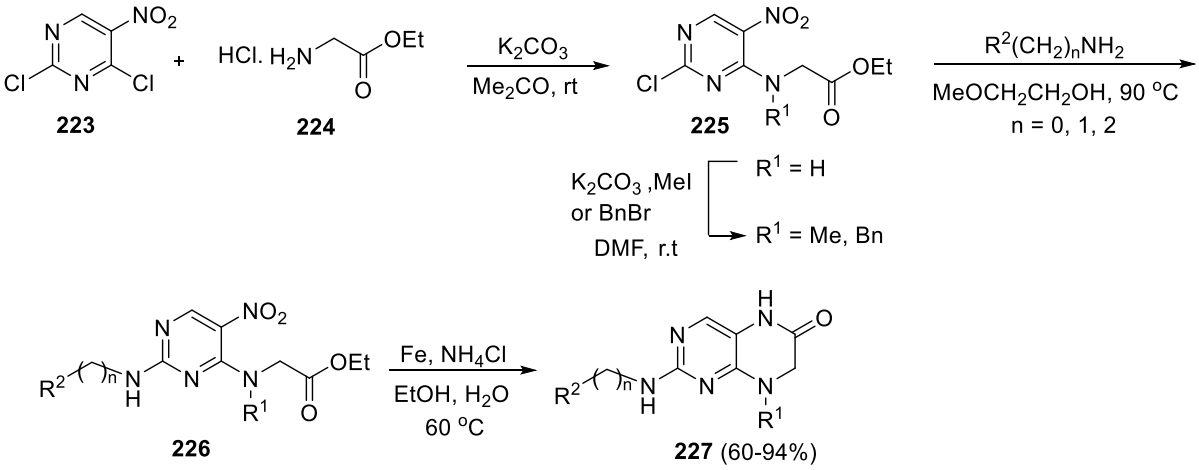

Scheme 50

The same Polonovsky-Boon ring-closing strategy was applied to give the 7,8-dihydropteridin-6(5*H*)-one scaffold for the synthesis of isoform selective Polo-like kinase-2 inhibitors[119], bifunctional Polo-like kinase 1 inhibitors[120] and BRD4 inhibitors.[121]

Routes to substituted pteridine trione/dione scaffolds were reported using the alkylation of pyrimidine **228** with isobutyl iodide giving an inseparable 5:1 mixture of *N*- and *O*-alkylated products (Scheme 51). After nitration, the *N*-alkyl regioisomer **229** separated in 75% yield using column chromatography. Reaction of **229** with protected naphthylalanine **230** under basic conditions afforded **231** in 67% yield. Reduction of the nitro group followed by cyclization gave an intermediate lactam that readily aromatized in the presence of DDQ (2,3-dichloro-5,6-dicyano-1,4-benzoquinone) giving pteridine 2,4,6-trione **232** in good yield. This was further functionalized via *N*-alkylation or by conversion to the 6-triflate, which enabled diversification at position 6 (as described in Section 10.18.7.7).[73]

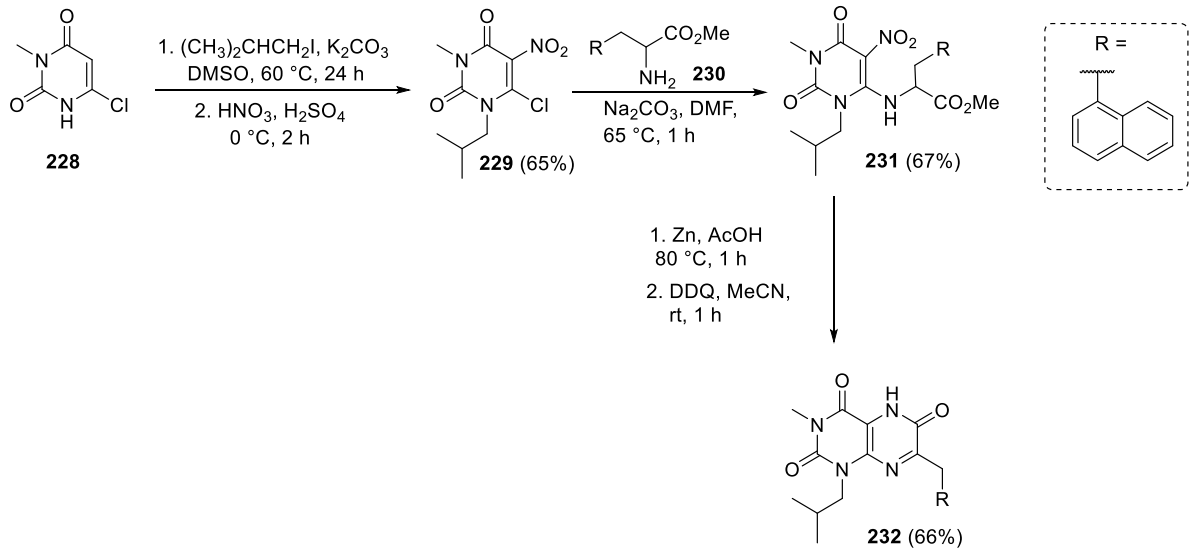

Scheme 51

Often, semi-synthetic or biological techniques are used to obtain homochiral pteridines. A totally synthetic methodology allows diversity for molecules containing the stereochemistry of natural coenzymes at C-6, using amine **233** derived from (2*S*)-malic acid (Scheme 52). The benzyl derivative was reacted with 2-amino-6-chloro-5-nitro-4-(3*H*)-pyrimidinone **235** to give pyrimidine **236**, which was treated with triflic anhydride and pyridine to give the triflate intermediate, which was hydrogenated to give the tetrahydropteridine **237** in good yield. Product **237** has a tendency to oxidize, and was treated with freshly prepared formic acetic anhydride to give the desired protected homochiral tetrahydropteridine **238**. Using methoxymethylene protection, the triformyltetrahydropteridine **239** was obtained, which exists as the 4-phenol tautomer instead of the usual 3,4-amide (Scheme 52).[122]

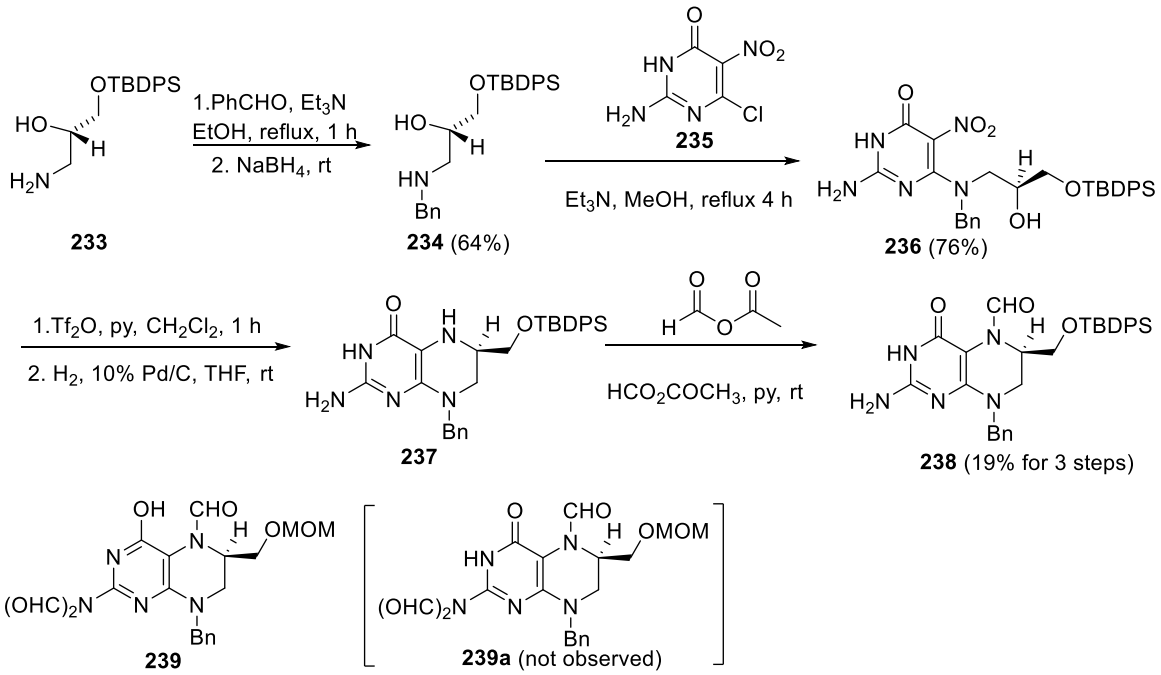

233 234 (64%) 236 (76%) 237 238 (19% for 3 steps) 239 239a (not observed)

Scheme 52

An optimal and broadly applicable method for construction of chiral 4,6-dihydropteridinones **242** was developed by applying the design of experiments (DoE) analysis for a S_NAr-amidation cyclization between 4-chloropyrimidin-5-amine **240** and (*S*)-*N*-methylalanine **241** (Scheme 53). Using DoE, five quantitative reaction variables were optimized, such as solvent, temperature, time, concentration, equivalents of amino acid and base. Optimized conditions maximized conversion and optical purity and gave a significant reduction in reaction time. The substrate scope was expanded to cover a diverse range of amino acids and variety of pyrimidines.[123]

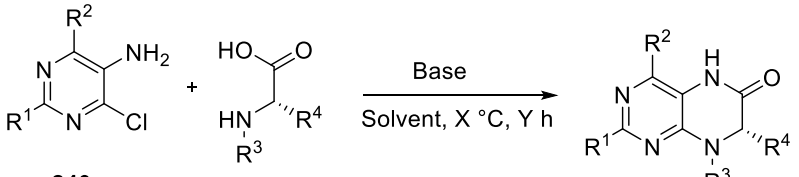

Defined parameters by DoE study:
Solvent : DMSO
Temp: 80-120 °C
Time : 3-22 h
Conc : 0.1-1 M
equiv. of amino acid : 1.5-2
equiv. of $NaHCO_3$: 1.1-3

Scheme 53

(*R*)-2-Chloro-7-ethyl-8-isopropyl-7,8-dihydropteridin-6(5H)-one **245** was a key intermediate for a new series of 5,6-dihydroimidazolo[1,5-*f*]pteridines. Methyl ester **243** was obtained in high yield by esterification of (*R*)-2-aminobutanoic acid followed by a reductive alkylation of the amine moiety with acetone. Reaction with 2,4-dichloro-5-nitropyrimidine **223** furnished the intermediate **244**, which was hydrogenated under carefully controlled conditions to avoid side reactions. The intramolecular cyclization afforded **245** in 78% yield (Scheme 54).[124] The chiral 7-ethyl-substituted dihydropteridin-6(7*H*)one **245** is the core for a number of pteridine

analogues based upon the Polo-like kinase inhibitor BI 2536.[71, 125] This compound and the diverse series of related scaffolds are discussed in more detail in Section 10.18.10.8.

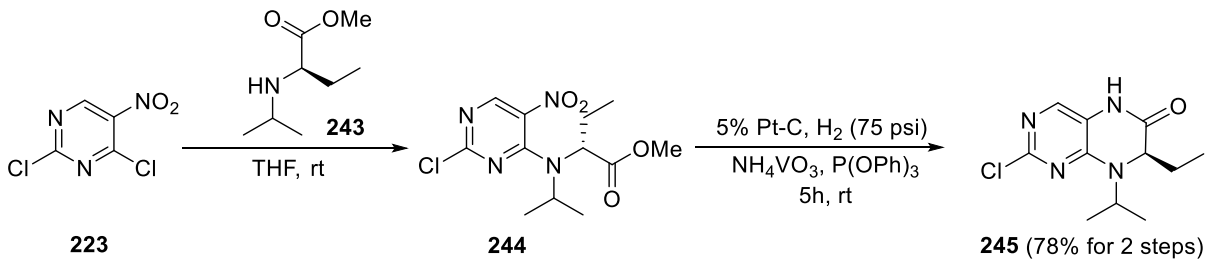

Scheme 54

The synthesis of 7-(benzimidazol-2-yl)pteridin-4(1*H*)-ones **247** was based on the acid-catalyzed rearrangement of quinoxalin-2-one **246**, when exposed to 4,5-diamino-6-hydroxy-2-mercapto- and 2,4,5-triamino-6-oxypyrimidines **152** and **198** in *n*-butanol (Scheme 55).[126] 7-(Benzimidazol-2-yl)-6-(2-fluorophenyl)-2-thioxo-2,3-dihydropteridin-4(1*H*)-one analogues of **247** go through intramolecular nucleophilic substitution of fluorine by the nitrogen of the benzimidazole fragment to give benzo[4′,5′]imidazo[1′,2′:1,2]quinolino[4,3-*g*]pteridine2,4(1*H*,3*H*)-diones **248**.[126]

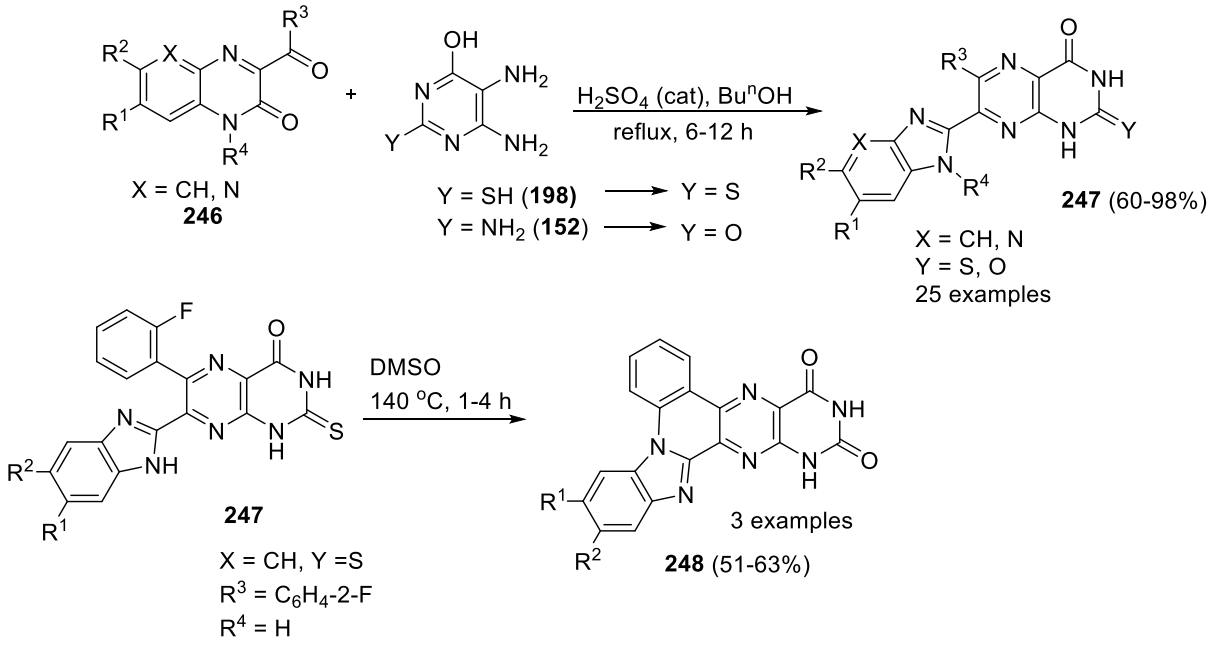

Scheme 55

10.18.9.2 Ring Syntheses from Pyrazines

5,8-Dichloro-2,3-dicyanoquinoxaline **251** was synthesized from tetrachlorocyclohexanedione **249** and diaminomaleonitrile **250** (Scheme 56). Compound **251** behaved as a dielectrophile towards dinucleophile, benzamidine .[127]

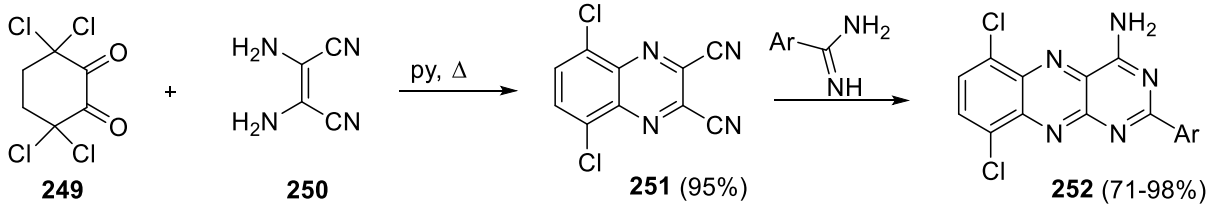

Scheme 56.

Synthesis of the 2-arylpteridines **257** as hepatitis C virus (HCV) inhibitors from 3-amino-pyrazine-2-carboxylic acid ethyl ester **253** involved the initial formation of the diacylated derivatives **254**, as the major products (Scheme 57). Esters **254** reacted with ammonia in refluxing ethanol to afford monoacetylated amides **255**, which underwent cyclization in presence of NaOH producing the corresponding pteridinones **256**. Treatment with benzotriazole-1-yloxy-tris-pyrrolidino-phosphonium hexafluorophosphate (PyBOP) formed a very reactive *O*-benzotriazole iminoether intermediate, and treatment with the appropriate aromatic aminestr gave the final 4-arylamino-substituted products **257**.[128]

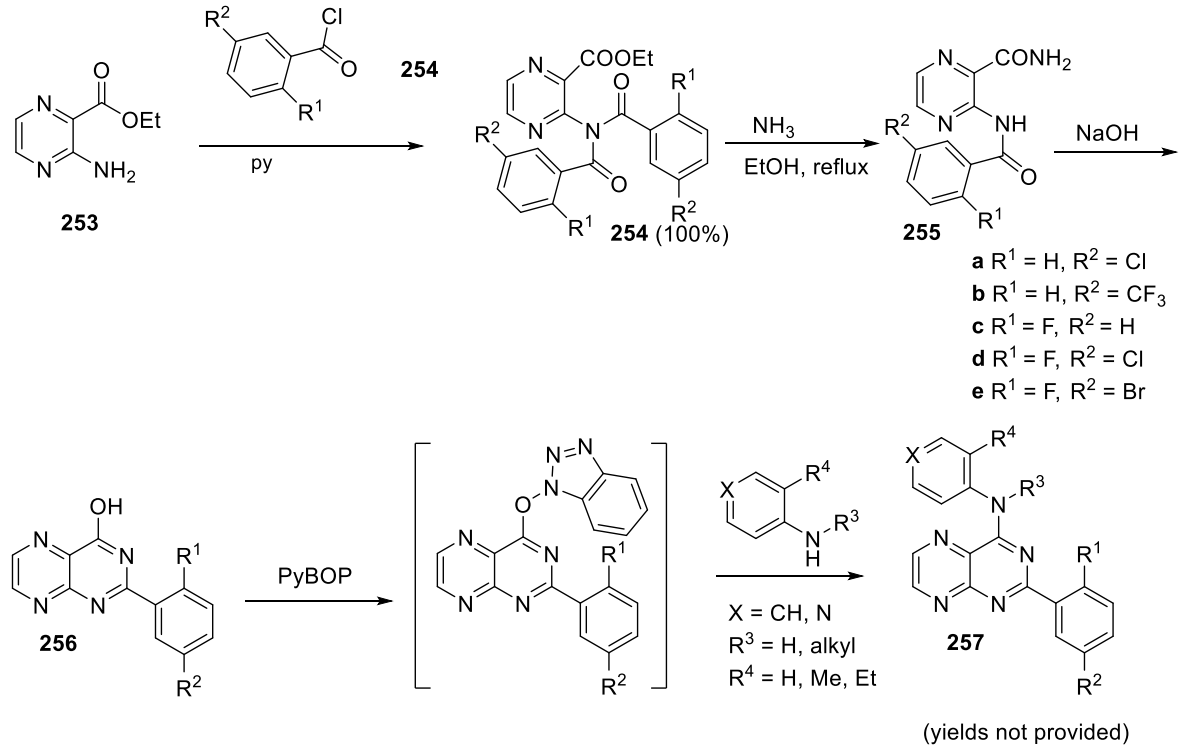

Scheme 57

The molybdopterin/molybdenum cofactor oxidation product *rac*-dephospho Form A **264** was synthesized by a novel approach (Scheme 58). The bicycle assembly occurs after the installation of the C6 side chain with selective iodination of methyl 3-aminopyrazine-2-carboxylate (**258**) at C-6 using *N*-iodosuccinimide (NIS) affording **259**. The alkynyl moiety at C-6 was introduced under Sonogashira conditions using alkyne **260** giving 6-alkynyl-3-aminopyrazine **261**, which was converted to pterin over two steps by treatment with excess ethoxycarbonylisothiocyanate to give the thioureido intermediate **262** followed by cyclization to **263** using hexamethyldisilazane/EDCI. Eventually, alkynylated pterin **263** was converted to the rac-dephospho Form A, *rac*-**264** over three steps.[129]

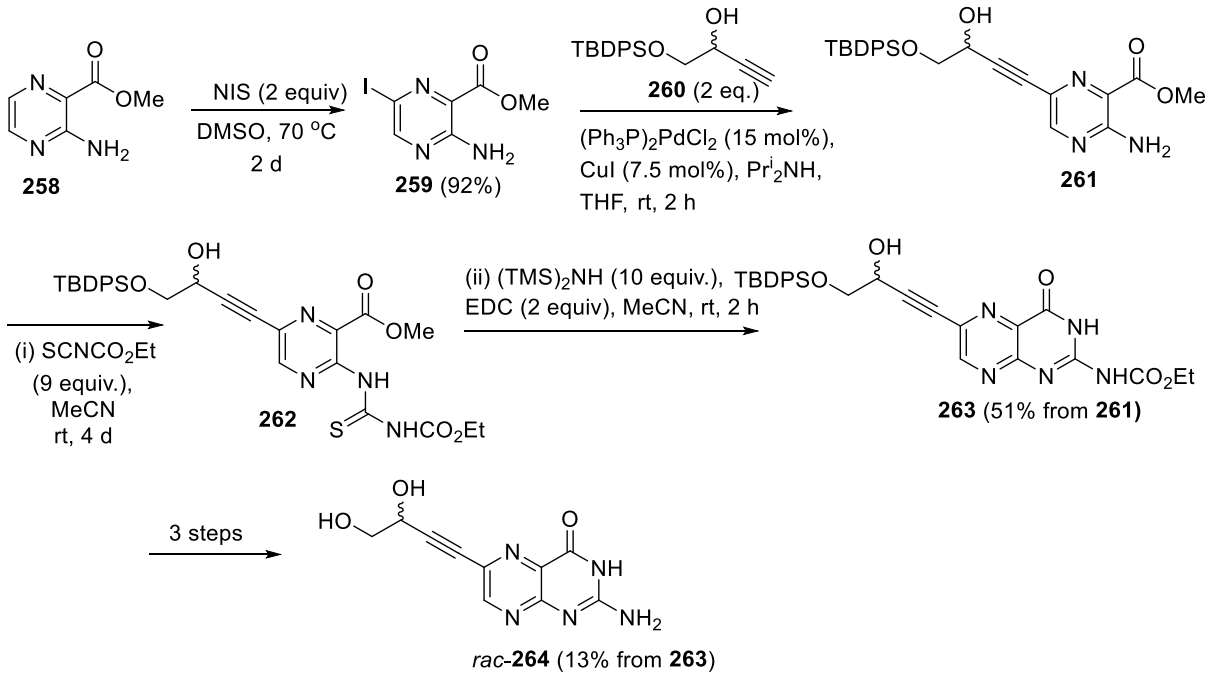

Scheme 58

10.18.9.3 Ring Syntheses by Transformation of Other Rings

Other than the previously described synthesis employing a 5,6-diaminopyrimidine and a rearranged quinoxalin-2-one as the dicarbonyl moiety to construct the pyrazine ring,[126] there are no further reported examples.

10.18.10 Important Compounds and Applications

10.18.10.1 Synthesis of Special Classes of Pteridines

The naturally occurring pterins have continued to be of interest synthetically. A critical review on synthesis of biopterin **43** and related pterin glycosides is available (Figure 4). The syntheses of natural pterin glycosides are commonly achieved through appropriately protected *N*^{2}-(*N*,*N*-dimethylaminomethylene)-3-[2-(4-nitrophenyl)ethyl]pterin derivatives as glycosyl acceptors.[130] Synthesis of tetrahydrobiopterin **45** analogues is also recently reported.[131]

The synthesis of cyclic pyranopterin monophosphate cPMP **270** (Scheme 59), a key intermediate in molybdenum cofactor (MoCo) biosynthesis involved multiple *N*-Boc-protection of the tricyclic Viscontini reaction product **202** giving **265** and **266**. Cyclic phosphorylation of deprotected **267** to **268** and a Swern secondary alcohol oxidation to **269**, followed by immediate deprotection of the two remaining Boc-groups *in situ* gave the HBr salt of cPMP **270**. [114]

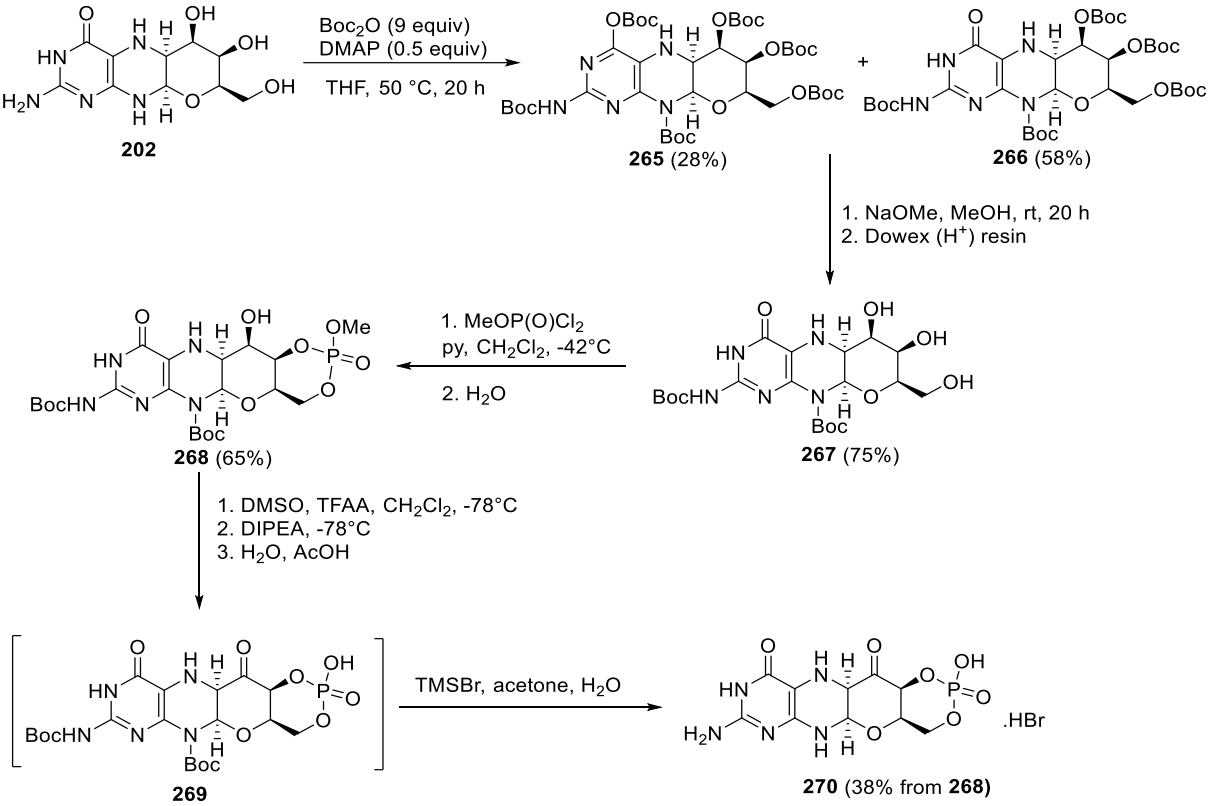

Scheme 59

The molybdenum cofactor **271** coordinates molybdenum through dithiolene ligands and there has been much interest in elucidating binding and mechnisms of action. A number of ligands have been prepared to synthesize model compexes, including alkynyl[132] and pyranopterin-dithiolene complexes,[133] as discussed in sections 10.18.10.3 and 10.18.10.6.

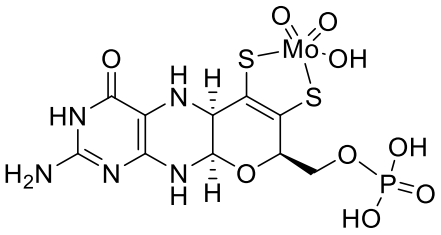

271 MoCo

<Figure 7>

A traditional use of pteridines in medicine has been as antifolates, to inhibit folate-dependent pathways, often in oncology, inflammatory disease and anti-infective applications. A route to *p*-aminophenyl-*H*-phosphinic acids, e.g. **274**, as potential antifolates involves displacement of bromide from **272** by methylamine **273** (Scheme 60). The phosphinic acid acts as a mimic for the tetrahedral phosphorylated intermediate **276** in the biosynthesis of dihydrofolate **49** by dihydrofolate synthase (DHF), *via* phosphorylation of dihydropteroate (DHP) **275** and coupling with L-glutamate.[134]

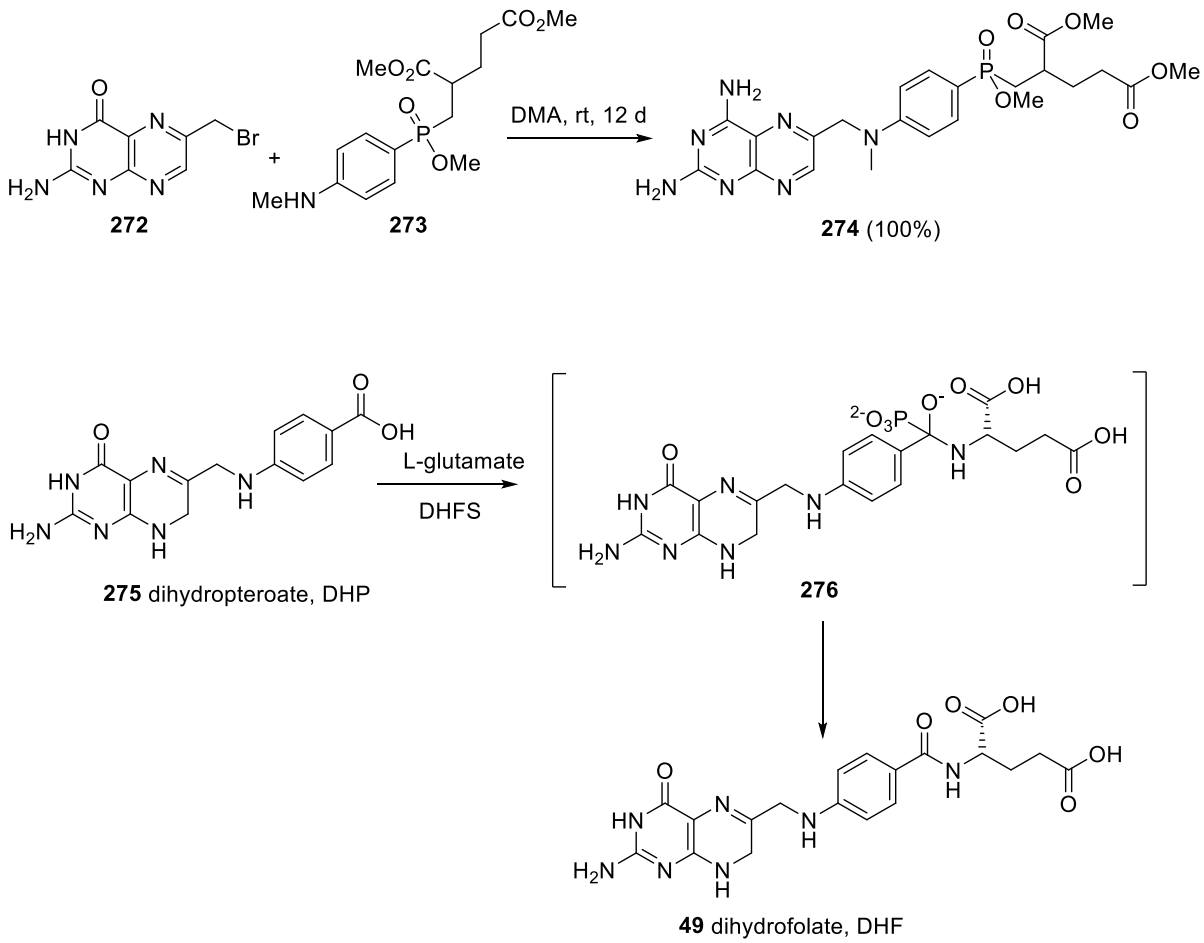

272 **273** **274** (100%)

275 dihydropteroate, DHP **276**

49 dihydrofolate, DHF

Scheme 60

10.18.10.2 Photochemistry and associated redox activity

The photochemistry of pteridines has continued to be of great interest, particularly in terms of the effects of natural pteridines *in vivo*. Their photochemical properties have led to their use as photosensitizers for a variety of biological applications. There is also much interest in applications of their fluorescence in biology, particularly as nucleic acid analogues, see Section 10.18.10.4, and in optoelectronics. Some recent developments in elucidating mechanisms and applications are summarized below.

A quantitative structure-property relationship (QSPR) study was applied to the singlet oxygen generation by pteridines, in order to predict photosensitizing properties. Quantum yield, Φ_{Δ}, correlates with HOMO energy, so this was used to generate an electronegativity descriptor. A functional model was generated, using a range of descriptors. The best model was based on descriptors of electronegativity, electrostatic charge on N3 and dipole density.

$\log\Phi_{\Delta}$ = -13:958 - 4:659*Electrostatic N3 + 2:371*Electronegativity - 6:571* Dipole density

Where Electronegativity = – (*E* HOMO - *E* LUMO)/2

This model could predict the quantum yield of a range of pterin and flavin photosensitizers (pred R^2 = 0.873).[135]

Photo-oxidation of folate sensitized by diffusion-controlled singlet or the slower triplet state excited riboflavin involved electron-transfer to the pterin.[136] Lumazine **3** used as a photosensitizer caused decomposition of deoxyguanosine monophosphate (dGMP) inducing death of HeLa cells,[45] and oxidation of deoxyadenosine monophosphate (dAMP).[137] Iodide deactivated the triplet excited states of **3** and pterin **2** via a non-radiative $T_1 \rightarrow S_0$ transition.[138] The stability and volatility of lumazine **3** at the absorption maximum of 350 nm makes it useful as a MALDI matrix for complex phospholipid analytes.[139] The interactions and differing photophysical properties of the cofactor 6,7-dimethyl-8-ribityllumazine and riboflavin in complexes with the lumazine protein of a bacterial species (*Photobacterium leiognathi*) were compared by spectroscopic characterization.[140] The photostability and photoexcitation properties of pyrene-flavin and phenothiazine-flavin dyads were characterized *via* absorption and fluorescence spectroscopy.[141, 142] Photodynamics of roseoflavin and riboflavin have been measured in aqueous and organic solvents. Roseoflavin shows a bi-exponential fluorescence decay from an initial fast electron transfer from the dimethylamino group to the pteridine carbonyl, followed by a slower intramolecular process.[143]

A series of decyl-chain pterin conjugates showed decreased fluorescence and increased singlet oxygen quantum yield.[144] The *O*-decylpterin was used for intercalation with and photo-oxidation of unilamellar vesicles, as a model for cell membrane damage by UVA-mediated singlet oxygen oxidation processes.[145] Peroxide oxidation of folic acid **8** leads to a strongly fluorescent product with the potential to use for reactive oxygen species (ROS) detection.[146] The photosensitized decomposition of both folic acid and methotrexate in D_2O leads to a strongly fluorescent product, offering a fluorimetric method for determination of quantum yield (Φ_Δ) of water-soluble photosensitizers, with potential applications in photodynamic therapy.[147] 5-Methyltetrahydrofolate acts as a scavenger of singlet oxygen, thereby inhibiting UVA/UVB photosensitization-induced DNA strand breaks.[148] Pteridine-2,4-dione acceptor units have been incorporated into oligothiophenes with potential optoelectronic applications.[149] Neutral and cationic riboflavin exhibit different optoelectronic performance, with the latter giving higher fluorescence quantum yields.[150] A triamterene grafted graphitic carbon nitride photocatalyst was reported.[151]

6,7-Diphenyl-2-morpholinylpterin (DMPT, **277**) and 6-thienyllumazine (TLM, **278**) were synthesized and were amongst a number of pteridine derivatives modelled as fluorescence-based pH sensors for use in physiological pH ranges. DMPT gives an emission signal from blue to cyan at pH values close to its pK_a of 7.2. These sensors can be pH-tuned and have potential for measurement of pH in living cells.[152]

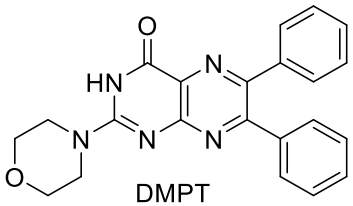

DMPT

277

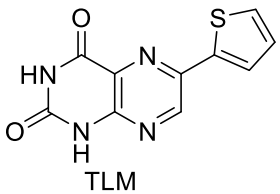

TLM

278

<Figure 8>

A disposable solid state pH sensor based upon a polymeric flavin analogue 10-(4-hydroxyphenyl) benzo[g]pteridine-2,4(3*H*,10*H*)-dione **279-280** probed both with and without ferrocyanide as internal standard.[153]

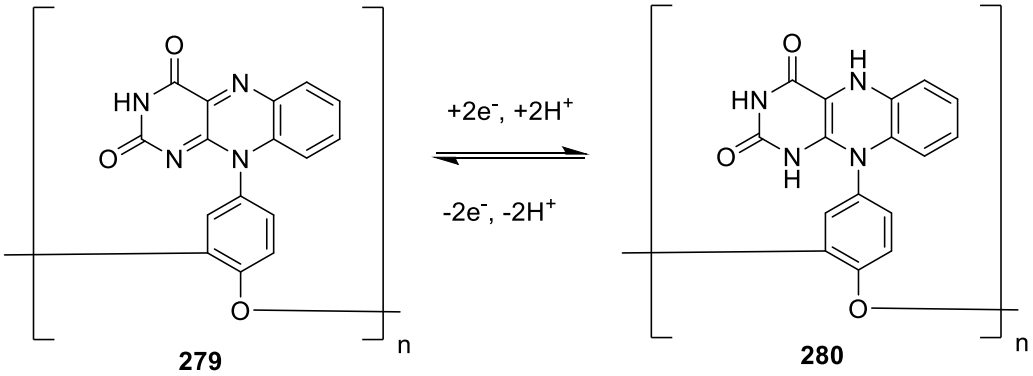

279 **280**

<Figure 9>

Pteridine redox centers inspired by natural redox activity of flavins, alloxazines and lumazines were developed for use in lithium and sodium rechargeable batteries. The pteridine electrodes demonstrated reversible alloxazine–isoalloxazine tautomerism and high capacity.[154]

10.18.10.3 Metal Complexes

Pteridines can complex through a nitrogen, often the pyrazine N5, whereas pteridine-4(3*H*)-ones offer a second binding site at O4. Often pterin ligand substitution confers greater stability. A new water soluble Re^{I} complex was synthesized containing an unsubstituted pterin ligand, $Re(CO)_3(pterin)(H_2O)$.[155] ^1H NMR and FTIR spectroscopy provided evidence for the coordination of the pterin ligand via the O4 and N5 atoms. The binding mode of pterin was confirmed by X-ray diffraction, which also illustrated facial conformation of three carbonyl ligands in the complex. The water molecule in the complex completes the octahedral coordination of the central metal atom. Strong H-bonds between the 2-amino functionality and crystallization water molecules results in a polymeric arrangement of $Re(CO)_3$ -(pterin)(H_2O) complexes in the network with stability across the entire pH range studied.

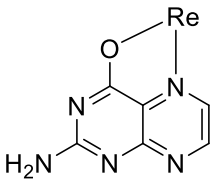

281

<Figure 10>

This complex and related rhenium(I)-pterin complexes have been extensively studied for protein association, photochemical, photophysical and redox properties.[156-158]

Synthesis and characterization of neutral mixed P/S-donor two-coordinate Au^{I} complexes containing a thiol-derived pteridine ligand and a tertiary phosphane as supporting ligand is exemplified by corresponding complexes prepared from the treatment of pteridine with a suitable [ClAu(PR'_3)] precursor (PR_3 = PPh_3 or PCy_3) to form the desired Au^{I} agents, [(L)Au(PR'_3)] (L = pteridine). The reactions at room temperature in the absence of light resulted in Au^{I} complexes characterized using variety of spectroscopic methods. The crystal structure shows a dimeric complex through an Au-Au interaction. Interestingly, the obtained complexes are soluble in a broad range of solvents and contain luminescence originating from ligand-centered excited states.[159]

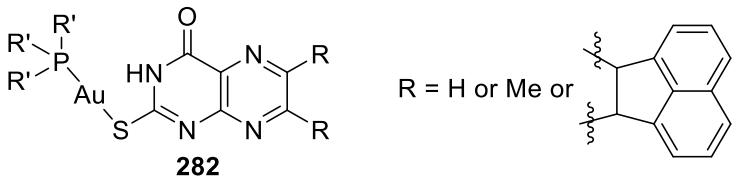

282

<Figure 11>

A multinuclear ferrocenylcopper(I) complex with 2-pivaloylpterin coordinated through all four nitrogen atoms and O4, as well as a pivaloyl oxygen.[160] A novel tetranuclear iridium(III) complex, $[Ir_4(Allo)(Cp^*)_4(Hallo)_2Cl_2](PF_6)_2$ **283**, was prepared from the mononuclear complex **144** with the use of a flavin analogue, alloxazine, as a bridging ligand. This complex consists of unusual coordination modes of alloxazine (coordinating through N1/N3) to connect the Ir(III) centers to form a U-shaped structure with a pocket for enclosing a counter-anion. Alloxazine ligands have the ability to form a closed π-space via intermolecular H-bonding and exchangeable anions confined in the supramolecular cage could be exchanged via self-reorganization.[89]

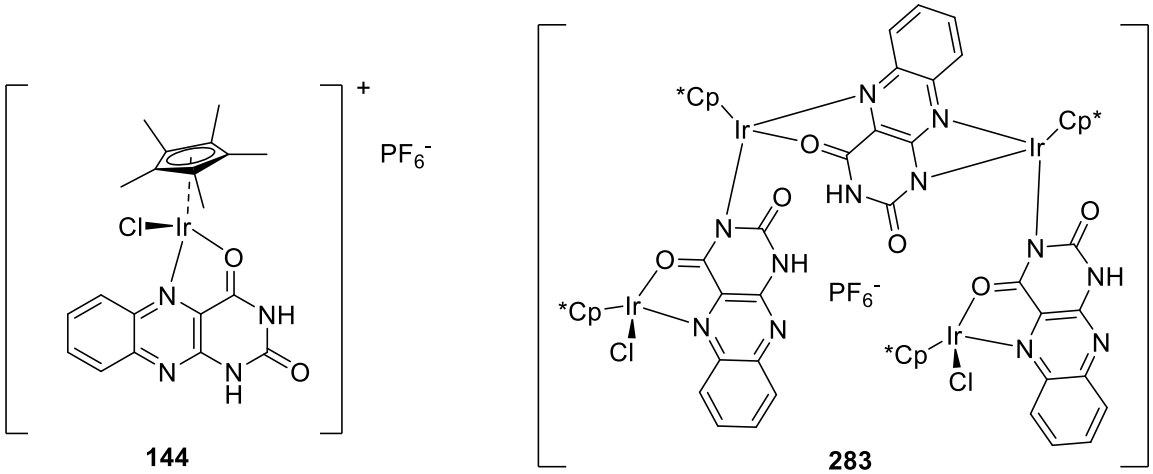

144 **283**

<Figure 12>

The effects of silver (I) complexes of 6-hydroxylumazine on the activity of aminopeptidases A and N (renin-angiotensin system regulators) in neuroblastoma and glioma cell lines are reported.[161] A methotrexate-copper (II) complex wth DNA-cleaving properties has been

characterized. The copper coordinates to the amide and carboxylate groups of the glutamate moiety, with no involvement of the pterin ring.[162]

Complexes using lumazine-based ligands and their condensation products have been studied, including a five-coordinated bis-(triphenylphosphine) copper(I) complex of 6-acetyl-1,3,7-trimethyl-pteridine-2,4(1H,3H)-dione (6 acetyl-1,3,7-trimethyllumazine) **182**. The copper is coordinated to two phosphorus atoms and a nitrogen of the pyrazine, with further semi-coordination of two O atoms (O4 and acetyl) at 2.48 Å.[163]

Condensation of hydrazinyl derivatives with the 6-acetyl group has led to a series of azomethine derivatives. Metal complexes of Mn(II), Co(II), Cd(II), Hg(II), Ag(I), Rh(III), and Ir(I) with a ligand **284**, BZLMH, the benzoylhydrazone of 6-acetyl-1,3,7-trimethyllumazine, are described. The structures of these complexes showed that the ligand is coordinated to the metals in tridentate form via N5, N61 and O63 or tetradentate form through O4, N5, N61 and O63 atoms. Molecular structures of Co(II) and Rh(III) complexes were resolved by single crystal X-ray diffraction, which confirmed the two aforementioned coordination modes.[88] The ligand's novel coordination behavior with Ni(II), Zn(II) and Hg(II) was further studied using luminescence and theoretical calculations.[164]

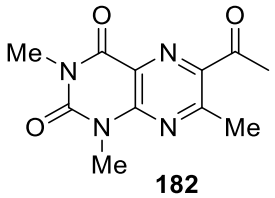

182

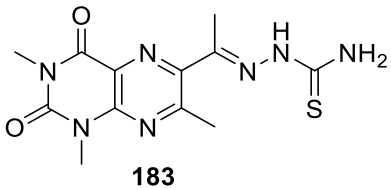

183

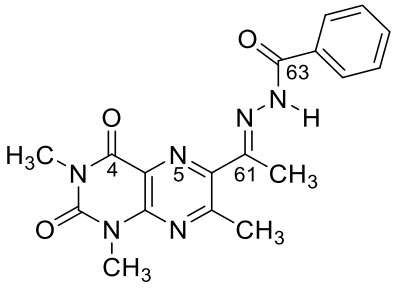

284

<Figure 13>

Ni(II), Cu(I), Zn(II), and Cd(II) complexes of the thiosemicarbazone ligand **183** have four potential predicted modes of binding; double bidentate, tetradentate, tridentate, and bidentate with bidentate, double bidentate and tetradentate modes confirmed.[102]

Reaction of **182** with stoichiometric hydrazine led to the formation of a dimeric symmetric diazine, DHzD **285** (Scheme 61). This forms binuclear complexes with Re(I) and Ag(I). Results from X-ray diffraction studies show two very different binuclear modes for the complexes, dependent on the number of ligands and the capacities of coordinating counteranion. In the Re complex, $(Re(CO)_3Cl)_2(DHzD)$, one molecule of **285** participates and each pteridine ring is bidentate, through O4 and N5. In the Ag complex, the stoichiometry is 1:1, $[(Ag(DHzD))_2]^{2+}$, i.e. two DHzD ligands span the binuclear complex; each binding to both Ag through O4, N5 and the hydrazone N, thereby occupying all coordination sites.[165]

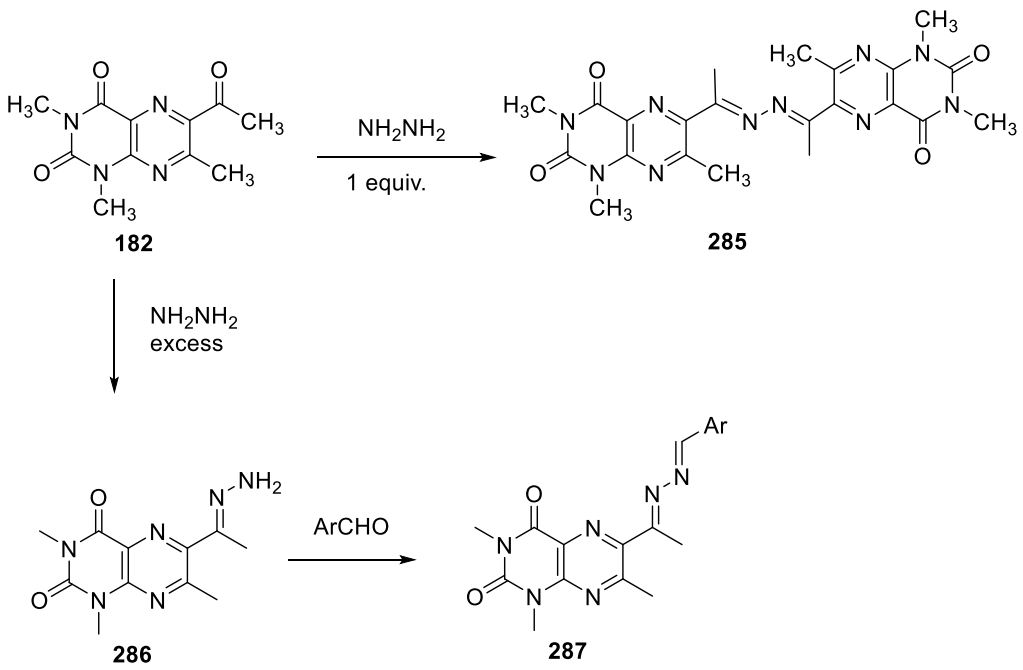

Scheme 61

Reaction of **182** with excess hydrazine leads to the hydrazone **286** additionally substituted by condensation with an aromatic aldehyde (Scheme 61). Rhenium complexes of these diazine-lumazine ligands **287** exhibit growth inhibition properties against human tumor cell lines.[166] Polyhedral silver complexes of *N,N,O-E*-[6-(hydroxyimino)ethyl]-1,3,7-trimethyllumazine are also reported.[167] Transition metal complexes of the thiocarbazone[168] and pyridinylhydrazone[169] of 6-acetyl-1,3-7-trimethyllumazine were reported recently.

Bis-pteridinebenzodiazepine ligand **274** complexes with zinc(II), cadmium(II) and mercury(II) halides have been prepared. The X-ray structures of the free ligand and the complexes showed the ligand folds so that there is capacity for σ-π interactions and π-π interactions between the two pteridine rings, the metal and the halogens. The dihedral angle between the two-pteridine rings closes from 160° to 30-50°. Luminescent properties were determined using absorption and emission spectra indicating that emissions are ligand-based.[170]

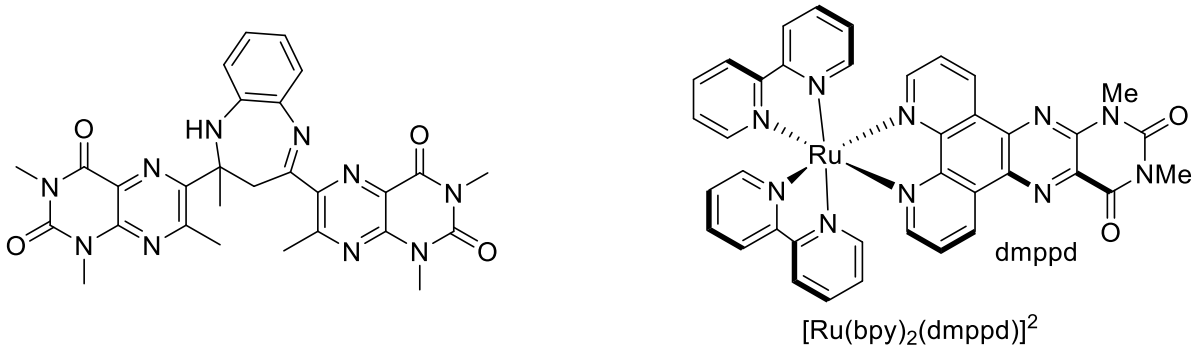

288

$[Ru(bpy)_2(dmppd)]^2$

289

<Figure 14>

The groups of Ji and Nieter Burgmayer have reported a number of DNA-binding ruthenium complexes of pteridinophenanthroline ligand systems, such as dmppd,[171] (10,12-dimethylpteridino[6,7-*f*][1,10]phenanthroline-11,13(10*H*,12*H*)-dione) prepared by Gabriel-Isay condensation of 1,10-phenanthroline-5,6-dione and 5,6-diamino-1,3-dimethyluracil. Two derived chiral ruthenium(II) complexes Δ-[Ru(bpy)$_2$(py)$_2$] [*O,O'*-dibenzoyl-D-tartrate].12H$_2$O and Λ-[Ru(bpy)$_2$(py)$_2$][*O,O'*-dibenzoyl-L-tartrate].12H$_2$O (py = pyridine) were treated with dmppd to afford chiral ruthenium(II) complexes, as the perchlorate salts. These complexes were shown to intercalate DNA complexes of pteridino[6,7-*f*] [1,10]phenanthroline-11,13(10*H*,12*H*)-dione, also acting as DNA photocleavage agents.[172] DNA-binding ruthenium (II) complexes incorporating the pteridino[6,7-*f*] [1,10]phenanthroline-11,13- diamine ligand demonstrated "light-switch" properties, becoming strongly luminescent in the presence of DNA.[173] In a separate study, the intercalation of DNA by ruthenium (II) bis-(bipyridine)pterin complexes was measured by viscometry, thermal denaturation, and absorbance and fluorescence spectroscopy. Fluorescence emission (quenched in buffer, observed when bound to DNA) enables these complexes to be used as a molecular "light-switch" for detection of DNA binding. H-bonding with the major groove results in changes to DNA thermal stability.[174] DNA-intercalating pteridin-4-one-phenanthroline complexes, e.g. **290,** undergo cleavage of the pteridine upon heating in water, leading to complex **291** that facilitates photocleavage of DNA (Scheme 62).[175] Luminescent iridium(III) complexes containing the pteridino[7,6–*f*][1,10]phenanthroline-1,13(10*H*,12*H*)-dihydroxy (ppdh) ligand are recently reported.[176]

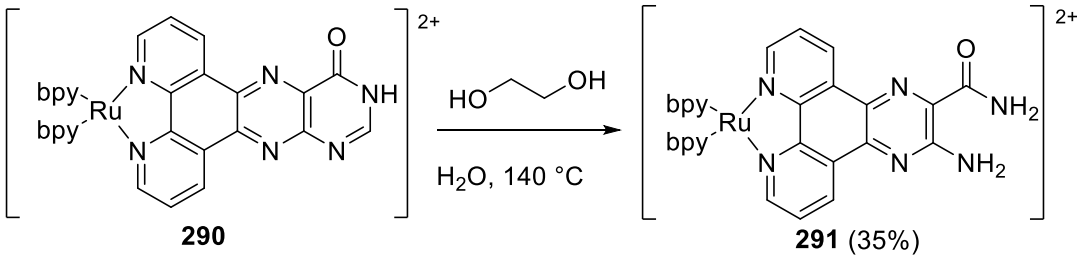

290 **291** (35%)

Scheme 62

Model molybdenum cofactor complexes of the general formula Tp*MoX(pterin-R-dithiolene), (where X = O, S, R = aryl and Tp*= tris(3,5,-dimethylpyrazolyl)-borate) containing pterin-substituted dithiolene, chelate oxo and sulfido Mo(IV) and Mo(V). Only the sulfido species **292** reacts with activated alkynes with the Mo=S species (**293**) converted to Mo=O (**294**) after thiolene formation. Pterinyl alkynes show a range of reactivities towards Mo(S4) moieties with alkyne electron-withdrawing substituents favouring dithiolene formation on molybdenum. Coupling reactions of five alkynes, 2-pivaloyl-6-phenyl ethynyl pterin (PEPP) **295**, 2-pivaloyl-6-(2,4-difluorophenyl) ethynyl pterin (DIFPEPP) **296**, 2-pivaloyl-6-(3-hydroxybutyne)pterin (BOPP) **297**, 2-pivaloyl-6-(3-hydroxy-3-methylbutyne)pterin (BMOPP) **298** and 2-pivaloyl-6-acetylethynyl pterin (AEP) **299**, with molybdenum tetrasulfide reagents showed AEP and DIFPEPP were the most reactive and PEPP reacted most sluggishly in the formation of

chelated pterin-dithiolene ligands (Scheme 63).[132] Pyranopterin dithiolene complexes have also been prepared. [133]

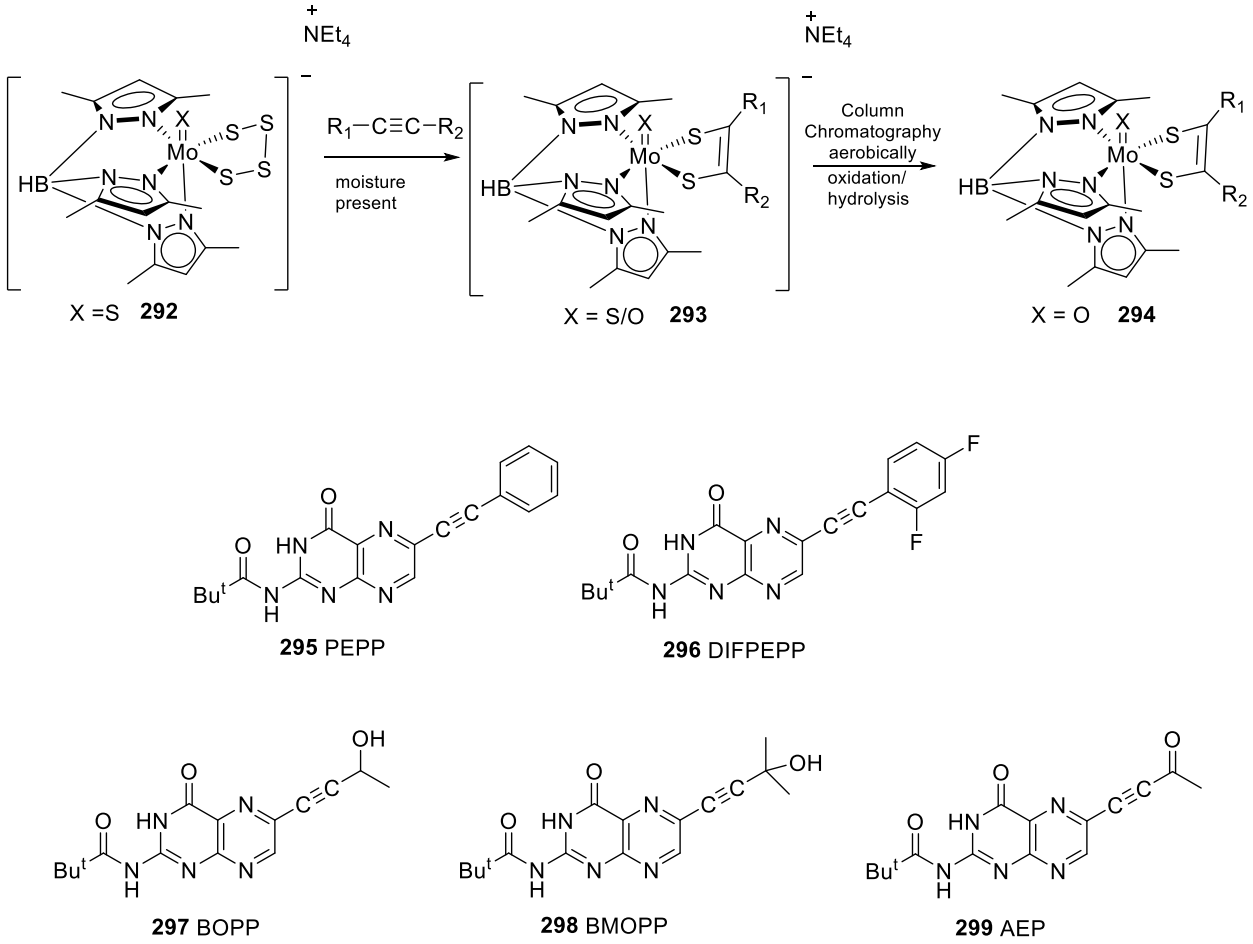

Scheme 63

10.18.10.4 Nucleoside and nucleotide analogues

The fluorescent properties of pteridines have led to their increasing use in nucleoside and nucleotide analogues, particularly as DNA probes. A recent review details the wider range of fluorescent nucleobase analogues, including the pteridines.[177] Fluorescent pteridine adenosine analogues 6MAP **300** and DMAP **301** have wide applications.[178] 6,7-Bistrifluoromethylpterin **302** has been used as a fluorescent ligand for single nucleotide polymorphism (SNP)-typing.[179]

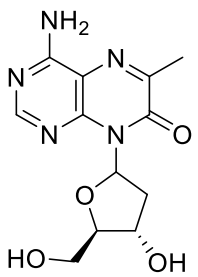

300 6MAP

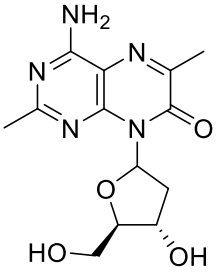

301 DMAP

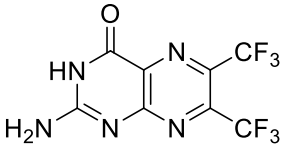

302

<Figure 15>

Analogues of isoxanthopterin **5** are fluorescent base analogues for a variety of DNA-sensing applications. Isoxanthopterin **5** and its 3- and 8-methyl analogues detect thymine (T) and cytosine (C) nucleobases. 3-Methylisoxanthopterin (3-MI) **303** shows selectivity for thymine, whereas the 8-methyl analogue **305** has higher selectivity for cytosine (Figure 16).[180] It was demonstrated that 3-MI-labelled **303** oligonucleotides can enter LLC-PK1 cells via a nucleotide-uptake channel[181] and **303** has also been used in quadruplex primers for DNA amplification.[182]

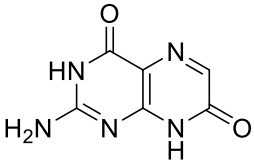

5

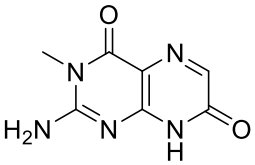

303 3-MI

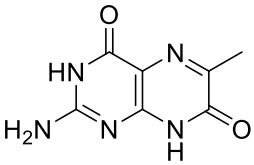

304 6-MI

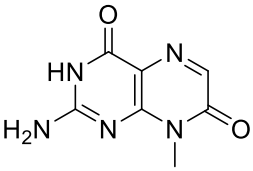

305 8-MI

<Figure 16>

3-Methyl- and 6-methyl-isoxanthopterin (6-MI, **304**) were employed to gain insight into ribosomal decoding-site RNA flexibility.[183] The 6-methyl analogue **304** has been explored extensively and six low-energy electronic transitions were identified via both experimental (absorption spectroscopy and linear dichroism) and theoretical quantum mechanical methods. DNA and RNA base pair conformations were derived.[184] Excitation-emission spectroscopy (EES) of **304** elucidated DNA conformational states.[185] A dimer of 6-methylisoxanthopterin, acting as a substitute for a GG (guanine-guanine) sequence, was shown to be a useful DNA probe, particularly its low energy CD (circular dichroism) spectrum, which can give useful information on conformations of adjacent guanine residues in DNA and RNA.[186]

Internal probes, that is, fluorescent probes incorporated into a nucleic acid chain, have been limited in sensitivity by the reduction in quantum yield when in a duplex DNA chain. Mukerji and co-workers have identified two pentameric probes, ATFAA and AAFTA (where A = adenine, T – thymine and F = fluorescent pteridine 6-MI) that maintain a high quantum yield in duplex DNA. These monitored DNA-protein interactions at picomolar concentrations.[187] The base-binding affinity and selectivity of a number of pteridine derivatives in AP-site (abasic site) duplex DNA demonstrated that pterin **2** is selective for guanine, and lumazine **3** for adenine, with 6,7-dimethyl analogues exhibiting the same selectivity with higher affinity. Alloxazine was also selective for adenine, whereas the 7,8-dimethyl analogue, lumichrome, was selective for thymine.[188] 2,4-Diamino-6,7-dimethylpteridine selectively binds to an orphan cytosine

opposite an AP site in duplex RNA. The 4-amino moiety allows for facile protonation of N1, giving fully complementary H-bonding to cytosine.[189] Modified 2-guanidinopteridines selectively bind to orphan guanines.[190]

Wolfgang Pfleiderer (1927-2018) published extensively on the synthesis of pteridine-based and pteridine-labelled nucleic acid analogues. Work published in this review period includes the 4-amino-7(8*H*)pteridinone-*N*8-nucleosides discussed in section 10.18.5.4[49], pterin *N*1-ribonucleosides[191], alloxazine-labelled oligonucleotides[115] and thymidine labelled with a fluorescent pteridine at the 3'-*O* position.[192]

Guanine quartets, where the four monomeric units interact by resonance assisted H-bonding (RAHB) are the basis of the G-quadruplexes found in DNA. The structures of purine and analogous pteridine quartets elucidated the relationship between π-conjugation and stability.[193]

10.18.10.5 Natural Products

Pteridines are widespread across the plant and animal kingdom. A small number of novel pteridine-based natural products were identified during this period. There has also been interest in the identification and quantification of the natural pteridines in plants and animal species for a variety of applications[194-196], including potential diagnostic detection of pteridines as cancer biomarkers.[197-199]

Isoxanthopterin **5** is a reflective material in the mirrored eyes of some crustaceans. The high reflective properties of this material offer potential for use in optical devices. The crystallization of **5** from DMSO leads to an alternative polymorphic crystalline form with lower refractive indices than the natural biogenic crystals.[200] Asteropterin **306**, an inhibitor of cathepsin B, was isolated from the marine sponge *Asteropus simplex*, with *p*artial elucidation of the pteridinyl and 2-aminoethylimidazolyl substructures.[201] A number of pteridines and tricyclic derivatives from leech species are reported. Hirudinoidines A-C, thieno[3,2,*g*]lumazines **307** were extracted from *Hirudo nipponica* Whitman. The X-ray structure of hirudinoidine A was obtained.[202] The hirudinoidine C structure was separately reported as being isolated from *Whitmania pigra* Whitman.[203] Two further related tricyclic analogues **308** and **309** were also extracted from *Whitmania pigra.*[204]

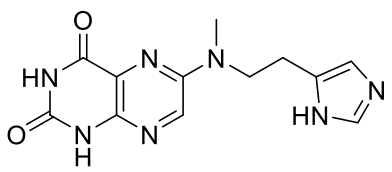

306

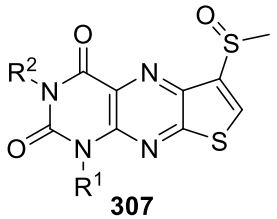

307

Hirudinoidine A: R^1= Me, R^2 = Me
Hirudinoidine B: R^1 = Me, R^2 = H
Hirudinoidine C: R^1= H, R^2 = H

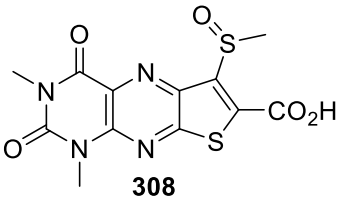

308

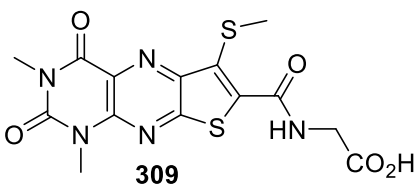

309

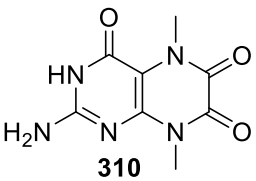

310

<Figure 17>

Pterin-6-carboxylic acid was identified as a fluorescent component of the cuticle of the train millipede *Parafontaria laminate armigera*.[205] Two pteridines have been isolated from monofloral mānuka honey, as potential markers for identification of counterfeit honey products. The first, named lepteridine, was confirmed spectroscopically and by total synthesis as being 3,6,7-trimethyllumazine (3,6,7-trimethyl-2,4(1*H*,3*H*)- pteridinedione) **311**. This pteridine was found in mānuka honeys and at a low level in one kānuka honey sample, but was not present in other honeys.[206] Lepteridine and a related lumazine derivative, 6,7-dimethyl-2,4(1*H*,3*H*)- pteridinedione **312** were independently isolated from mānuka honeys. Using UHPLC-PDA-MS/MS analysis, the two pteridines were detected only in mānuka honey samples. TLC visualization of these fluorescent pteridines at 366 nm provided a rapid method for discerning mānuka honey from kānuka honey and nine other monofloral honey samples.[207]

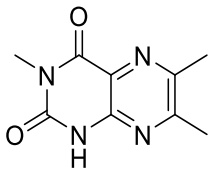

311

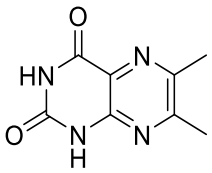

312

<Figure 18>

Penilumamide **313**, a lumazine peptide, was isolated from the marine *Penicillium* sp. CNL-338.[208] Penilumamide (now suffixed with A) and three new related peptides, penilumamides B, C and D (**314-316**) were isolated from *Aspergillus* sp. XS-20090B15.[209] Two further related lumazine peptides, named terrelumamides A **317** and B **318** were isolated from *Aspergillus terreus*.[210] Compound **317** was later reported from *Aspergillus terreus* with the alternate name penilumamide E.[211]

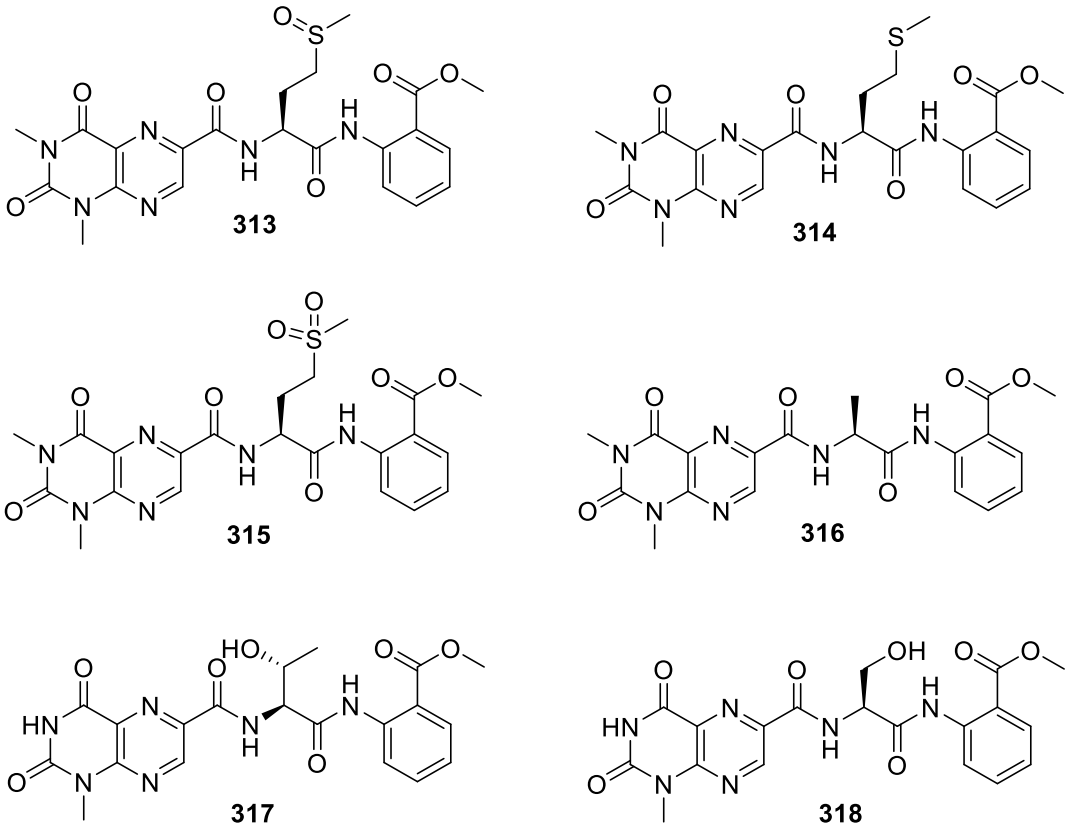

<Figure 19>

Another lumazine peptide, aspergilumamide A **319**, has been extracted from a mangrove-derived *Aspergillus* species.[212] Duramidines A-D **320**, the first glyceryl-3-(O-carboxyhydroxymethylcholine) alkaloids to be reported from an animal source, were isolated from the Australian ascidian *Leptoclinides durus*.[213]

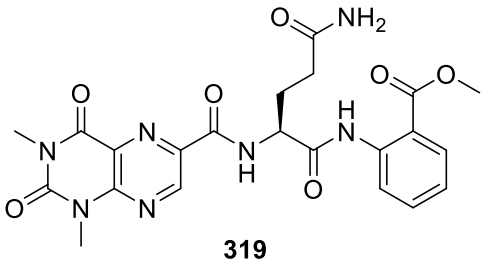

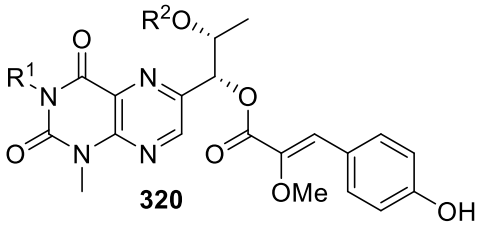

Duramidine A: R^1 = Me, R^2 = SO_3H
Duramidine B: R^1 = Me, R^2 = H
Duramidine C: R^1 = H, R^2 = SO_3H
Duramidine D: R^1 = H R^2 = H

<Figure 20>

10.18.10.6 Biosynthetic Pathways

Biosynthetic pathways for the synthesis of pteridines or involving pteridine cofactors are a subject of great interest, with several mechanistic pathways stil not fully elucidated. An overall review of the biological roles of folates and other pteridine cofactors is provided by Rébeillé *et al.* and highlights the ubiquity and importance of this class of heterocycle.[214] The genetic control of riboflavin and flavin nucleotide biosynthesis[215] and the lumazine synthase/riboflavin synthase complex have been reviewed.[216]

The biosynthesis of riboflavin involves the reaction of two molecules of 6,7-dimethyl-8-ribityllumazine **321** to form riboflavin **323** plus 5-amino-6-(ribitylamino)uracil **324**, and is believed to proceed via the pentacyclic intermediate **322** (Scheme 64).[1]

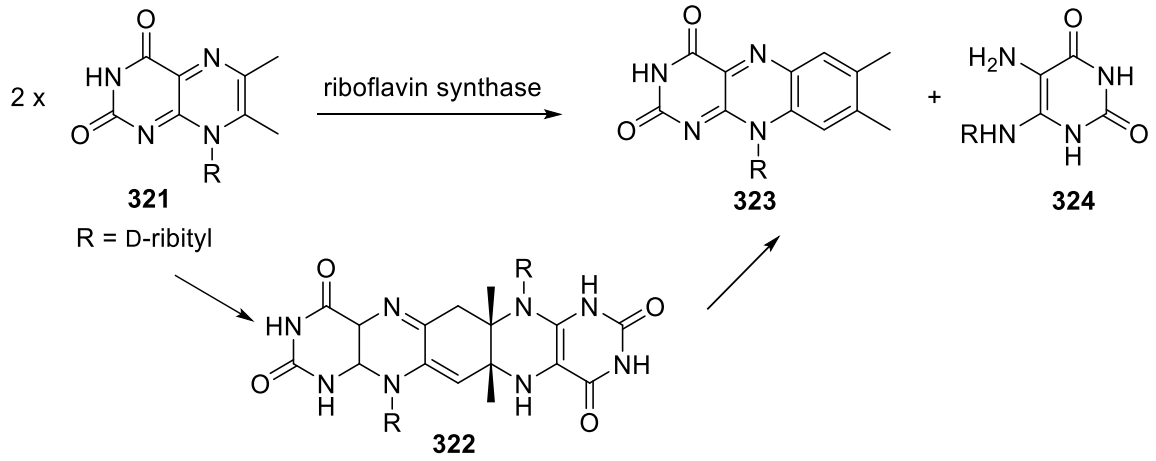

Scheme 64

A high throughput platform screened inhibitors of lumazine synthase and riboflavin synthase, for exploration of the riboflavin biosynthesis pathway.[217] Studies to elucidate the mechanism of this transformation have continued. Proposed mechanisms include the participation of a nucleophile, although it is unclear if any residue in the enzyme active site can act in this role as an internal nucleophile and an external nucleophilic addition, e.g. water, is a feasible alternative. The other proposed mechanisms involve H atom or hydride transfer. Fischer, Bacher and co-workers studied the *N*-terminal domain of *E. coli* riboflavin synthase by NMR and observed that the enzyme interacted with the 6,7-dimethyl-8-ribityllumazine exomethylene anion. The proposed mechanism therefore was that this anion engaged in hydride transfer to another 6,7-dimethyl-8-ribityllumazine, followed by a [4+2]-cycloaddition.[218] There has continued to be literature disagreement on whether the riboflavin synthase enzyme active site cysteine acts as a catalytic nucleophile in this process. It was observed that this reaction can also proceed non-enzymatically at elevated temperatures, therefore theoretical studies were carried out to elucidate the possible mechanisms of this reaction. DFT was used to analyze four proposed mechanisms. Simple nucleophilic addition was calculated to be the lowest energy pathway, although nucleophilic catalysis was also an energetically viable pathway from these analyses. Alternative H atom or hydride transfer mechanisms, as previously proposed, were calculated to be 30-45 kcal mol^{-1} higher in energy. [219]

A review of folate biosynthesis and the transformations of folate and derivatives is available.[220] Biosynthesis of folate by bacteria involves nine steps from guanosine triphosphate (GTP). The first four steps are GTP→ dihydroneopterin triphosphate (DHN-P_3), → monophosphate (DHN-P)→ dihydroneopterin, (DHN)→ 6-hydroxymethyldihydropterin (HMDHP). This fourth step is catalyzed by dihydroneopterin aldolase (FolB). In bacteria lacking the FolB gene, a novel enzyme, 6-pyruvoyltetrahydropterin synthase (PTPS) was found to catalyze the direct synthesis of HMDHP from DHN triphosphate.[221] Two archeal enzyme families involved in the biosynthesis of 6-hydroxymethyldihydropterin phosphate have been discovered. Enzymes from the COG2098 family catalyze synthesis from 7,8-dihydroneopterin and those from the COG1634 family catalyze the synthesis from 6-hydroxymethyl-7,8-dihydropterin.[222]

Tetrahydromonapterin, H_4-MPt, a bacterial pterin, is biosynthesized from dihydroneopterin. Two enzymes on this pathway, FolM, a short-chain dehydrogenase/reductase, and FolX, a dihydroneopterin-triphosphate-epimerase, were found to be essential in the biosynthetic pathway in *Escherichia coli and Pseudomonas aeruginosa*.[223] 10-Formyltetrahydrofolate (10-CHO-THF) is essential for the mitochondrial biosynthesis of methionyl-tRNA. In the parasite *Leishmania major*, the enzymes for this biosynthetic pathway are found exclusively in the cytosol, raising the possibility of the transport of 10-CHO-THF from the cytosol to the mitochondria as a potential drug target.[224]

Tetrahydrobiopterin (BH_4) is a cofactor for NOS and in the synthesis of several neurotransmitters. Kapatos has reviewed the biosynthetic pathways to tetrahydrobiopterin and the importance of GTP cyclohydrolase I in the brain for these pathways.[225] The nitric oxide synthase in the bacterium *Deinococcus radiodurans* uses tetrahydrofolate (FH_4) instead of tetrahydrobiopterin (BH_4) as a cofactor. Pulse radiolysis studies of the tetrahydrofolate bound enzyme have demonstrated that decay of the ferrous-dioxygen bound intermediate occurs to give a further intermediate, where the tetrahydrofolate is reduced to an FH_4 radical. It has been suggested that in other NOSs, tetrahydrobiopterin may also be involved in an analogous electron-transfer step.[226] The drosopterins, eye pigments of Drosophila fruit flies, are biosynthesized from 7,8-dihydropterin.[227]

Metal-pterin complexes are a feature of the important family of enzyme cofactors, notably the molybdenum cofactor (MoCo/Moco), found in many species of prokaryotes and eukaryotes, and the analogous tungsten-pterin cofactors, found mainly in archaea and some other prokaryotes.A number of reviews are available on this subject, covering pterin chemistry related the molybdenum cofactor,[228] its biosynthesis,[229, 230] the shared functions of proteins in this pathway with other biosynthetic pathways[231] and the regulation of bacterial MoCo biosynthesis by molybdenum and iron.[232]

The overall pathway, as shown catalyzed by bacterial enzymes, with the corresponding human enzymes as shown in brackets (Scheme 65), involves conversion of GTP **325** to cyclic pyranopterin phosphate (cPMP) **270**, followed by conversion to the dithiolene **326** and molybdenum insertion via an AMP-adduct **327** to give MoCo **271**.[233]

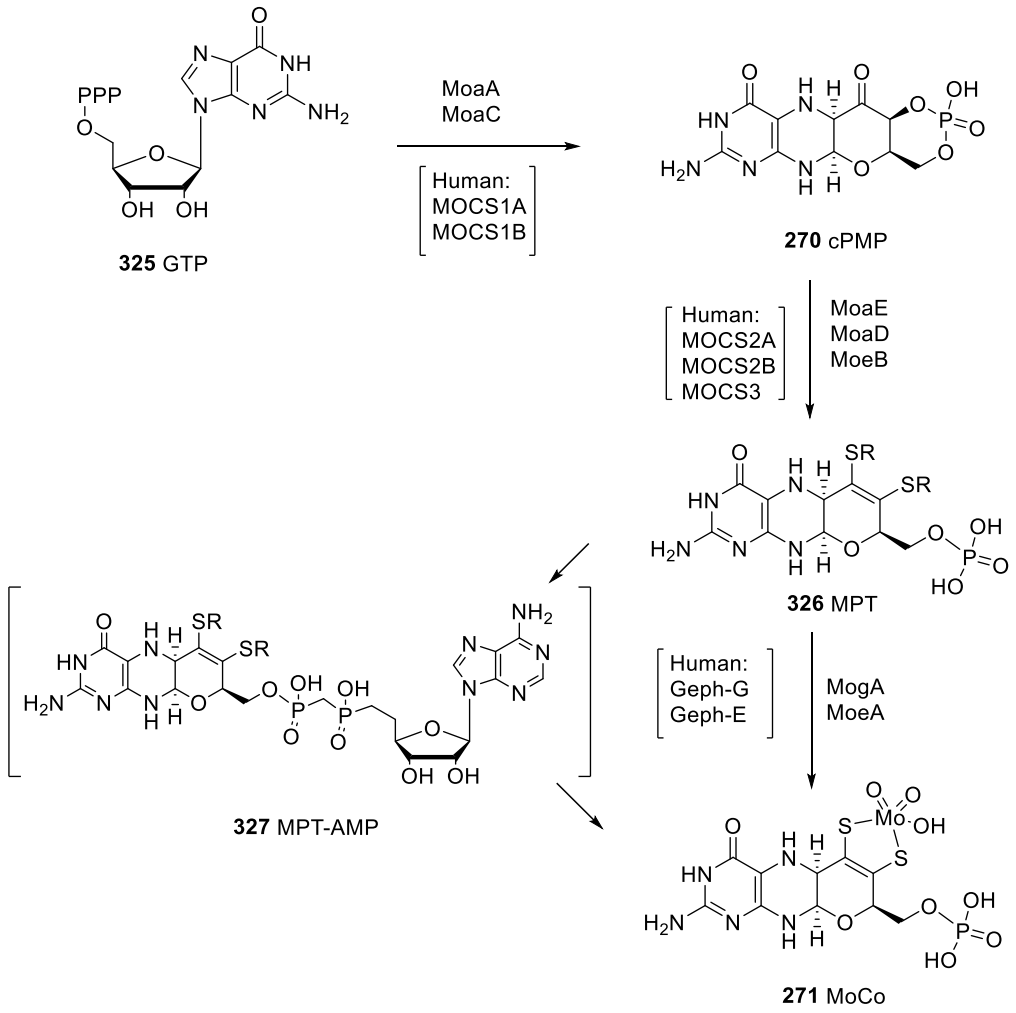

Scheme 65

Further information about these enzymes and possible alternative enzymatic pathways has come to the fore in the past 10 years. In the human biosynthesis pathway, Hover and Yokoyama elucidated that the cPMP synthesis in humans involves enzymes MOCS1A, together with a MOCS1B gene product. A terminal glycine motif (GG) in MOCS1A is necessary for the enzyme to function in its role of catalyzing *S*-adenosyl methionine radical cleavage.[233]

Gephyrin catalyzes the final step in the human MoCo biosynthetic pathway. Splicing studies demonstrated that the insertion of a C5 cassette or deletion of the C6 cassette in the G domain abolishes activity.[234] The G domain adenylates molybdopterin and the E domain carries out the final step of molybdenum incorporation, with loss of AMP. X-Ray structures of gephyrin E domain-nucleotide and nucleotide-metal complexes have offered more insight into these previously poorly understood steps.[235] In the plant species *Arabidopsis*, the mitochondrial ABC transporter ATM3 has been shown to be essential for the final step of MoCo synthesis. Mutants lacking this transporter accumulate cPMP in high levels due to reduced levels of MoCo. Possible mechanisms of ATM3 involvement include direct transport of cPMP or Fe-S cluster precursors from the mitochondria to the cytosol, where the final biosynthetic step takes place.[236] Rhodanese-like protein YnjE enhances the rate of the final molybdopterin synthesis step in *Escherischia coli*.[237]

The MoAB enzyme from *Pyrococcus furiosus* was found to catalyze pterin adenylation in an analogous way to the enzymes in other bacteria and eukaryotes.[238] A bis-molybdopterin (bis-MPT) intermediate in the *Escherischia coli* MoCo biosynthesis pathway has been identified. X-ray absorption spectroscopy, using XANES (X-ray absorption near edge structure) and EXAFS (extended X-ray absorption fine structure) experiments, was used to confirm Mo oxidation state and first coordination sphere in the bis-MPT biosynthetic intermediate.[239] MoCo is involved in many enzymatic pathways. The reaction mechanisms of MoCo in xanthine oxidoreductase have been reviewed.[240]

10.18.10.7 Chemical Mechanism of Action of Pteridine-Synthesizing or -Transforming Enzymes

Some major advances in recent years towards the greater understanding of MoCo and the mechanistic steps in MoCo biosynthesis, include the model dithiolene-molybdenum complexes constructed to help elucidate the proposed potential for pyran scission-recyclization.[132, 133] Complex **328** was found to undergo spontaneous cyclization to furnish a pyran **329** in the crystal structure. NMR data suggest a reversible process in solution (Scheme 66).[133]

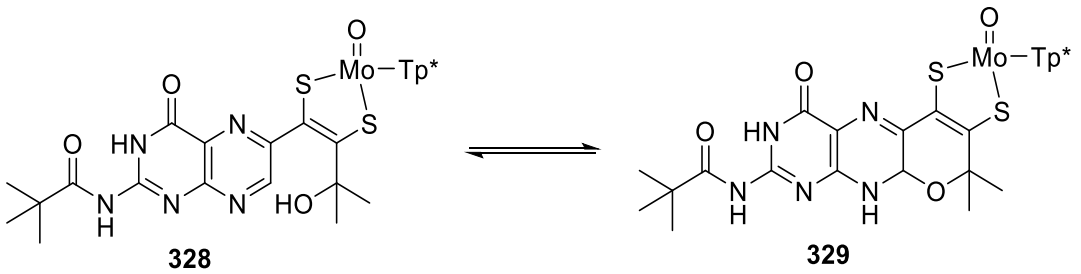

Scheme 66

A recent review discusses radical *S*-adenosyl-L-methionine (SAM) enzymes, including those involved in MoCo.[241] Further information on a key step in the biosynthesis of MoCo and the genetic mutations that cause MoCo deficiency have been elucidated. The formation of cPMP from GTP has been the subject of several recent studies. The biosynthesis of cPMP involves an interesting insertion of guanine C8 into the ribose C2'-C3' bond. In 2013, two groups independently reported the unusual guanine-C8-ribose-C3' adduct **330** as an intermediate in this cPMP synthesis pathway.[242-244]

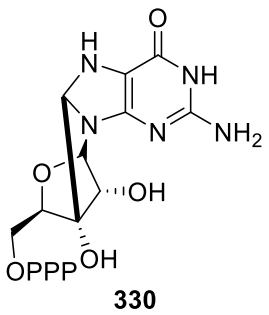

<Figure 21>

Yokoyama and co-workers isolated and characterized intermediate **330** in the MoaA-catalyzed synthesis of cPMP.[242] Begley and coworkers proposed intermediate **332** was formed by generation of the 3'-ribosyl radical (via H-abstraction by an adenosyl radical), which cyclizes onto position 8 of the guanine and is then reduced. Confirmation of this intermediate was achieved using an analogue, 2′,3′-dideoxyGTP **331**, and trapping the cyclized intermediate, whereby a C8-C3'-linked product **333** was obtained (Scheme 67).[245, 246]

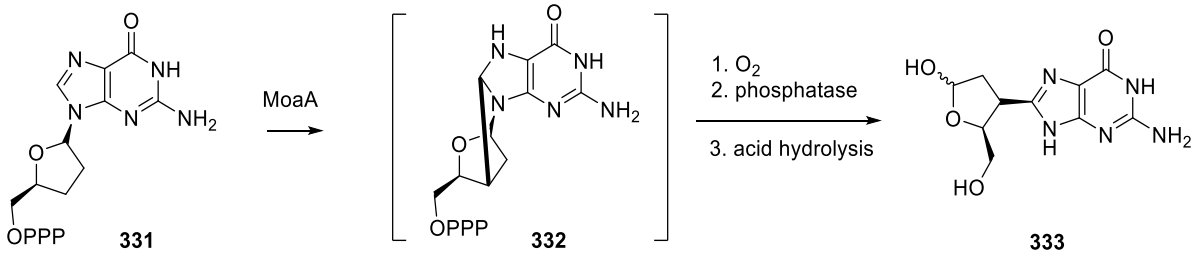

Scheme 67

The site of initial H-abstraction was further elucidated[245], using 2'-ChloroGTP, which traps the C3' radical of GTP, and 2'-deoxyGTP, which blocks a later step. This resulted in an amended proposed mechanistic pathway for the MoaA transformation. Aminal hydrolysis of **330** is followed by rearrangement of the furan to a pyran, which ring-opens, Tautomerization to an enone allows for conjugate addition to close the pteridine ring, followed by pyran ring closure as the final step. (Scheme 68).[246]

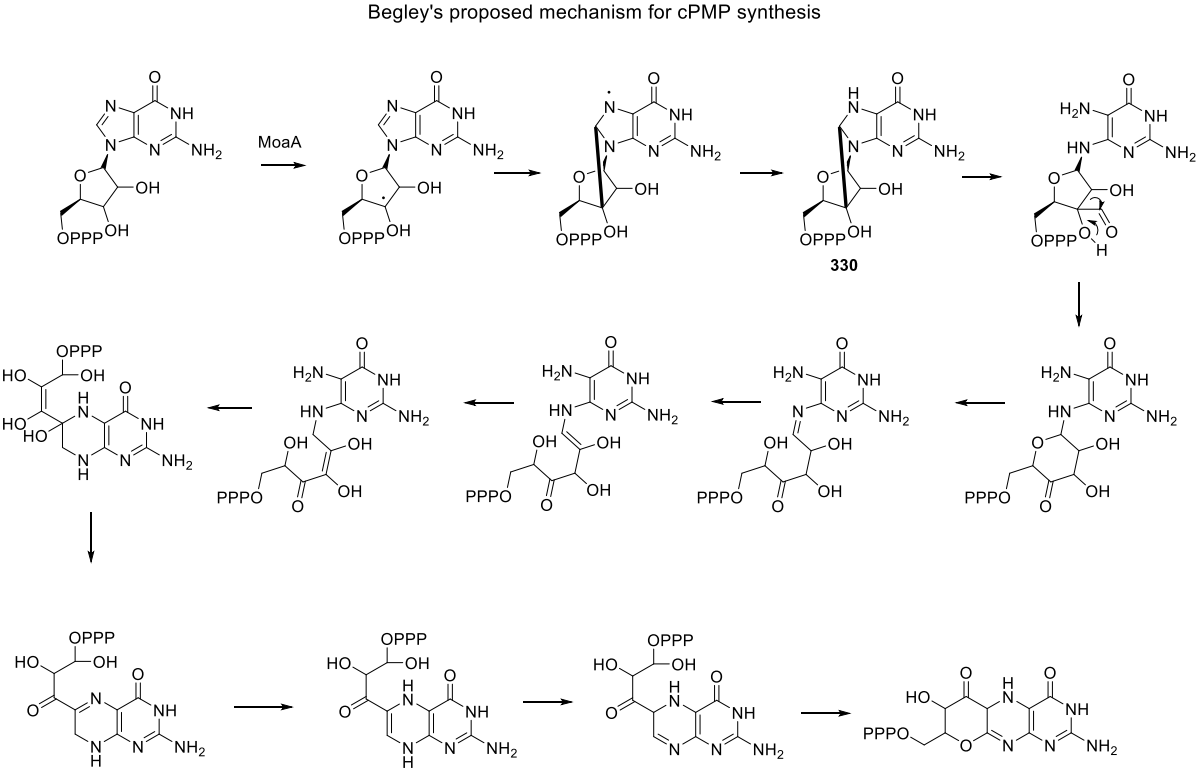

Scheme 68

MoaA was believed to catalyze all steps of the pyranopterin formation. The Yokoyama group provided evidence that MoaA catalyzes the formation of the initial 3'-8 cyclized intermediate,

but that MoaC catalyzes the following rearrangement steps leading to the cPMP product **270**. Therefore proposing that these enzymes should be designated as GTP 3′,8-cyclase and cPMP synthase respectively.[247] The Yokoyama group proposed an alternative mechanistic pathway based upon the interactions with key residues in the MoaC protein, whereby the pyran ring is formed before the pyrazine (Scheme 69).

The ring cleavage of the 3'-8 cyclized intermediate **330** can proceed via two potential pathways aided by M113/E112 stabilization of the pyrimidine O4 and D128 interaction with 3'-OH. In pathway A (Scheme 69), rearrangement occurs *via* aminal hydrolysis followed by C2'-C3' ring cleavage. In pathway B, C2'-C3' ring cleavage is followed by enamine/iminium tautomerism and hydrolysis; both lead to the same intermediate X. Residue K131 stabilizes the enediol and may be involved in proton transfer for pathway **B**. In both pathways, closure of Loop 3 brings K51 into the proximity of D128, further facilitating the following steps. Formation of the pyran ring, is followed by dehydration, the conjugate addition of N to close the pterin ring system and the formation of the cyclic phosphate.[247]

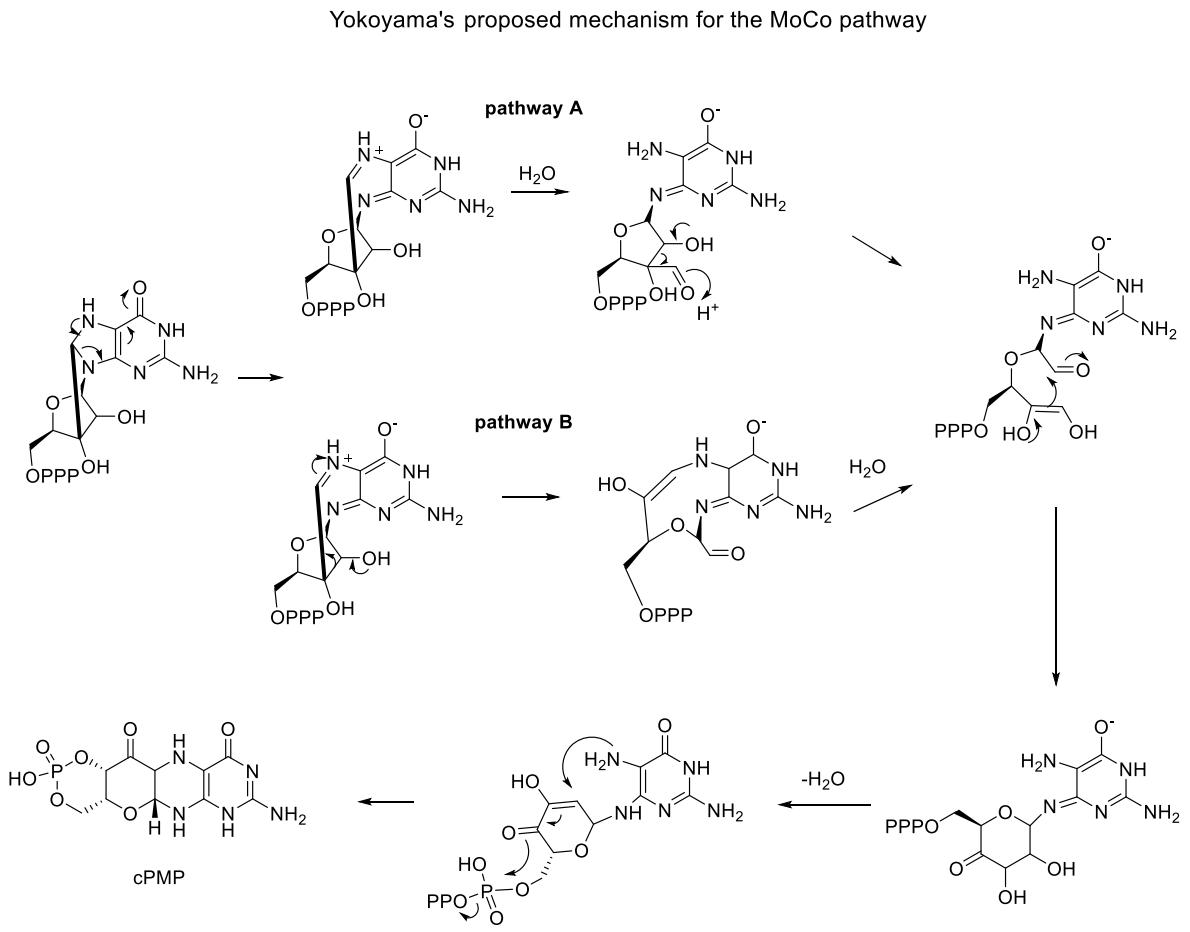

Scheme 69

A non-cleavable substrate for MoaC was used to confirm that closure of the pterin ring and cyclic phosphate formation does occur in a concerted fashion in the final step of cPMP **270** synthesis from **330** (Scheme 70).[248] These interesting radical reactions involve FeS clusters.[249, 250]

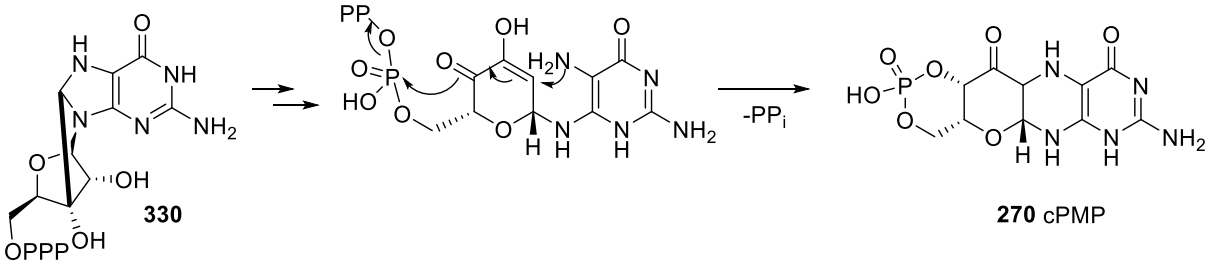

Scheme 70

10.18.10.8 Medicinal Chemistry

Pteridines and derivatives have been widely investigated for a number of medicinal applications and there have been several new areas of research in the past 15 years. There is a recent review of medicinal/therapeutic applications of pteridines.[251]

A traditional use of pteridines in medicine has been as antifolates, which inhibit folate-dependent pathways and are used in oncology, inflammatory disease and anti-infective applications. Methotrexate is a folate analogue antimetabolite used in cancer therapy and autoimmune/inflammatory disease management. There have been some further developments around folic acid or methotrexate analogue development. Ketone analogues of methotrexate have demonstrated antifolate ability with potentially reduced toxicity.[252] Substituted 3-(pteridin-6-yl)propanamides were developed as cytotoxic antifolate analogues; these were synthesized from 5,6-diamino-1-methyluracil via reaction with 2-oxopentanedioic acid to give the intermediate lactone.[253]

Dual substrate inhibitors of the folate biosynthetic pathway enzyme 6-hydroxymethyl-7,8-dihydropterin pyrophosphokinase (HPPK) have been developed, linking 7,7-dimethyl-7,8-dihydropterin or the 6-carboxylate derivative to adenosine via a piperidine-thioether linker.[254] Folic acid **8** enters the cell via binding to the folate receptor and receptor-mediated endocytosis. Overexpression of folate receptors occurs in cancer and in inflammatory disease leading to the use of folate conjugates for delivery of therapeutic agents.[255] A conjugate of a hydrazide derivative of the antifolate drug aminopterin with folic acid has been developed, using carbohydrate and peptidic spacers with a disulfiide reductive-release linker.[256] Delivery of methotrexate-amino derivatives through carboxylate-linked PEG peptide or protein carriers demonstrated superior *in vitro* inhibition of dihydrofolate reductase (DHFR) and growth inhibition of glioma cells in comparison to traditional cysteine or amine-linked systems.[257] Pteridinyl-sulfonamide conjugates were developed as potential dual DHFR and carbonic anhydrase (CA) inhibitors with inhibition in the 2-20 micromolar range, compared to IC_{50} of 5 nM for the reference compound and market drug methotrexate. Activity against carbonic anhydrase was comparable in potency to reference compounds, with inhibition constant (K_i) in the nanomolar range, but the novel conjugates demonstrated significant isozyme selectivity for CA IX (a cancer associated isozyme) over CA II (ubiquitously expressed). Compound **334** is a typical example with 369-fold isozyme selectivity. However, the compounds had only modest anti-proliferative effects in cancer cells attributed to poor physicochemical properties. Nevertheless, the authors report the potential for rational design of selective carbonic anhydrase inhibitors (Figure 22).[258]

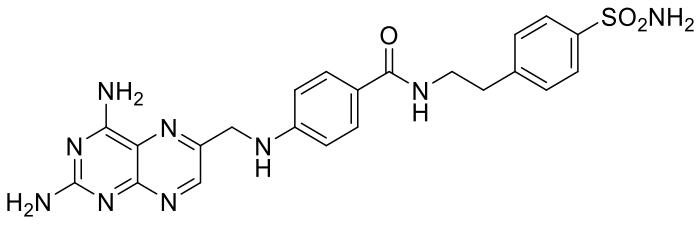

334

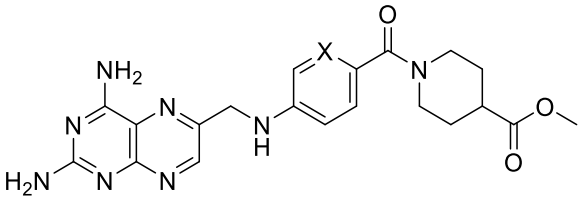

335: X = C
336, X = N

<Figure 22>

Pteridine reductase (PTR1) is an enzyme drug target in *Leishmania* and *Trypanosoma* parasites, as it can replace DHFR in metabolic pathways, leading to antifolate resistance. Structure-based design of potential PTR1 inhibitors based upon the interactions with substrates and methotrexate, led to three scaffolds, based on 6,7-substituted 2,4-dimainopteridine, pyrrolo[2,3-*d*]pyrimidine and 2,4-diaminopyrimidine. The pteridine scaffold demonstrated greater selectivity for *Leishmania* PTR1 over *Trypanosoma* PTR1.[259] The search for selective PTR1 inhibitors led to compound **335**, a cyclized piperidinyl analogue of methotrexate, with 100-fold selectivity for leishmanial PTR1 over human DHFR.[260] This was used as the basis for structure-based design of analogues leading to the more selective pyridyl analogue **336**, which demonstrated synergistic antiparasitic effects, in combination with a DHFR inhibition.[261]

A pteridine library was screened to identify potential dual immunosuppressive and anti-inflammatory compounds, by assays of inhibition of both T cell production (immunosuppressive) and tumor necrosis factor-alpha (TNF)-α production (anti-inflammatory). A library of analogues based upon hit **337** was initially explored by varying alkoxy substituents at position 4 and substitution of the aryl group (Figure 23). The 3,4-dimethoxyphenyl motif at position 6 was found to be essential. Exploration of amino-substituents led to a final series of 4-substituted piperazinyl analogues **338**, which exhibited nanomolar or sub-nanomolar T cell inhibition combined with retained inhibition of TNF-α in the sub-micromolar range.[105]

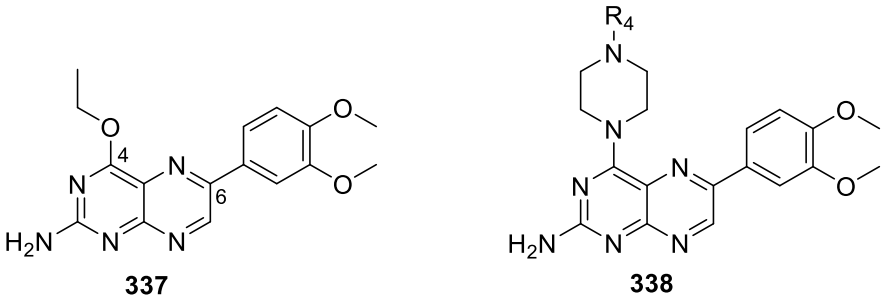

<Figure 23>

4-Amino-2-aryl-6,9-dichlorobenzo[g]pteridines **237** (Figure 24) synthesized from 5,8-dichloro-2,3-dicyanoquinoxaline, have been reported as micromolar inhibitors of TNF-α and interleukin-6 (IL-6)[127] and to have anti-leukemic activity against HL60 and K562 cell lines.[262] Pteridine 2,4-diamine derivatives act as antioxidants *via* radical scavenging and lipoxygenase inhibition, down to 100 nM. The analogues with the best profile (**339** and **340**) exhibited some efficacy in preventing tissue damage in a rat model of colitis and one analogue exhibited greater efficacy than indomethacin in a paw edema model.[56]

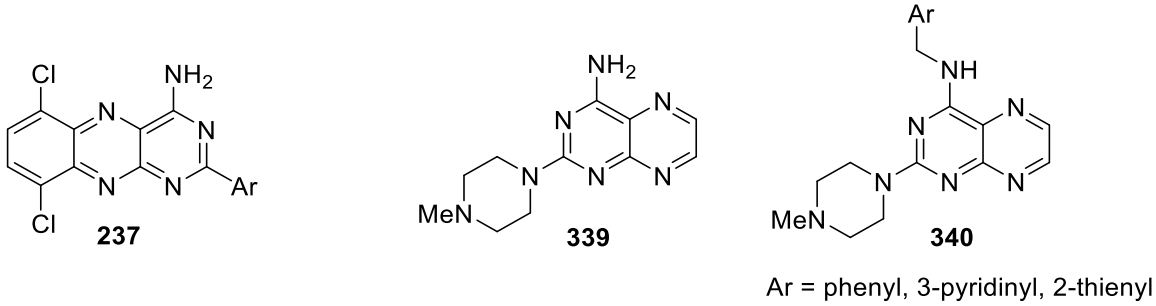

<Figure 24>

The structure-based design of pterin-based inhibitors of the cytotoxic protein ricin has been reviewed.[263] The DNA-binding and antiviral activity of a short series of 6-substituted pteridine derivatives **341** was determined with some modest activity for those with non-aromatic substituents (Figure 25).[96]

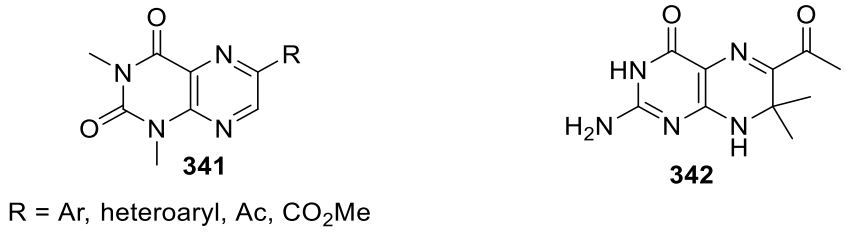

<Figure 25>

The role of tetrahydrobiopterin **45** in NOS, a key messenger molecule, has led to further pteridine-based medicinal chemistry studies. 6-Acetyl-7,7-dimethyl-5,6,7,8-tetrahydropterin **342** activated NOS by acting as a cofactor replacement for **45**.[264] 6-Aryl,2,4-diaminopteridine derivatives **343** were designed as inhibitors of inducible nitric oxide synthase (iNOS), via

interaction with the tetrahydrobiopterin (BH_4) cofactor binding site (Figure 26).[104] Several analogues inhibited iNOS with IC_{50} values in the range 14-42 μM, exhibiting similar or better potency, compared to the reference pharmaceutical, methotrexate. Two compounds, **344** and **345**, were evaluated in an *in vivo* sepsis model, demonstrating similar activity to aminoguanidine.[103] A 3-D QSAR (quantitative structure activity relationship) study of pteridine inhibitors of iNOS is reported.[265]

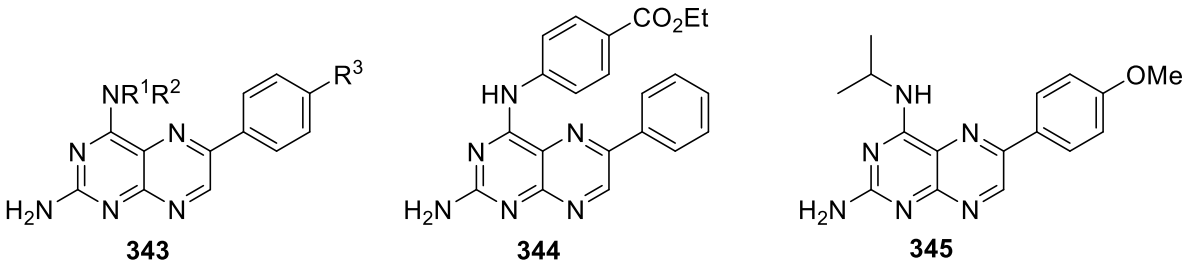

343 **344** **345**

<Figure 26>

The 6-styrylpteridine-2,4-dione analogue **346** demonstrates potent inhibition of monoamine oxidase B (Figure 27). However, it does not inhibit NOS and it is likely that the styryl side chain prevents interaction with the tetrahydrobiopterin **45** binding site.[266] A series of pteridines/pteridinones **347**[267] and, later, 4-aryl-8-alkylpteridin-7[8*H*]-ones leading to the analogue **348**,[110] were investigated as inhibitors of corticotropin releasing factor (CRF). Hypersecretion of CRF is associated with altered stress response, anxiety and depression. These showed less potent inhibitory activity than the deaza-analogues, pyridino[3,2-*b*]pyrazines, but had improved physicochemical properties, with lower calculated log of partition coefficient (clog*P*) and correspondingly lower plasma protein binding.

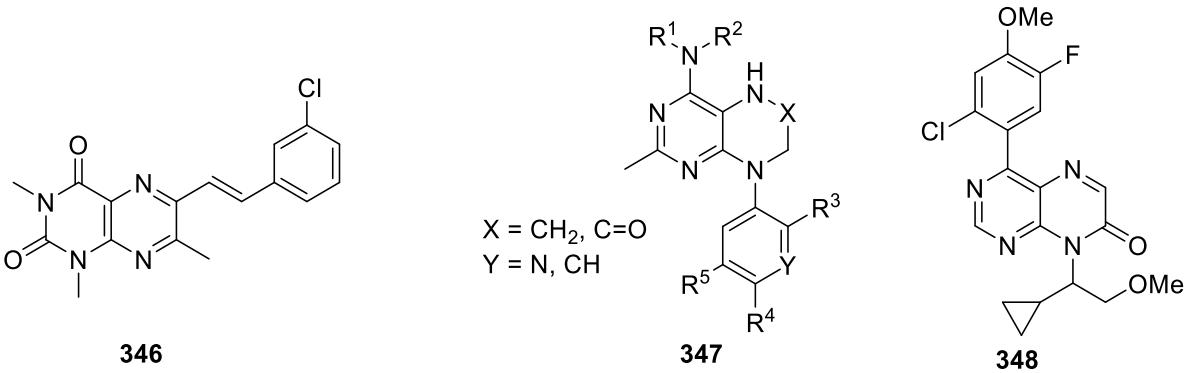

346 **347** **348**

<Figure 27>

Pteridines have emerged as interesting compounds against oncology targets. The pteridine skeleton has appeared in a number of recent publications as a replacement for pyrimidine-based hits. 3-Substituted pteridines with a 1,3,4-thiadiazole linker, of the general structure **349** (Figure 28), were found to have potent antiproliferative activities.[268] Substituted 2-amino-7,8-dihydropteridin-6(5*H*)-ones **350** were shown to have micromolar antiproliferative effects, arresting cells at the G1 phase of the cell cycle.[118] Antitumor properties of 4-(*N*-arylamino)-6-alkoxypteridines are reported.[269] Pteridin-7(8H)-ones were investigated for antiproliferative activity, of which **351** was the most active against four cancer cell lines, promoting pro-apoptotic pathways.[109] The same group developed related 5,8-dihydropteridine-6,7-diones, of

which **352** was the most potent in inducing apoptosis and reducing cell migration in MGC-803 colon cancer cells.[68]

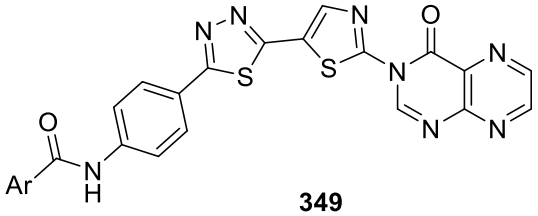

349

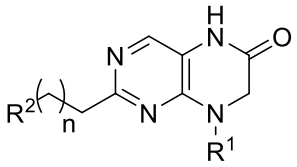

350

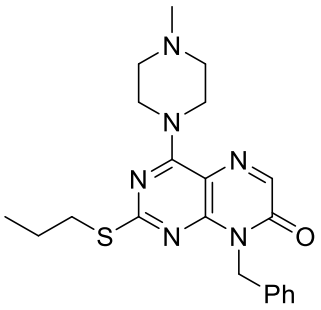

351

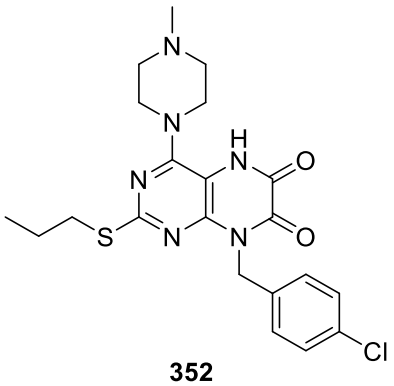

352

<Figure 28>

The benzo[*g*]pteridine **353** (Figure 29) was selected from a high-throughput screen as a micromolar inhibitor of the RNA-binding protein MSI2, a key protein in acute myeloid leukemia (AML). The compound effected increased differentiation and apoptosis in myeloid leukemia cells and demonstrated an anti-leukemogenic effect in an *in vivo* model.[270] 5,7--Substituted 2-amino-4-chloro-8-((4-methoxy-3,5-dimethylpyridin-2-yl)methyl)-7,8-dihydropteridin-6(5H)-ones **354** are potent inhibitors of Hsp90, a heat shock protein of interest as an oncology drug target.[107]

Pteridine diones and triones were developed as inhibitors of monocarboxylate transporter 1 (MCT-1) inhibitors. This transporter is of interest as an oncology target, as it is overexpressed in aggressive tumors, which have upregulated aerobic glycolysis, thereby requiring increased rate of removal of acidic glycolysis products from the cell. Compounds **355** and **356** demonstrated sub-micromolar IC_{50} in a ^{14}C lactate transport assay and an EC_{50} in the range 37-150 nM in MCT1-expressing Raji lymphoma cells.[73]

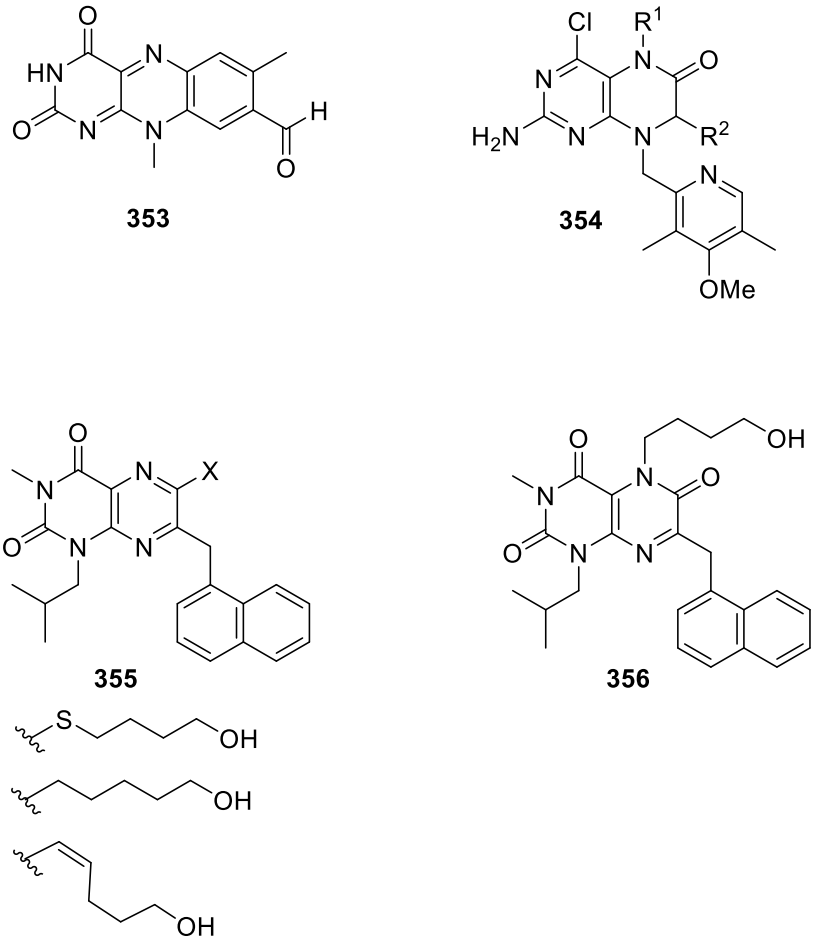

<Figure 29>

There is growing interest in pteridines as kinase inhibitors, including 3,3′-(2,4-diaminopteridine-6,7-diyl)diphenol **357** reported as a selective phosphatidylinositol-3-kinase (PI3K) inhibitor, with isoform selectivity for PI3Kγ, for prevention of ischemia-reperfusion injury (Figure 30).[94] 4-Methylpteridinones act as a dual PI3K/mTOR inhibitors, including compound **358** with nanomolar activity against both enzymes. Pteridine **358** has good predicted human PK parameters and oral bioavailability, effecting 75% tumor growth inhibition at 20 mg kg^{-1} in a U97 glioma mouse tumor xenograft model.[271]

The Nagamatzu group have investigated flavin **7** and alloxazine **6** analogues, as potential c-Kit receptor protein tyrosine kinase inhibitors with antitumor properties.[100] The same group reported the synthesis and anti-tumor activities of further 2-deoxoflavin-5-oxides and 2-deoxoalloxazine-5-oxides. In particular, the 2-methylthio-derivatives exhibited favorable antitumor properties.[272] The active compounds were docked into c-Kit protein tyrosine kinase (PTK) and some correlation of docking scores with cell activity was determined.[87] Pteridin-6-ones based on the Boehringer-Ingelheim compound BI-D1870 **359** have been reported as inhibitors of p90 ribosomal S6 protein kinase (RSK), another promising cancer drug target.[273]

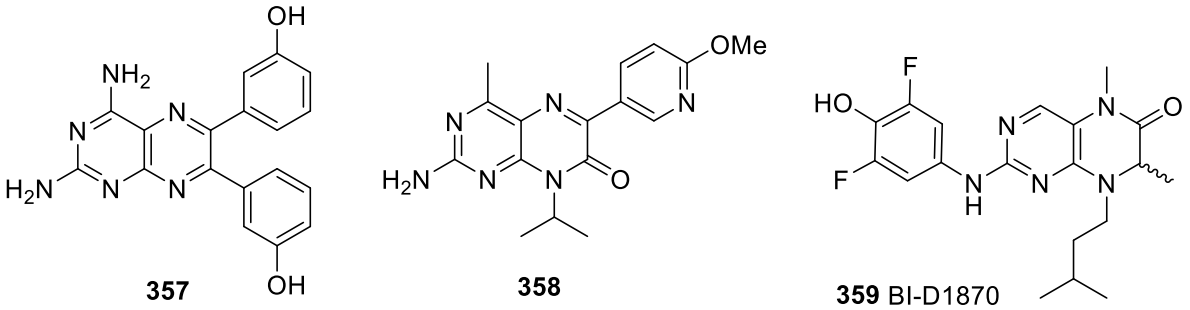

<Figure 30>

Pteridine-7[8*H*]-ones have demonstrated activity against T790M/L858R mutants of epidermal growth factor (EGFR) kinase. The T790M mutation is a major mechanism of resistance EGFR kinase inhibitors. Scaffold hopping from a pyrimidine hit compound, led to compounds **360** bearing a Michael acceptor on the 8-aryl substituent (Figure 31). These act as irreversible inhibitors with ~60 nM activity against gefitinib-resistant cells and antitumor effects *in vivo*.[108] Compound **360** (R = OMe) was used in structure-based design with the differences between the T790M mutant and wild-type EGFR, leading to the 5-isopropyl-6,7-dione analogue **361** exhibiting relatively modest 6.7-fold enzyme selectivity for T790M/L858R mutant vs wild-type EGFR. Compound **361** demonstrated over 400-fold selectivity for H1975 cells bearing the double mutation, with IC_{50} of 18 nM, compared to A431 cells without the mutation. The compound is orally bioavailable and, in an, *in vivo* model, was more potent in reducing tumor growth in an H1975 xenograft model than in an A431 xenograft model.[112] Reversible pteridine-7(8*H*)-one inhibitors of FMS-like tyrosine kinase 3 (FLT3) **362**, a target for acute myeloid leukemia were developed from the structure of the irreversible EGFR inhibitor **360**, replacing the Michael acceptor with an amine. These exhibited nanomolar inhibition of FLT3 and selectivity against leukemia cells with the FLT3 mutation.[111]

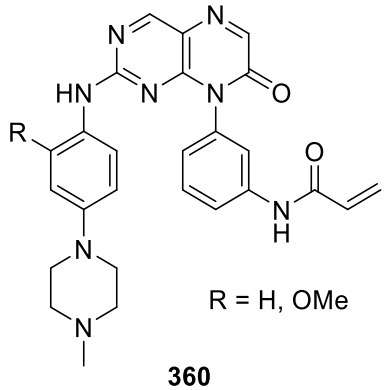

360

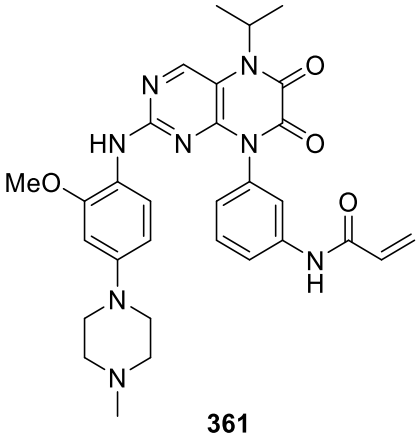

361

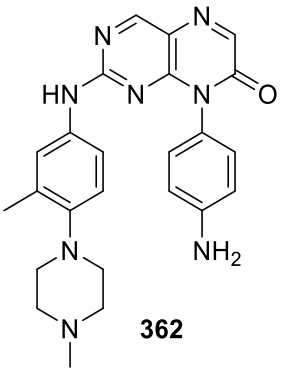

362

<Figure 31>

Polo-like kinases 1-3 (Plk1/Plk2/Plk3) have been targets of interest in cancer and other therapies. Plk1 is a specific serine-threonine kinase that is of interest as a target in cancer and Plk1 inhibitor drug development was the subject of a recent mini-review.[274] Dihydropteridinones were identified as an inhibitor class from a screening program and from this, BI2536 **363** was developed by Boehringer Ingelheim (Figure 32). BI2536 has reached Phase II clinical trials. The related volasertib (BI6727) **364** is in Phase III trials.

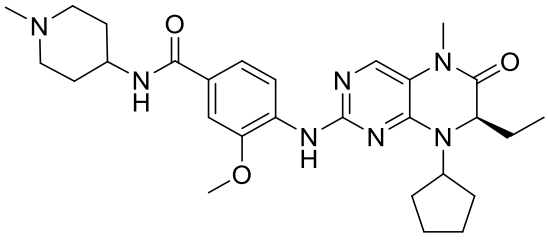

BI2536

363

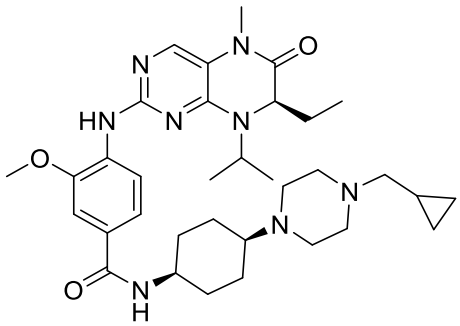

BI6727, Volasertib

364

<Figure 32>

BI2536 inhibits Plk1 with an IC_{50} of 0.83 nM and with 1000-fold selectivity over other kinases.[275] A fluorescent kinase probe based upon a 4,4-difluoro-4-bora-3a,4a-diaza-s-indacene (BODIPY) conjugate of BI2536 has been reported to act as latency reversing agent, reactivating HIV-1 from dormant virus reservoirs, potentially allowing eradication of latent virus reservoirs when administered with an antiretroviral. [276, 277] Plk-1 has a protein-protein interaction domain known as the polo-box domain (PBD), which is unique to a small group of polo-like kinases representing a potentially useful target for selective Plk inhibition. Bifunctional inhibitors linking the BI2536 scaffold to a peptide polo-box domain inhibitor exhibit nanomolar activity against PLk1 PBD with selectivity over the PBDs of Plk2 and Plk3.[120] This scaffold has since generated much interest for development of anti-tumor pteridines. A series of antiproliferative hydrazine-substituted pteridin-6,7-diones, based upon the BI2536 scaffold has recently been reported.[69] Further selective Plk-1 inhibitors have been developed based upon the tetrahydropteridine scaffold of BI2536. Design with a pendant hydroxyl side-chain **365** (Figure 33) targets interactions with polar residues Arg57, Glu69 and Arg134 of Plk-1, in order to enhance potency and selectivity over Plk2/PLk3.[72] BRD4, a member of the BET (bromodomain and extra terminal domain family) is a potential cancer target. BI2536 exhibits activity against BRD4 as well as Plk1. A perspective on dual kinase-bromodomain inhibitors, including the pteridines BI2536, BI6727 and BI-D1870 is available.[278] A library of BI2536 analogues was prepared to explore the SAR against the two targets, Plk1/BRD4. Activity improved by replacing the *N*8-cyclopentyl moiety with a 3-bromobenzyl group. Replacing N at position 2 with O gave 1000-fold selectivity for BRD4 over Plk1, demonstrating the potential for further tuning of activity.[125] Structure guided design has led to alternative analogues that exhibit dual Plk1/BRD4 activity. Introduction of a 7-(*R*)-propyl group increased selectivity for Plk1, whereas replacement of the aromatic methoxy group by cyclopentyloxy led to a series of compounds with potent dual Plk1/BRD4 activity.[279] Assessment of BI2536 and a series of analogues achieved using bioluminescence resonance energy transfer (BRET) gave bromodomain binding measured *via* displacement of a fluorophore-tagged BET bromodomain ligand.[280] Structure-based design based on BI2536 has also enabled tuning of kinase selectivity, to give **366**, with increased activity against anaplastic lymphoma kinase (ALK) and maintaining BRD4 activity, whilst exhibiting reduced Plk-1 activity.[281]

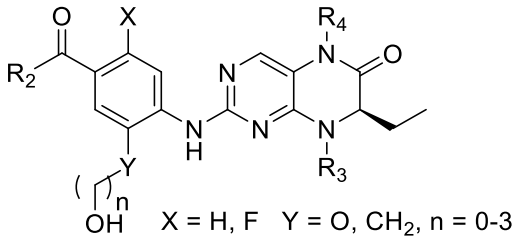

365

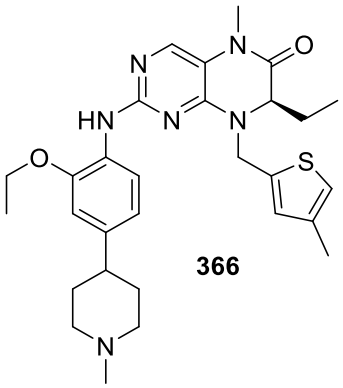

366

<Figure 33>

BI2536 was used as the scaffold for development of dual TAF1 and BET bromodomain inhibitors, eventually moving away from the pteridine scaffold to a dihydropyridopyrazinone core.[282] Further advances developed fused tricyclic analogues, of which recent examples include the 5,6-dihydroimidazolo [1,5-*f*]pteridine[124], [1,2,4]triazolo[4,3-*f*]pteridinone[61, 70, 121] and

7-aminotetrazolo[1,5-*f*]pteridinone[71] scaffolds. Selective polo-like kinase-2 (Plk2) inhibitors based on the modelling of the tetrahydropteridinyl scaffold in BI2536 with the Plk isoenzymes led to two inhibitor series, including an arylsulfonamide **367** (Figure 34), to target Lys86 or an indole **368** to target Tyr161. These most active compounds inhibited Plk2 in the single nanomolar range and exhibited selectivity for Plk2 over Plk1 and Plk3 with antitumor activity in six Plk2-epxressing cancer cell lines.[71]

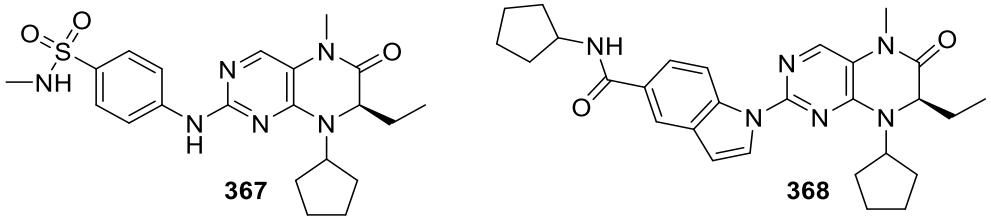

367 **368**

<Figure 34>

Plk2 is also a potential target in Parkinson's disease. A series of dihydropteridinones was prepared, giving nanomolar activity against Plk-2, with selectivity for Plk-2 over Plk-1. Compound **369** represents the analogue chosen for Plk-2 selectivity and favorable bioavailability, being able to cross the blood-brain barrier and not acting as a substrate for Pgp-mediated efflux (Figure 35). Functional effects in animal models reduce levels of Ser-129 phosphorylated α-synuclein in the cerebral cortex.[119] Investigation of a number of bicyclic heterocycle scaffolds identified the substituted 4-amino-2-thiopteridine-7[8*H*]-one **370**, as a potent inhibitor of the CXCR2 chemokine receptor, IC_{50} 1 nM. Although these were superseded by the thiazolo[4,5-*d*]pyrimidine-2(3*H*)-one scaffold as the preferred core.[283] The ionotropic glutamate receptor iGluA2 is a potential drug target for a number of neurological conditions, with *in silico* screening identifing four potential scaffolds, including 10-2 (methoxyethyl)-3-phenylbenzo[*g*]pteridine-2,4-dione **371**.[284]

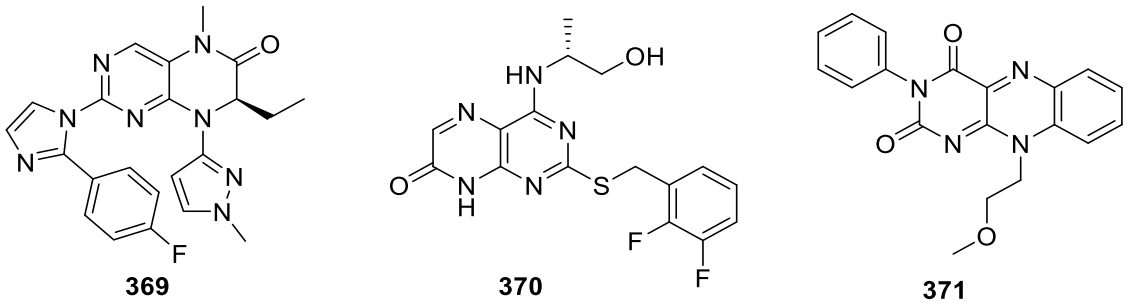

369 **370** **371**

<Figure 35>

The bis-isoalloxazine **372** demonstrated activity relevant to neurodegenerative conditions such as Alzheimer and Creuzfeld-Jakob disease, where there is aggregation of harmful amyloid peptides or prion proteins. Compound **372** strongly inhibited the association of amyloid-β peptide and reduced association of pathogenic prion protein, as measured by flow cytometry, using fluorescence-labelled peptides (Figure 36).[285]

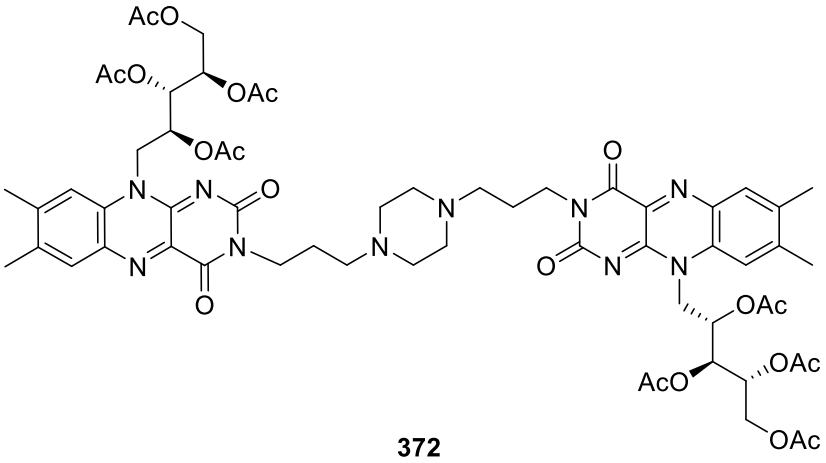

372

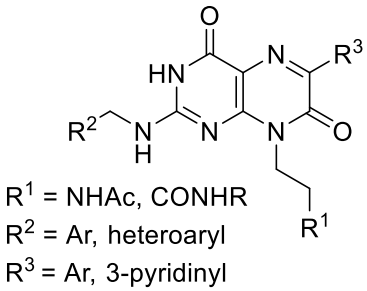

373

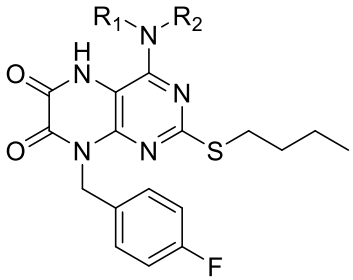

374

<Figure 36>

Screening hits were the starting point for development of selective inhibitors **373** of stearoyl-CoA desaturase, a potential target against obesity and type II diabetes.[286] Pteridinones have demonstrated activity against Gram-positive bacterial glutamate racemase, MurI, a key enzyme in the biosynthesis of a peptidoglycan precursor. Scaffold hopping from 9-benzylpurines and further elaboration in positions 2, 4 and 8 furnished analogues of general structure **374** with MurI IC_{50} values in the micromolar range, favourable solubility profiles and some modest antibacterial activity against *S. aureus*.[101]

A series of pterin-sulfonamide structures, based upon the hybrid concept of sulfonamide antibacterials bound to a mimic of the natural enzyme substrate, act as dihydropteroate synthase (DHPS) inhibitors. The compounds inhibit DHPS in a competition assay at lower concentrations than sulfamethoxazole, however in an antibacterial assay against *E. coli*, they are around 10 times less potent than the parent sulfonamide. A crystal structure of compound **375** (Figure 37) bound to *Yersinia pestis* DHPS (5JQ9) demonstrates that this compound occupies the substrates' pterin and *p*ABA binding pockets, closely mimicking binding modes. Therefore, the lower antibacterial activity could be attributed to poorer cell penetration and/or increased drug efflux.[79] Pteridine-2,4,7(1*H*,3*H*,8*H*)-triones **376** exhibit some radical scavenging activity, weak antibacterial activity and good antifungal activity (equivalent MICs to ketoconazole against *C. albicans*).[85] Computational pharmacophore design led to a series of thirty pteridines as potential HIV-1 integrase inhibitors, of which six were synthesized and

evaluated for inhibition of HIV-1 replication *in vitro*.[113] TGFβ-R_1 kinase inhibitors were the starting point for discovery and optimization of pteridines with antiviral effects against the hepatitis C virus. 4-[2-(5-Bromo-2-fluoro-phenyl)pteridin-4-ylamino]-*N*-[3-(2-oxopyrrolidin-1-yl)propyl]nicotinamide **377** was the most potent of the series, with EC_{50} for replication inhibition of 64 nM.[128] Toll-like receptor 7 (TLR7) is an important component of the immune system response to viral pathogens, particularly hepatitis B and C. Development of pteridinone TLR7 agonists led to GS-9620 **378**, which entered clinical trials for chronic hepatitis B infection.[63]

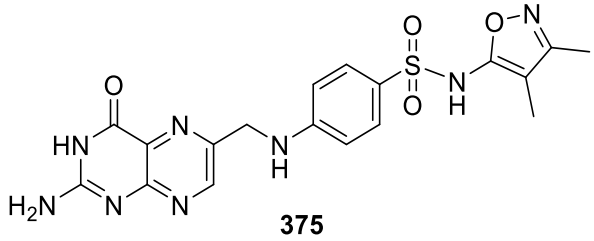

375

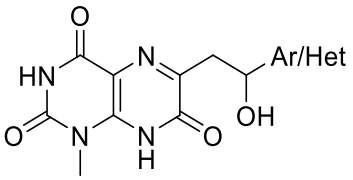

376

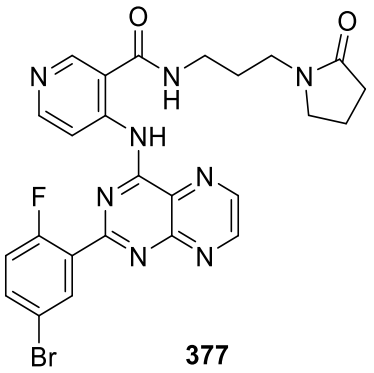

377

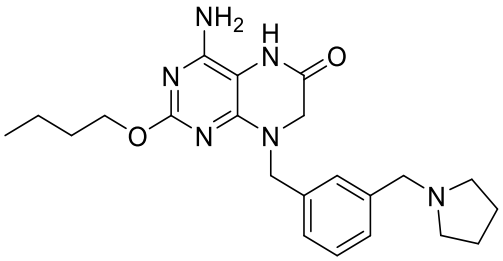

378, GS-9620

<Figure 37>

10.18.10.9 Toxicology

Folic acid **8** was shown to be phototoxic and photogenotoxic in cells by two separate mechanisms. Extracellular folic acid photoexcitation by irradiation with 360 nm UVA, leads to photodegradation and the production of H_2O_2, causing DNA strand breaks. A second mechanism via photoexcitation of intracellular folic acid leads to DNA damage by oxidative modification of purine bases.[287] Neopterin **46** is of interest for its physiological effects and acts as an endogenous cognitive enhancer.[288] Neopterin **46** is a biomarker for exhaustive exercise-induced inflammation due to the inflammatory upregulation of GTP cyclohydrolase-1. This leads to a metabolic “block” on the tetrahydrobiopterin biosynthetic pathway, leading to higher levels of the **46** precursor. Raised **46** levels induce improved cellular antioxidant response.[289] Tetrahydrobiopterin **45** is vital for a number of processes and is essential for immune response to cancer through T cell production. Low levels of **45** are associated with reduced T cell proliferation and immune response. However, in autoimmune diseases T cell proliferation leads to inflammation. Reduction of tetrahydrobiopterin **45** production by administering an inhibitor of sepiapterin reductase (the final step of the biosynthesis) leads to a reduction in T

cell mediated inflammation.[290] Pathologically high levels of **45** are also associated with chronic inflammatory and neuropathic pain. Damaged sensory neurons and macrophages produce excess tetrahydrobiopterin **45**, which is associated with pain hypersensitivity. Administration of a sepiapterin reductase inhibitor reduces hypersensitivity without affecting normal pain sensations.[291]

10.18.10.10 Nanochemistry

Nanoparticles for delivery of folates, in both a therapeutic setting and for use in diagnostic applications, have attracted recent interest. Mixed molecular nanostructures of folic acid and gallium(II)-deferrioxamine (contrast agent) attached to a gold-mercaptopropionic surface were able to capture 4T1 mouse breast cancer cells via binding with tumor folate receptors, demonstrating potential for use in a diagnostic and/or therapeutic application. The folic acid was attached at the 2-amino position of the pteridine to ensure no interference with the receptor binding regions of the molecule.[292] Theranostic nanoparticles of methotrexate linked to manganese oxide by a pH-sensitive polyacrylic acid linker have potential as MRI contrast agents and were able to selectively capture 4T1 mouse breast cancer cells.[293] Folic acid - magnetite nanoparticles were prepared and characterized. Magnetite particles were functionalized with aminopropyltriethoxysilane, and the resulting amine-functionalized nanoparticles conjugated to folic acid **8** using DCC coupling. The pterin ring remained available for folate receptor binding, so that these nanoparticles have potential for use in therapeutic and diagnostic settings.[294] Surface-enhanced Raman scattering (SERS) spectroscopy was used to determine the adsorption of **8** onto gold nanopillar structures,[295] and onto a gold nanoparticle surface in the absence and presence of surface modifiers.[296] Folic acid-conjugated boron nitride nanoparticles have been prepared for targeted cancer delivery. Boron nitride nanoparticles (BNNPs) were functionalized by plasma surface polymerization with ethene and carbon dioxide. The carboxylate nanoparticles were coupled to ethylenediamine, and the resulting amino-functionalized BNNPs conjugated to the γ-COOH of folic acid via DCC activation.[297]

References

1. Suckling, C.; Gibson, C.; Huggan, J. in *Comprehensive Heterocyclic Chemistry III*, Jones, R., Ed.; Katritzky, A. R., Ramsden C. A., Scriven, E. F. V., Taylor, R. J. K., Eds.; Elsevier Science: Oxford, UK, 2008; vol. 10, pp 915-975. Chapter 10.18.
2. Ohta, K.; Wrigglesworth, R.; Wood, H. C. S. In *Rodd's Chemistry of Carbon Compounds: A Modern Comprehensive Treatise* 2nd Ed., Coffey, S., Ed., Elsevier Science: Oxford, UK, 2008, Vol. 4, pp 237-289.
3. Pfleiderer, W. *Second Supplements to the 2nd Edition of Rodd's Chemistry of Carbon Compounds: A Modern Comprehensive Treatise,* Coffey, S., Ed., Elsevier Science: Oxford, UK, 2008, Vol. 4, pp 269-330.
4. Hamon, C. G. B.; Blair, J. A. In *Supplements to the 2nd Edition of Rodd's Chemistry of Carbon Compounds: A Modern Comprehensive Treatise* Coffey, S., Ed., Elsevier Science: Oxford, UK, 2009, Vol. 4-4, pp 129-154.
5. Rinderspacher, K. A. *Progress in Heterocyclic Chemistry.* **2016**, *28*, 439-492. http://dx.doi.org/10.1016/B978-0-08-100755-6.00013-2
6. Rinderspacher, K. A. *Progress in Heterocyclic Chemistry.* **2017**, *29*, 441-4828. https://doi.org/10.1016/B978-0-08-102310-5.00013-8
7. Rinderspacher, K. A. *Progress in Heterocyclic Chemistry.* **2018**, *30*, 357-398. https://doi.org/10.1016/B978-0-08-102788-2.00013-1
8. Hiebel, M.-A.; Suzenet, F. *Progress in Heterocyclic Chemistry*. **2020**, *31*, 505-531. https://doi.org/10.1016/B978-0-12-819962-6.00014-2
9. Rinderspacher, K. A. *Progress in Heterocyclic Chemistry.* **2020**, *31*, 465-504. https://doi.org/10.1016/B978-0-12-819962-6.00013-0
10. Fuqua, C.; Feirer, N. *Pteridines.* **2017**, *28*, 23-36. https://doi.org/10.1515/pterid-2016-0012
11. Goswami, S.; Das, M. K.; Sain, D.; Goswami, B. *Pteridines*. **2018**, *29*, 15-41. https://doi.org/10.1515/pteridines-2018-0002
12. Daubner, S. C.; Fitzpatrick, P. F. *In Encyclopedia of Biological Chemistry, 2*nd Ed., Academic Press, London, UK, 2013, pp 666-669.
13. Reibnegger, G. *Pteridines.* **2014**, *25*, 41-48. https://doi.org/10.1515/pteridines-2014-0005
14. Reibnegger, G. *Pteridines.* **2015**, *26*, 135-142. https://doi.org/10.1515/pterid-2015-0008
15. Soniat, M.; Martin, C. B. *Pteridines.* **2008**, *19*, 120-124.
16. Soniat, M.; Martin, C. B. *Pteridines.* **2009**, *20*, 124-128.
17. Nekkanti, S.; Martin, C. B. *Pteridines.* **2015**, *26*, 13-22. https://doi.org/10.1515/pterid-2014-0011
18. Ji, H.-F.; Shen, L. *Pteridines.* **2011**, *22*, 73-76.
19. Reibnegger, G. *ChemistrySelect.* **2018**, *3*, 10925-10931. https://doi.org/10.1002/slct.201802368
20. Vargas, R.; Martinez, A. *Phys. Chem. Chem. Phys.* **2011**, *13*, 12775–12784. https://doi.org/10.1039/c1cp20134d
21. Illán-Cabeza, N. A.; Peña-Ruiz, T.; Moreno-Carretero, M. N. *J. Mol. Model.* **2012**, *18*, 815-824. https://doi.org/10.1007/s00894-011-1109-1
22. Biaso, F.; Burlat, B.; Guigliarelli, B.; *Inorg. Chem.* **2012**, *51*, 3409-3419. http://dx.doi.org/10.1021/ic201533p

23. Li, L.; Cai, T.; Wang, Z.; Zhou, Z.; Geng, Y.; Sun, T. *Spectrochim. Acta, Part A.* **2014**, *120*, 106-118. https://doi.org/10.1016/j.saa.2013.10.011
24. Ayyappan, S.; Sundaraganesan, N.; Aroulmoji, V.; Murano, E.; Sebastian, S. *Spectrochim. Acta, Part A.* **2010**, *77*, 264-275. http://dx.doi.org/10.1016/j.saa.2010.05.021
25. Prabavathi, N.; Nilufer, A.; Krishnakumar, V. *Spectrochim. Acta, Part A.* **2012**, *99*, 292-302. https://doi.org/10.1016/j.saa.2012.09.003
26. Sakai, K.; Nagahara, K.; Yoshii, Y.; Hoshino, N.; Akutagawa, T. *J. Phys. Chem.* A. **2013**, *117*, 3614-3624. https://doi.org/10.1021/jp401528c
27. Baisya, S. S.; Ghosh, B.; Roy, P. S. *Acta Crystallogr., Sect. E: Crystallogr. Commun.* **2015**, *71*, m162-m163. http://dx.doi.org/10.1107/S2056989015014619
28. Stevenson, R.; Stokes, R. J.; MacMillan, D.; Armstrong, D.; Faulds, K.; Wadsworth, R.; Kunuthur, S.; Suckling, C. J.; Graham, D. *Analyst.* **2009**, *134*, 1561-1564. http://dx.doi.org/10.1039/b905562b
29. Pauszek, R. F. III; Kodali, G.; Stanley, R. J. *J. Phys. Chem. A*, **2014**, *118*, 8320-8328. https://doi.org/10.1021/jp501143u
30. Kodali, G.; Narayanan, M.; Stanley, R. J. *J. Phys. Chem.* B. **2012**, *116*, 2981-2989. http://dx.doi.org/10.1021/jp2110083
31. Yang, K.-D.; Peng, P.; Ge, L.; Wen, Y.-X.; Long, Y.-F.; Song, Y. *J. Chem. Eng. Chin. Univ.* **2011**, *25*, 699-702.
32. Zimnicka, M.; Troć, A.; Ceborska, M.; Jakubczak, M.; Koliński, M.; Danikiewicz, W. *Anal. Chem.* **2014**, *86*, 4249-4255. http://dx.doi.org/10.1021/ac4039042
33. Miyazaki, S.; Okhubo, K.; Kojima, T.; Fukuzumi, S. *Angew. Chem. Int. Ed.* **2008**, *47*, 9669 –9672. https://doi.org/10.1002/anie.200802835
34. DiScipio, R. M.; Santiago, R. Y.; Taylor, D.; Crespo-Hernández, C. E. *Phys. Chem. Chem. Phys.* **2017**, *19*, 12720-12729. https://doi.org/10.1039/C7CP01574G
35. Xiang, D.; Magana, D.; Dyer, R. B.; *J. Am. Chem. Soc.* **2014**, *136*, 14007-14010. http://dx.doi.org/10.1021/ja5081103
36. Saveant, J.-M.; Tard, C.; *J. Am. Chem. Soc.* **2016**, *138*, 1017-1021. https://doi.org/10.1021/jacs.5b12138
37. Lim, C.-H.; Holder, A. M.; Hynes, J. T.; Musgrave, C. B. *J. Phys. Chem. B.* **2017**, *121*, 4158-4167. https://doi.org/10.1021/acs.jpcb.7b01224
38. He, R.-X.; Zha, D.-W. *J. Electroanal. Chem.* **2017**, *791*, 103-108. https://doi.org/10.1016/j.jelechem.2017.03.026
39. Hoke, K. R.; Crane, B.R. *Nitric Oxide.* **2009**, *20*, 79-87. https://doi.org/10.1016/j.niox.2008.11.002.
40. Milletti, F.; Storchi, L.; Goracci, L.; Bendels, S.; Wagner, B.; Kansy, M.; Cruciani, G. *Eur. J. Med. Chem.* **2010**, *45*, 4270-4279. https://doi.org/10.1016/j.ejmech.2010.06.026.
41. Suckling, C. J. *IUBMB Life*. **2013**, *65*, 283–299. https://doi.org/10.1002/iub.1148.

42. 42 Lorente, C.; Petroselli, G.; Dántola, M. L.; Oliveros, E.; Thomas, A. H. *Pteridines*. **2011**, 22,111 – 119.
43. Liu, L.; Yang, D.; Li, P. *J. Phys. Chem, B.* **2014**, *118*, 11707-11714. http://dx.doi.org/10.1021/jp5082017.
44. Denofrio, M. P.; Thomas, A. H.; Braun, A. M.; Oliveros, E.; Lorente, C. *J. Photochem. Photobiol., A.* **2008**, *200*, 282-286. http://dx.doi.org/10.1016/j.jphotochem.2008.08.003.

45. Denofrio, M. P.; Hatz, S.; Lorente, C.; Cabrerizo, F. M.; Ogilby, P. R.; Thomas, A. H. *Photochem. Photobiol. Sci*. **2009**, 8, 1539–1549. https://doi.org/10.1039/B9PP00020H.
46. Simkovitch, R.; Huppert, D. *J. Phys. Chem. B.* **2017**, *121*, 129-142. https://doi.org/10.1021/acs.jpcb.6b10828.

47. Juzeniene, A.; Grigalavicius, M.; Ma, L. W.; Juraleviciute, M.; *J. Photochem. Photobiol., B.* **2016**, *155*, 116-121. http://dx.doi.org/10.1016/j.jphotobiol.2016.01.001 .

48. Hsu, M.-H.; Tsai, C.-J.; Lin, A. Y.-C. *J. Hazard. Mater.* **2019**, *373*, 468-475. https://doi.org/10.1016/j.jhazmat.2019.03.095.
49. Jungmann, O.; Pfleiderer, W. *Nucleosides*, *Nucleotides Nucleic Acids*. **2009**. *28*, 550–585. https://doi.org/10.1080/15257770903054241.
50. Abbas, Z. A. A.; Abu-Mejdad, N. M. J.; Atwan, Z. W.; Al-Masoudi, N. A. *J. Heterocyclic Chem.*, **2017**, *54*, 895-903. https://doi.org/10.1002/jhet.2651.
51. Das, M. K.; Goswami, S.; Quah, C. K.; Fun, H.–K. *Tetrahedron Lett*. **2016**, 57, 3277–3280. https://doi.org/10.1016/j.tetlet.2016.06.031
52. Khalymbadzha, I. A.; Fatykhov, R. F.; Chupakhin, O. N.; Charushin, V. N.; Tseitler. T. A.; Sharapov, A. D.; Inytina, A. K.; Kartsev, V. G. *Synthesis.* **2018**, *50*, 2423–2431. https://doi.org/10.1055/s-0037-1609482
53. Žurek, J.; Svobodová, E.; Šturala, J.; Dvořáková, H.; Svoboda, J.; Cibulka, R. *Tetrahedron: Asymmetry*. **2017**, *28*, 1780–1791. https://doi.org/10.1016/j.tetasy.2017.10.029
54. Pruet, J. M.; Robertus, J. D.; Anslyn. E. V*. Tetrahedron Lett*. **2010**, *51*, 2539–2540. https://doi.org/10.1016/j.tetlet.2010.03.008
55. Perez, C. E.; Park, H. B.; Crawford, J. M. *Biochemistry.* **2018**, *5*7, 354−361. https://doi.org/10.1021/acs.biochem.7b00863
56. Pontiki, E.; Hadjipavlou-Litina, D.; Patsilinakos, A.; Tran, T. M.; Marson, C. M. *Future Med. Chem.* **2015**, *7*, 1937–1951. https://doi.org/10.4155/fmc.15.104
57. Gliszczyńska-Świgło, A.; Muzolf, M. *J. Agric. Food. Chem.* **2007**, *55*, 8237-8242. https://doi.org/10.1021/jf070986x
58. Baxter-Parker, G.; Prebble, H. M.; Cross, S.; Steyn, N.; Shchepetkina, A.; Hock, B. D.; Cousins, A. Gieseg, S. P. *Free Radical Biol. Med.* **2020**, *152*, 142-151. https://doi.org/10.1016/j.freeradbiomed.2020.03.002
59. Vignoni, M.; Lorenter, C.; Cabrerizo, F. M.; Erra-Balsells, R.; Oliveros, E.; Thomas, A. H. *Photochem. Photobiol. Sci.* **2012**, *11*, 979-987. https://doi.org/10.1039/C2PP05363B
60. Mokaber-Esfahani, M.; Eshghi, H.; Shiri, A.; Akbarzadeh, M.; Mirzaei, M. *J. Chem. Res.* **2015**, *39*, 216-219. https://doi.org/10.3184/174751915X14271341601550
61. Wang, N. –Y.; Xu, Y.; Xiao, K. –J.; Zuo, W. -Q.; Zhu, Y. -X.; Hu, R.; Wang, W. –L.; Shi, Y. –J.; Yu, L. –T.; Liu, Z. –H. *Eur. J. Med. Chem*. 2020, 191, 112152. https://doi.org/10.1016/j.ejmech.2020.112152
62. Greco, G. E.; Conrad, Z. A.; Johnston, A. M.; Li, Q.; Tomkinson, A. E.; *Tetrahedron Lett*. **2016**, *57*, 3204–3207. https://doi.org/10.1016/j.tetlet.2016.06.037
63. Roethle, P. A.; McFadden, R. M.; Yang, H.; Hrvatin, P.; Hui, H.; Graupe, M.; Gallagher, B.; Chao, J.; Hesselgesser, J.; Duatschek, P.; Zheng, J.; Lu, B.; Tumas, D. B.; Perry, J.; Halcomb, R. L. *J. Med. Chem*. **2013**, *56*, 7324−7333. https://doi.org/10.1021/jm400815m

64. Gliszczynska-Swiglo, A.; Szymusiak, H. *Acta Toxicol.* **2007**, *15*, 63-68.
65. Estarellas, C.; Frontera, A.; Quiñonero, D.; Deyà, P. M. *Phys. Chem. Chem. Phys*. **2011**, *13*, 16698–16705. https://doi.org/10.1039/C1CP21685F
66. Telegina, T. A.; Lyudnikova, T. A.; Bluglak, A. A.; Vechtomova, Y. L.; Biryukov, M. V.; Demin, V. V.; Kritsky, M. S. *J. Photochem. Photobiol., A.* **2018**, *354*, 155-162. https://doi.org/10.1016/j.jphotochem.2017.07.029
67. Adcock, J.; Gibson, C. L.; Huggan, J. K.; Suckling, C. J. *Tetrahedron*. **2011**, *67*, 3226-3237. https://doi.org/10.1016/j.tet.2011.03.011
68. Geng, P. F.; Wang, C. C.; Li, Z. H.; Hu, X. N.; Zhao, T. Q.; Fu, D. J.; Zhao, B.; Yu, B.; Liu, H. M. *Eur. J. Med. Chem*. **2018**, *143*, 1959-1967. https://doi.org/10.1016/j.ejmech.2017.11.009
69. Li, Z.; Xu, L.; Zhu, L.; Zhao, Y.; Hu, T.; Yin, B.; Liu, Y.; Hou, Y. *Bioorg. Med. Chem. Lett.* **2020**, *30*, 127329. https://doi.org/10.1016/j.bmcl.2020.127329
70. Hou, Y.; Zhu, L.; Li, Z.; Shen, Q.; Xu, Q.; Li, W.; Liu, Y.; Gong, P. *Eur. J. Med. Chem.* **2019**, *163*, 690-709. https://doi.org/10.1016/j.ejmech.2018.12.009
71. Zhan, M. -M.; Yang, Y.; Luo, J.; Zhang, X. -X.; Xiao, X.; Li, S.; Cheng, K.; Xie, Z.; Tu, Z.; Liao, C. *Eur. J. Med. Chem.* **2018**, *143*, 724-731. https://doi.org/10.1016/j.ejmech.2017.11.058
72. Lv, X.; Yang, X.; Zhan, M. –M.; Cao, P.; Zheng. S.; Peng, R.; Han, J.; Xie, Z.; Tu. Z.; Liao, C. Eur. *J. Med. Chem*. **2019**, *184*,111769. https://doi.org/10.1016/j.ejmech.2019.111769
73. Wang, H.; Yang, C.; Doherty, J. R.; Roush, W. R.; Cleveland, J. L.; Bannister, T. D. *J. Med. Chem*. **2014**, *57*, 7317−7324. https://doi.org/10.1021/jm500640x
74. Gulevskaya, A. V.; Dang, S. V.; Tyaglivy, A. S.; Pozharskii, A. F.; Kazheva, O. N.; Chekhlov, A. N.; Dyachenko, O. A. *Tetrahedron*. **2010**, *66*, 146–151. http://dx.doi.org/10.1016/j.tet.2009.11.039

75. Shi, G.; Ji, X. *Tetrahedron Lett*. **2011**, *52*, 6174–6176. https://doi.org/10.1016/j.tetlet.2011.09.047
76. Kuroda, Y.; Isarai, K.; and Murata, S. *Heterocycl. Commun*. **2012**; *18*, 117–122. https://doi.org/10.1515/hc-2012-0046
77. Nxumalo, W.; Dinsmore, A. *Nat. Prod. Commun.* **2014**, *9*, 37-38. https://doi.org/10.1177%2F1934578X1400900112
78. Quotadamo, A.; Linciano, P.; Costi, M. P.; Venturelli, A. *ChemistrySelect.* **2019**, *4*, 4429 –4433. https://doi.org/10.1002/slct.201900721
79. Zhao, Y.; Shadrick, W. R.; Wallace, M. J.; Wu, Y.; Griffith, E. C.; Qi, J.; Yun, M.; White, S. W.; Lee, R. E. *Bioorg. Med. Chem. Lett*. **2016**, *26*, 3950–3954. https://doi.org/10.1016/j.bmcl.2016.07.006

80. Heizmann, G.; Pfleiderer, W. *Helv. Chim. Acta*. **2007**, *90*, 1856-1873. https://doi.org/10.1002/hlca.200790195
81. Bockman, A. R.; Pruet, J. M. *Beilstein J. Org. Chem*. **2020**, *16*, 509–514. https://doi.org/10.3762/bjoc.16.46
82. Gulevskaya, A. V.; Dang, S. V.; Tyaglivy, A. S.; Pozharskii, A. F.; Kazheva, O. N.; Chekhlov, A. N.; Dyachenko, O. A. *Tetrahedron*. **2010**, 66, 146–151. https://doi.org/10.1016/j.tet.2009.11.039

83. Gulevskaya, A. V.; Nguyen, H. T. L.; Tyaglivy, A. S. Pozharskii, A. F. *Tetrahedron*. **2012**, *68*, 488-498. https://doi.org/10.1016/j.tet.2011.11.018
84. Gulevskaya, A. V.; Pozharskii, A. F. *Russ. Chem. Rev.* **2011**, *80*, 495-529. https://doi.org/10.1070/rc2011v080n06abeh004168
85. Kazunin, M. S.; Voskoboynik, O. Y.; Nosulenko, I. S.; Berest, G. G.; Kholodniak, S. V.; Pryymenko, B. O.; Kovalenko, S. I. *J Heterocyclic Chem*. **2020**, *57*, 268–280. https://doi.org/10.1002/jhet.3774
86. Steinlin, T.; Sonati, T.; Vasella, A. *Helv. Chim. Acta.* **2008**, *91*, 1879-1887. https://doi.org/10.1002/hlca.200890201
87. Ali, H. I.; Ashidab, N.; Nagamatsu. T. *Bioorg. Med. Chem*. **2008**, *16*, 922–940. https://doi.org/10.1016/j.bmc.2007.10.014
88. Jiménez-Pulido, S. B.; Linares-Ordóñez, F. M.; Martínez-Martos, J. M.; Moreno-Carretero, M. N.; Quirós-Olozábal, M.; Ramírez-Expósito, M. J. *J. Inorg. Biochem.* **2008**, *102*, 1677-1683. https://doi.org/10.1016/j.jinorgbio.2008.04.004
89. Kojima, T.; Inui, Y.; Miyazaki, S.; Shiro, M.; Fukuzumi, S. *Chem. Commun.* **2009**, 6643-6645. https://doi.org/10.1039/b911033j
90. Martinez, A.; Vargas, R. *New J. Chem.* **2010**, *34*, 2988-2995. https://doi.org/10.1039/b9nj00805e
91. Ahmed, S. A.; Elghandour, A. H.; Elgendy, H. S. *Der Pharma Chimica.* **2014**, *6*, 194-219.
92. Pfleiderer, W.; in *Comprehensive Heterocyclic Chemistry II*, Ramsden, C. A., Ed.; Katritzky, A. R.; Rees, C. W.; Scriven, E. F. V.; Eds.; Elsevier Science: Oxford, UK, 1996: vol. 7, pp 679-736. Chapter 7.18.
93. Taghavi-Moghadam, S.; Pfleiderer, W. *Tetrahedron Lett*. **1997**, 38, 6835. https://doi.org/10.1016/S0040-4039(97)01619-5
94. Palanki, M. S. S.; Dneprovskaia, E.; Doukas, J.; Fine, R. M.; Hood, J.; Kang, X.; Lohse, D.; Martin, M.; Noronha, G.; Soll, R. M. Wrasidlo, W.; Yee, S.; Zhu, H. *J. Med. Chem*. **2007**, *50*, 4279-4294. https://doi.org/10.1021/jm051056c
95. Giorgi, I.; Biagi, G.; Livi, O.; Leonardi, M.; Scartoni, V.; Pietra, D. *Arch*. *Pharm. Chem. Life Sci*. **2007**, *340*, 81–87. https://doi.org/10.1002/ardp.200600168
96. El-Sabbagh, O. I.; El-Sadek, M. E.; El-Kalyoubi, S.; Ismail, I. *Arch. Pharm. Chem. Life Sci*. **2007**, *340*, 26–31. https://doi.org/10.1002/ardp.200600149
97. Hanaya, T.; Baba, H.; Yamamoto, H. *Carbohydrate Res*. **2007**, *342*, 2159–2162. https://doi.org/10.1016/j.carres.2007.06.017
98. Hanaya, T.; Baba, H.; Toyota, H.; Yamamoto, H. *Tetrahedron*. **2008**, *64*, 2090-2100. https://doi.org/10.1016/j.tet.2007.12.042
99. Zhang, F.L.; Schweizer, W. B.; Xu, M.; Vasella, A. *Helv.Chim. Acta*. **2007**, *90*, 521-534. https://doi.org/10.1002/hlca.200790054
100. Ali, H.; Tomita, K.; Akaho, E.; Kambara, H.; Miura, S.; Hayakawa, H.; Ashida, N.; Kawashima, Y.; Yamagishi, T.; Ikeya, H.; Yoneda, F.; Nagamatsu, T. *Bioorg. Med.Chem.* **2007**, *15*, 242–256. https://doi.org/10.1016/j.bmc.2006.09.063
101. Breault, G. A.; Comita-Prevoir, J.; Eyermann, C. J.; Geng, B.; Petrichko, R.; Doig, P.; Gorseth, E.; Noonan, B. *Bioorg. Med. Chem. Lett*. **2008**, *18*, 6100–6103. https://doi.org/10.1016/j.bmcl.2008.10.022.
102. Jiménez-Pulido, S. B.; Linares-Ordóñez, F. M.; Moreno-Carretero, M. N.; Quirós-Olozábal, M. *Inorg. Chem*. **2008**, *47*, 1096-1106. https://doi.org/10.1021/ic701994s.

103. Ma, F.; Lü, G.; Zhou, W. F.; Wang, Q. J.; Zhang, Y. H; Yao, Q. Z. *Arch. Pharm. Chem. Life Sci*. **2009**, *342*, 274 – 280. https://doi.org/10.1002/ardp.200800192.
104. Ma, F.; Lü, G.; Zhou, W. F.; Wang, Q. J.; Zhang, Y. H; Yao, Q. Z. *Chin. Chem.Lett.* **2009**, *20*, 420–422. https://doi.org/10.1016/j.cclet.2008.12.012.
105. De Jonghe, S.; Marchand, A.; Gao, L. J.; Calleja, A.; Cuveliers, E.; Sienaert, I.; Herman, J.; Clydesdale, G.; Sefrioui, H.; Lin, Y.; Pfleiderer, W.; Waer, M.; Herdewijn. P. *Bioorg*. *Med. Chem. Lett*. **2011**, *21*,145–149. http://dx.doi.org/10.1016/j.bmcl.2010.11.053.
106. Sun, C. L.; Li, X.; Yan, Z. Bioactive compounds for treatment of cancer and neurodegenerative diseases. WO2009,139834,A1, 2009.
107. Li, X.; Shocron, E.; Song, A.; Patel, N.; Sun, C. L. *Bioorg. Med. Chem. Lett*. **2009**, *19*, 2860–2864. http://dx.doi.org/10.1016/j.bmcl.2010.11.053
108. Zhou, W.; Liu, X.; Tu, Z.; Zhang, L.; Ku, X.; Bai, F.; Zhao, Z.; Xu, Y.; Ding, K.; Li, H. *J. Med. Chem*. **2013**, 56, 7821−7837. https://doi.org/10.1021/jm401045n.
109. Li, Z. H.; Zhao, T. Q.; Liu X. Q.; Zhao, B.; Wang, C.; Geng, P. F.; Cao, Y. Q.; Fu, D. J.; Jiang, L. P.; Yu, B.; Liu, H. M. *Eur. J. Med. Chem*. **2018**, *143*, 1396-1405. https://doi.org/10.1016/j.ejmech.2017.10.037
110. Dzierba, C. D.; Sielecki, T. M.; Arvanitis, A. G.; Galka, A.; Johnson, T. L.; Takvorian, A. G.; Rafalski, M.; Kasireddy-Polam, P.; Vig, S.; Dasgupta, B.; Zhang, G.; Molski, T. F.; Wong, H.; Zaczek, R. C.; Lodge, N. J.; Combs, A. P.; Gilligan, P. J.; Trainor, G. L.; Bronson, J. J.; Macor, J. E. *Bioorg. Med. Chem. Lett*. **2012**, *22*, 4986–4989. http://dx.doi.org/10.1016/j.bmcl.2012.06.034
111. Sun, D.; Yang, Y.; Lyu , J.; Zhou, W.; Song, W.; Zhao, Z.; Chen, Z.; Xu, Y.; Li, H. *J. Med. Chem*. **2016**, *59*, 6187−6200. https://doi.org/10.1021/acs.jmedchem.6b00374
112. Hao, Y.; Wang, X.; Zhang, T.; Sun, D.; Tong, Y.; Xu, Y.; Chen, H.; Tong, L.; Zhu, L.; Zhao, Z.; Chen, Z.; Ding, J.; Xie, H.; Xu, Y.; Li, H. *J. Med. Chem*. **2016**, *59*, 7111−7124. https://doi.org/10.1021/acs.jmedchem.6b00403
113. Bhatt, H.; Patel, P.; Pannecouque, C. *Chem Biol Drug Des*. **2014**, *83*, 154-166. https://doi.org/10.1111/cbdd.12207
114. Clinch, K.; Watt, D. K.; Dixon, R. A.; Baars, S. M.; Gainsford, G. J.; Tiwari, A.; Schwarz, G.; Saotome, Y.; Storek, M.; Belaidi, A. A.; Santamaria-Araujo, J. A. *J. Med. Chem*. **2013**, *56*, 1730−1738. https://doi.org/10.1021/jm301855r
115. Kvassiouk, E.; Charubala, R.; Pfleiderer, W. *Helvetica Chimica Acta*. **2010**, *93*, 1038-1047. https://doi.org/10.1002/hlca.200900413.
116. Hanaya, T.; Yamamoto, H. *Pteridines*. **2013**, *24*, 3–6. https://doi.org/10.1515/pterid-2013-0005.
117. Isbera, M.; Bognár, B.; Gulyás-Fekete, G.; Kish, K.; Kálai, T. *Synthesis*. **2019**, *51*, 4463–4472. https://doi.org/10.1055/s-0039-1690678.
118. Li, Q.; Yang, H. K.; Sun, Q.; You, W. W.; Zhao, P. L. *Bioorg & Med. Chem. Lett*. **2017**, *27*, 3954–3958. http://dx.doi.org/10.1016/j.bmcl.2017.07.076.
119. Bowers, S.; Truong, A. P.; Ye, M.; Aubele, D. L.; Sealy, J. M.; Neitz, R. J.; Homa, R. K.; Chan, W.; Dappen, M. S.; Galemmo Jr., R. A.; Konradi, A. W.; Sham, H. L.; Yong, L. Z.; Beroza, P.; Tonn, G.; Zhang, H.; Hoffman, J.; Motter, R.; Fauss, D.; Tanaka, P.; Bova, M. P.; Ren, Z.; Tam, D.; Ruslim, L.; Baker, J.; Pandya, D.; Diep, L.; Fitzgerald, K.; Artis, D. R.; Anderson, J. P.; Bergeron, M. *Bioorg*. *Med. Chem. Lett*. **2013**, *23*, 2743–2749. http://dx.doi.org/10.1016/j.bmcl.2013.02.065.

120. Scharow, A.; Knappe, D.; Reindl, W.; Hoffmann, R.; Berg, T. ChemBioChem. 2016, 17, 759 – 767. https://doi.org/10.1002/cbic.201500535.
121. Bi, X.; Li, J.; Li, J.; Shi, W.; Dai, Y.; Li, Q.; Zhang, W.; Huang, W.; Qian, H.; Jiang, C. *Bioorg & Med Chem*. **2019**, *27*, 2813–2821. https://doi.org/10.1016/j.bmc.2019.05.006.
122. Baker, S. J.; Beresford, K. J. M.; Young, D. W. *Tetrahedron*. **2014**, *70*, 7221-7228. http://dx.doi.org/10.1016/j.tet.2014.06.048.
123. Stone, S.; Wang, T.; Liang, J.; Cochran, J.; Green, J.; Gu, W. *Org. Biomol. Chem*. **2015**, *13*, 10471-10476. https://doi.org/10.1039/C5OB01154J.
124. Kiryanov, A.; Natala, s.; Jones, B.; McBride, C.; Feher, V.; Lam, B.; Liu, Y.; Honda, K.; Uchiyama, N.; Kawamoto, T.; Hikichi, y.; Zhang, L.; Hosfield, D.; Skene, R.; Zou, H.; Stafford, J.; Cao, X.; Ichikawa, T. *Bioorg & Med. Chem. Lett*. **2017**, *27*, 1311–1315. http://dx.doi.org/10.1016/j.bmcl.2016.10.009.
125. Chen, L.; Yap, J. L.; Yoshioka, M.; Lanning, M. E.; Fountain, R. N.; Raje, M.; Scheenstra, J. A.; Strovel, J. W.; Fletcher, S. *ACS Med. Chem*. *Lett*. **2015**, *6*, 764−769. https://doi.org/10.1021/acsmedchemlett.5b00084.
126. Mamedov, V. A.; Zhukova, N. A.; Gubaidullin, A. T.; Syakaev, V. V.; Kadyrova, M. S.; Beschastnova, T. N.; Bazanova, O. B.; Rizvanov, I. K.; Latypov, S. K. *J. Org. Chem.* **2018**, *83*, 14942−14953. https://doi.org/10.1021/acs.joc.8b02161.
127. Guirado, A.; López Sánchez, J.; Ruiz-Alcaraz, A. J.; García-Peñarrubia, P.; Bautista, D.; Gálvez. J. *Euro. J. Med. Chem*. **2013**, 66, 269-275. http://dx.doi.org/10.1016/j.ejmech.2013.05.020.
128. Raboisson, P.; Lenz, O.; Lin, T.; Surleraux, D.; Chakravarty, S.; Scholliers, A.; Vermeiren, K.; Delouvroy, F.; Verbinnen, T.; Simmen, K. *Bioorg & Med Chem Lett*. **2007**, 17, 1843–1849.. http://dx.doi.org/10.1016/j.bmcl.2007.01.046.
129. Klewe, A.; Kruse, T.; Lindel, T. *Chem. Eur. J*. **2017**, *23*, 11230-11233 https://doi.org/10.1002/chem.201702274.
130. Hanaya, T.; Yamamoto, H. *IUBMB Life*. **2013**, *65*, 300–309. https://doi.org/10.1002/iub.1137.
131. Yao, Q.; Pfleiderer, W. *Aust. J. Chem.* **2015**, 211-217. https://doi.org/10.1071/CH14421.
132. Burgmayer, S. J. N.; Kim, M.; Petit, R.; Rothkopf, A.; Kim, A.; BelHamdounia, S.; Hou, Y.; Somogyi, A.; Habel-Rodriguez, D.; Williams, A.; Kirk, M. L. *J. Inorg. Biochem.* **2007**, 101, 1601-1606. https://doi.org/10.1016/j.jinorgbio.2007.07.012.
133. Williams, B. R.; Fu, Y.; Yap, G. P. A.; Burgmayer, S. J. N. *J. Am. Chem. Soc.* **2012**, *134*, 19584-19587. https://doi.org/10.1038/mp.2011.182.doi.
134. Yang, Y.; Coward, J. K. *J. Org. Chem*. **2007**, *72*, 5748-5758. https://doi.org/10.1021/jo0707840.
135. Buglak, A. A.; Telegina, T. A.; Kritsky, M. S. *Photochem. Photobiol. Sci*., **2016**, *15*, 801–811. https://doi.org/10.1039/c6pp00084c.
136. Scurachio, R.S.; Skibsted, L.H.; Metzker, G.; Cardoso, D.R. *Photochem. Photobiol.* **2011**, *87*, 840-845. https://doi.org/10.1111/j.1751-1097.2011.00916.x
137. Denofrio, M. P.; Thomas, A. H.; Lorente, C.; *J. Phys. Chem. A.* **2010**, *114*, 10944-10950. https://doi.org/10.1021/jp1061336.
138. Denofrio, M. P.; Ogilby, P. R.; Thomas, A. H.; Lorente, C. *Photochem. Photobiol. Sci.* **2014**, *13*, 1058-1065. https://doi.org/10.1039/C4PP00079J.
139. Calvano, C. D.; Carulli, S.; Palmisano, F. *Anal. Bioanal. Chem.* **2010**, *398*, 499-507. https://doi.org/10.1007/s00216-010-3927-x.

140. Paulus, B.; Illarionov, B.; Nohr, D.; Roellinger, G.; Kacprzak, S.; Fischer, M.; Weber, S.; Bacher, A.; Schleicher, E. *J. Phys. Chem. B.* **2014**, *118*, 13092-13105. https://doi.org/10.1021/jp507618f.
141. Shirdel, J.; Penzkofer, A.; Procházka, R.; Shen, Z.; Strauss, J.; Daub, J. *Chem. Phys.* **2007**, *331*, 427-437. https://doi.org/10.1016/j.chemphys.2006.11.014.
142. Shirdel, J.; Penzkofer, A.; Procházka, R.; Shen, Z.; Daub, J. *Chem. Phys.* **2007**, *336*, 1-13. https://doi.org/10.1016/j.chemphys.2007.05.002.
143. Zirak, P.; Penzkofer, A.; Mathes, T.; Hegemann, P. *Chem. Phys.* **2009**, *358*, 111-122. http://dx.doi.org/10.1016/j.chemphys.2008.12.026.
144. Vignoni, M.; Wallawela, N.; Bonesi, S. M.; Greer, A.; Thomas, A. H. *Mol. Pharmaceutics.* **2018**, *15*, 798-807. https://doi.org/10.1021/acs.molpharmaceut.7b00136.
145. Vignoni, M.; Urrutia, M. N.; Junqueira, H. C.; Greer, A.; Reis, A.; Baptista, M. S.; Itri, R.; Thomas, A. H. *Langmuir* **2018**, *34*, 15578-15586. https://doi.org/10.1021/acs.langmuir.8b03302.
146. Hirakawa, K. In *Advances in Chemistry Research*; Nova Science Publishers Inc. 2015; Vol. 26, pp 111-126.
147. Hirakawa, K. *Anal. Bioanal. Chem.* **2009**, *393*, 999-1005. https://doi.org/10.1007/s00216-008-2522-x.
148. Offer, T.; Ames, B. N.; Bailey, S. W.; Sabens, E. A.; Nozawa, M.; Ayling, J. E. *FASEB J.* **2007**, *21*, 2101-2107. https://doi.org/10.1096/fj.06-7513com.
149. Wiles, A. A.; Fitzpatrick, B.; McDonald, N. A.; Westwater, M. M.; Long, D.-L.; Ebenhoch, B.; Rotello, V. M.; Samuel, I. D. W.; Cooke, G. *RSC Adv.* **2016**, *6*, 7999-8005. https://doi.org/10.1039/c5ra22402k.
150. Saltan, G. M.; Kiymaz, D.A.; Zafer, C.; Dinçalp, H. *J. Fluorescence.* **2017**, *27*, 1975-1984. https://doi.org/10.1007/s10895-017-2135-x.
151. Sun, M.; Li, K.; Zhang, W.-D.; Yu, Y.-X. *Chem. - Asian J.* **2018**, *13*, 3073-3083. https://doi.org/10.1002/asia.201801083.
152. Saleh, N.; Graham, J.; Afaneh, A.; Al-Soud, Y. A.; Schreckenbach, G.; Esmadi, F. T. *J. Photochem. Photobiol. A*: *Chemistry*. **2012**, *247*, 63–73. http://dx.doi.org/10.1016/j.jphotochem.2012.08.002.
153. Hegarty, C.; Kirkwood, S.; Cardosi, M. F.; Lawrence, C. L.; Taylor, C. M.; Smith, R. B.; Davis, J. *Microchem. J.* **2018**, *139*, 210-215. https://doi.org/10.1016/j.microc.2018.02.024.
154. Hong, J.; Lee, M.; Lee, B.; Seo, D.-H.; Park, C. B.; Kang, K. *Nat. Commun.* **2014**, *5*, 1-9. https://doi.org/10.1038/ncomms6335.
155. Ragone, F.; Ruiz, G. T.; Piro, O. E.; Echeverría, G. A.; Cabrerizo, F. M.; Petroselli, G.; Erra-Balsells, R.; Hiraoka, K.; Einschlag, F. S. G.; Wolcan, E. *Eur. J. Inorg. Chem*. **2012**, 4801–4810. https://doi.org/10.1002/ejic.201200681.
156. Ragone, F.; Ruiz, G.; Wolcan, E.; Ferraudi, G. *J. Argent. Chem. Soc.* **2013**, *100*, 61-65.
157. Ragone, F.; Martinez Saavedra, H. H.; García, P. F.; Wolcan, E.; Argüello, G. A.; Ruiz, G. T. *J. Biol. Inorg. Chem.* **2017,** *22*, 99-108. https://doi.org/10.1007/s00775-016-1410-7.
158. Ragone, F.; Gara, P. D.; Garcia Einschlag, F. S.; Lappin, A. G.; Ferraudi, G. J.; Wolcan, E.; Ruiz, G. T. *J. Photochem. Photobiol., A.* **2018**, *358*, 147-156. https://doi.org/10.1016/j.jphotochem.2018.02.015.

159. Mullice, L. A.; Mottram, H. J.; Hallett, A. J.; Pope, S. J. A. *Eur. J. Inorg. Chem*. **2012**, 3054–3060. https://doi.org/10.1002/ejic.201200147.
160. Jana, R.; Lissner, F.; Kaim, W. *Z. Anorg. Allg. Chem.* **2015**, *641*, 261-265. https://doi.org/10.1002/zaac.201400529.
161. Ramírez-Expósito, M. J.; Mayas-Torres, M. D.; Carrera-González, M. P.; Jiménez-Pulido, S. B.; Illán-Cabeza, N. A.; Sánchez- Sánchez, P.; Hueso-Ureña, F.; Martínez-Martos, J. M.; Moreno-Carretero, M. N. *J. Inorg. Biochem.* **2014**, *138*, 56-63. https://doi.org/10.1016/j.jinorgbio.2014.04.019.
162. Nagaj, J.; Kołkowska, P.; Bykowska, A.; Komarnicka, U. K.; Kyzioł, A.; Jeżowska-Bojczuk, M. *Med. Chem. Res.* **2015**, *24*, 115-123. https://doi.org/10.1007/s00044-014-1074-1.
163. Hueso-Ureña, F.; Jiménez-Pulido, S. B.; Fernández-Liencres, M. P.; Fernández-Gómez, M.; Moreno-Carretero, M. N.; *Dalton Trans.* **2008**, *4*, 6461-6466. https://doi.org/10.1039/b807634k.
164. Jiménez-Pulido, S. B.; Linares-Ordóñez, F. M.; Moreno-Carretero, M. N. *Polyhedron.* **2009**, *28*, 2641-2648. http://dx.doi.org/10.1016/j.poly.2009.05.061.
165. Jiménez-Pulido, S. B.; Illán-Cabeza, N. A.; Hueso-Ureña, F.; Moreno-Carretero, M. N. *Polyhedron*. **2013**, *50*, 10–15. https://doi.org/10.1016/j.poly.2012.10.033.
166. Picón-Ferrer, I.; Hueso-Ureña, F.; Illán-Cabeza, N. A.; Jiménez-Pulido, S. B.; Martínez-Martos, J. M.; Ramírez-Expósito, M. J.; Moreno-Carretero, M. N. *J. Inorg. Biochem.* **2009**, *103*, 94-100. http://dx.doi.org/10.1016/j.jinorgbio.2008.09.014.
167. Jiménez-Pulido, S. B.; Hueso-Ureña, F.; Fernández-Liencres, M. P.; Fernández-Gómez, M.; Moreno-Carretero, M. N. *Dalton Trans.* **2013**, *42*, 530-541. https://doi.org/10.1039/c2dt32044d.
168. El Azzouzi, N.; El Fadli, Z.; Metni, M. R. *J. Mater. Environ. Sci.* **2016**, *7*, 2636-2645.
169. El Azzouzi, N.; El Fadli, Z.; Metni, M. R. *J. Mater. Environ. Sci.* **2017**, *8*, 4323-4328. https://doi.org/10.26872/jmes.2017.8.12.455.
170. Illán-Cabeza, N. A.; Jiménez-Pulido, S. B.; Hueso-Ureña, F.; Peña-Ruiz, T.; Quirós-Olozábal, M.; Morenon-Carretero, M. N. *Dalton Trans.* **2016**, *45*, 17896-17909. https://doi.org/10.1039/c6dt03583c.
171. Gao, F.; Chao, H.; Zhou, F.; Xu, L.–C.; Zheng, K.–C.; Ji, L.-N. *Helv. Chim. Acta.* **2007**, *90*, 36-51. https://doi.org/10.1002/hlca.200790019.
172. Gao, F.; Chao, H.; Wei, Y.-F.; Yuan, Y.-X.; Peng, B.; Chen, X.; Zheng, K.-C.; Ji, L.-N. *Helv. Chim. Acta.* **2008**, *91*, 395-410. https://doi.org/10.1002/hlca.200890045.
173. Liu, X.-W.; Chen, J.-C.; Hu, X.; Li, H.; Zheng, K.-C.; Ji, L.-N. *Helv. Chim. Acta.* **2008**, *91*, 1374-1388. https://doi.org/10.1002/hlca.200890149.
174. Dalton, S. R.; Glazier, S.; Leung, B.; Win, S.; Megatulski, C.; Nieter Burgmayer, S. J. *J. Biol. Inorg. Chem.* **2008**, *13*, 1133–1148. https://doi.org/10.1007/s00775-008-0399-y.
175. Williams, B. R.; Dalton, S. R.; Skiba, M.; Kim, S. E.; Shatz, A.; Carroll, P. J.; Nieter Burgmayer, S.J. *Inorg. Chem.* **2012**, *51*, 12669-12681. https://doi.org/10.1021/ic301219z.
176. González, I.; Gómez, J.; Santander-Nelli, M,; Cortés-Arriagada, D.; Dreyse, P. *Polyhedron*. **2020**, *186*, 114621. https://doi.org/10.1016/j.poly.2020.114621.
177. Xu, W.; Chan, K. M.; Kool, E. T. *Nature Chem.* **2017**, *9*, 1043-1055. https://doi.org/10.1038/NCHEM.2859.

178. Matarazzo, A.; Hudson, R. H. E. *Tetrahedron.* **2015**, *71*, 1627-1657. http://dx.doi.org/10.1016/j.tet.2014.12.066.
179. Kanai, E.; Nishizawa, S.; Teramae, N. *Nucleic Acids Symp. Ser.* **2008**, *52*, 115–116. https://doi.org/10.1093/nass/nrn059.
180. Rajendar, B.; Rajendran, A.; Sato, Y.; Nishizawa, S.; Teramae, N. *Bioorg. Med. Chem.* **2009**, *17*, 351-359. https://doi.org/10.1016/j.bmc.2008.10.062.
181. Costa, J. A.; Leal-Pinto, E.; Henderson, S. C.; Zabel, T.; Hawkins, M. E.; Hanss, B. *Pteridines.* **2012**, *23*, 81-89.
182. Gogichaishvili, S.; Johnson, J.; Gvarjaladze, D.; Lomidze, L.; Kankia, B. *Biopolymers.* **2014**, *101*, 583-590. https://doi.org/10.1002/bip.22421.
183. Parsons, J.; Hermann, T. *Tetrahedron.* **2007**, *63*, 3548–3552. https://doi.org/10.1016/j.tet.2006.08.106.
184. Widom, J. R.; Rappoport, D.; Perdomo-Ortiz, A.; Thomsen, H.; Johnson, N. P.; von Hippel, P. H.; Aspuru-Guzik, A.; Marcus, A. H. *Nucleic Acids Res.* **2013**, *41*, 995-1004. https://doi.org/10.1093/nar/gks1148.
185. Johnson, N. P.; Ji, H.; Steinberg, T. H.; von Hippel, P. H.; Marcus, A. H. *J. Phys. Chem. B.* **2015**, *119*, 12798-12807. https://doi.org/10.1021/acs.jpcb.5b06361.
186. Datta, K.; Johnson, N. P.; Villani, G.; Marcus, A. H.; von Hippel, P. H. *Nucleic Acids Res.* **2012**, *40*, 1191-1202. https://doi.org/10.1093/nar/gkr858.
187. Moreno, A.; Knee, J.; Mukerji, I. *Biochemistry.* **2012**, *51*, 6847-6859. https://doi.org/10.1021/bi300466d.
188. Rajendar, B.; Rajendran, A.; Ye, Z.; Kanai, E.; Sato, Y. Nishizawa, S.; Sikorski, M.; Teramae, N. *Org. Biomol. Chem.* **2010**, *8*, 4949-4959. https://doi.org/10.1039/c0ob00057d.
189. Sato, Y.; Toriyabe, Y.; Nishizawa, S.; Teramae, N. *Chem. Commun.* **2013**, *49*, 9983-9985. https://doi.org/10.1039/c3cc46085a.
190. Sato, Y.; Asami, T.; Toriyabe, Y.; Sato, T.; Teramae, N.; Nishizawa, S. *Chem. Lett.* **2016**, *45*, 982-984. https://doi.org/10.1246/cl.160425
191. Pfadler, W.; Pfleiderer, W. *Arkivoc.* **2009**, *3*, 95-114. https://doi.org/10.3998/ark.5550190.0010.309.
192. Prykota, T.I.; Pfleiderer, W. *Nucleosides, Nucleotides Nucleic Acids*. **2011**, *30*, 544–551. https://doi.org/10.1080/15257770.2011.578089.
193. Paudel, H. R.; Das, R.; Wu, C.-H.; Wu, J. I. *Org. Biomol. Chem.* **2020**, *18*, 1078-1081. https://doi.org/10.1039/c9ob02412c.
194. Hurtado-Sánchez, M. d. C.; Espinosa-Mansilla, A.; Rodriguez-Cáceres, M. I.; Durán-Merás, I. *J. Agric. Food Chem.* **2014**, *62*, 97-106. https://doi.org/10.1021/jf404180t.
195. Kozlík, P.; Krajíček, J.; Kalíková, K.; Tesařová, E.; Čabala, R.; Exnerová, Štys, P.; Bosáková, Z. *J. Chromatogr. B*. **2013**, *930*, 82-89. https://doi.org/10.1016/j.jchromb.2013.05.004.
196. Xiong, X.; Liu, Y. *Talanta*, **2016**, *150*, 493-502 https://doi.org/10.1016/j.talanta.2015.12.066.
197. Xiong, X.; Zhang, Y.; Zhang, W. *Biomed. Chromatogr.* **2018**, *32*, e4244. https://doi.org/10.1002/bmc.4244
198. Kośliński, P.; Bujak, R.; Daghir, E.; Markuszewski, M. J. *Electrophoresis.* **2011**, *32*, 2044-2054. https://doi.org/10.1002/elps.201000664.
199. Burton, C.; Weng, R.; Yang, L.; Bai, Y.; Liu, H.; Ma, Y. *Analytica Chimica Acta.* **2015**, *853*, 442-450. https://doi.org/10.1016/j.aca.2014.10.044.

200. Hirsch, A.; Palmer, B. A.; Ramasubramaniam, A.; Williams, P. A.; Harris, K. D. M.; Pokroy, B.; Weiner, S.; Addadi, L.; Leiserowitz, L.; Kronik, L. *Chem. Mater.* **2019**, *31*, 4479-4489. https://doi.org/10.1021/acs.chemmater.9b01039.
201. Murayama, S.; Nakao, Y.; Matsunaga, S. *Tetrahedron Lett.* **2008**, *49*, 4186-4188. https://doi.org/10.1016/j.tetlet.2008.04.043.
202. Li, Y.-B.; Huang, W.-H.; Xiang, Y. *Helv. Chem. Acta.* **2008**, *91*, 303-307. https://doi.org/10.1002/hlca.200890035.
203. Li, T.; Wang, G.-C.; Wang, C.-H.; Ye, W.-C. *Chem. Lett.* **2013**, *42*, 983-985. https://doi.org/10.1246/cl.130349.
204. Zheng, Y. F.; Li, C. Y.; Peng, G. P.; Li, H. Y. *Chin. Chem. Lett.* **2010**, *21*, 603-605. http://dx.doi.org/10.1016/j.cclet.2010.01.031.
205. Kuse, M.; Yanagi, M.; Tanaka, E.; Tani, N.; Nishikawa, T. *Biosci. Biotechnol. Biochem.* **2010**, *74*, 2307–2309. https://doi.org/10.1271/bbb.100171.
206. Daniels, B. J.; Prijic, G.; Meidinger, S.; Loomes, K. M.; Stephens, J. M.; Schlothauer, R. C.; Furkert, D. P.; Brimble, M. A. *J. Agric. Food. Chem.* **2016**, *64*, 5079-5084. https://doi.org/10.1021/acs.jafc.6b01596.
207. Beitlich, N.; Lübken, T.; Kaiser, M.; Ispiryan, L.; Speer, K. *J. Agric. Food. Chem.* **2016**, *64*, 8886-8891. https://doi.org/10.1021/acs.jafc.6b03984.
208. Meyer, S. W.; Mordhorst, T. F.; Lee, C.; Jensen, P. R.; Fenical, W.; Köck, M. *Org. Biomol. Chem.* **2010**, *8*, 2158-2163. https://doi.org/10.1039/b910629d.
209. Chen, M.; Shao, C.-L.; Fu, X.-M.; Kong, C.-J.; She, Z.-G.; Wang, C.-Y. *J. Nat. Prod.* **2014**, *77*, 1601-1606. https://doi.org/10.1021/np5001686.
210. You, M.; Liao, L.; Hong, S. H.; Park, W.; Kwon, D. I.; Lee, J.; Noh, M.; Oh, D.-C.; Oh, K.-B.; Shin, J.; *Mar. Drugs.* **2015**, *13*, 1290-1303. https://doi.org/10.3390/md13031290.
211. Chaiyosang, B.; Kanokmedhakul, K.; Boonmak, J.; Youngme, S.; Kukongviriyapan, V.; Soytong, K.; Kanokmedhakul, S. *Nat. Prod. Res.* **2016**, *30*, 1017-1024. https://doi.org/10.1080/14786419.2015.1101107.
212. Zheng, C.-J.; Wu, L.-Y.; Li, X.-B.; Song, X.-M.; Niu, Z.-G.; Song, X.-P.; Chen, G.-Y.; Wang, C.-Y. *Helv. Chim. Acta.* **2015**, *98*, 368-373. https://doi.org/10.1002/hlca.201400197.
213. Rudolph, K. E.; Liberio, M. S.; Davis, R. A.; Carroll, A. R. *Org. Biomol. Chem.* **2013**, *11*, 261-270. https://doi.org/10.1039/c2ob26879e.
214. Rébeillé, F.; Ravanel, S.; Marquet, A.; Mendel, R.R.; Smith, A.G.; Warren, M. J. *Nat. Prod. Rep*. **2007**, *24*, 949–962. https://doi.org/10.1039/b703104c.
215. Abbas, C. A.; Sibirny, A. A. *Microbiol. Mol. Biol. Rev.* **2011**, *75*, 321-360. https://doi.org/10.1128/mmbr.00030-10.
216. Ladenstein, R.; Fischer, M.; Bacher, A. *FEBS J.* **2013**, *280*, 2537-2563. https://doi.org/10.1111/febs.12255.
217. Kaiser, J.; Illarionov, B.; Rohdich, F.; Eisenreich, W.; Saller, S.; Van den Brulle, J.; Cushman, M.; Bacher, A.; Fischer, M. *Anal. Biochem*. **2007**, *365*, 52–61. https://doi.org/10.1016/j.ab.2007.02.033.
218. Kim, R.-R.; Illarionov, B.; Joshi, M.; Cushman, M.; Lee, C. Y.; Eisenreich, W.; Fischer, M.; Bacher, A. *J. Am. Chem. Soc.* **2010**, *132*, 2983-2990. https://doi.org/10.1021/ja908395r.
219. Breugst, M.; Eschenmoser, A.; Houk, K. N. *J. Am. Chem. Soc.* **2013**, *135*, 6658-6668. https://doi.org/10.1021/ja402099f.

220. Green, J. M.; Matthews, R. G. *EcoSal Plus*. **2007**, *2*, https://doi.org/10.1128/ecosalplus.3.6.3.6.
221. Pribat, A.; Jeanguenin, L.; Lara-Núñez, A.; Ziemak, M. J.; Hyde, J. E.; de Crécy-Lagard, V.; Hanson, A. D. *J. Bacteriol.* **2009**, *191*, 4158-4165. https://doi.org/10.1128/JB.00416-09.
222. de Crécy-Lagard, V.; Phillips, G.; Grochowski, L. L.; El Yacoubi, B.; Jenney, F.; Adams, M. W. W.; Murzin, A. G.; White, R. H. *ACS Chem. Biol.* **2012**, *7*, 1807-1816. https://doi.org/10.1021/cb300342u.
223. Pribat, A.; Blaby, I. K.; Lara-Núñez, A.; Gregory, J. F. III; de Crécy-Lagard, V.; Hanson, A. D. *J. Bacteriol.* **2010**, *192*, 475-482. https://doi.org/10.1128/JB.01198-09.
224. Vickers, T. J.; Murta, S. M. F.; Mandell, M. A.; Beverley, S. M. *Mol Biochem Parasitol*. **2009**, *166*, 142–152. https://doi.org/10.1016/j.molbiopara.2009.03.009.
225. Kapatos, G. *IUBMB Life.* **2013**, *65*, 323-333. https://doi.org/10.1002/iub.1140.
226. Tsutsui, Y.; Kobayashi, K.; Takeuchi, F.; Tsubaki, M.; Kozawa, T. *Biochemistry.* **2018**, *57*, 1611-1619. https://doi.org/10.1021/acs.biochem.7b00887.
227. Kim, H.; Kim, K.; Yim, J. *IUBMB Life* **2013**, *65*, 334-340. https://doi.org/10.1002/iub.1145.
228. Basu, P.; Burgmayer, S. J. N. *Coord. Chem. Rev.* **2011**, *255*, 1016-1038. https://doi.org/10.1016/j.ccr.2011.02.010.
229. Mendel, R. R. *J. Biol. Chem.* **2013**, *288*, 13165-13172. https://doi.org/10.1074/jbc.R113.455311.
230. Iobbi-Nivol, C.; Leimkühler. S. *Biochim. Biophys. Acta* **2013**, *1827*, 1086-1101. http://dx.doi.org/10.1016/j.bbabio.2012.11.007.
231. Leimkühler. S. *Biol. Chem.* **2017**, *398*, 1009–1026. https://doi.org/10.1515/hsz-2017-0110.
232. Zupok, A. Iobbi-Nivol, C.; Méjean, V.; Leimkühler, S. *Metallomics*. **2019**, *11*, 1602-1624. https://doi.org/10.1039/c9mt00186g.
233. Hover, B. M.; Yokoyama, K. *J Am Chem Soc.* **2015**, *137,* 3352–3359. https://doi.org/10.1021/ja512997j.
234. Smolinksy, B.; Eichler, S. A.; Buchmeier, S.; Meier, J. C.; Schwarz, G. *J. Biol. Chem.* **2008**, *283*, 17370–17379. https://doi.org/10.1074/jbc.M800985200.
235. Karasgod, V.; Schindelin, H. *Structure*. **2016**, *24*, 782-788. http://dx.doi.org/10.1016/j.str.2016.02.023.
236. Teschner, J.; Lachmann, N.; Schulze, J.; Geisler, M.; Selbach, K.; Santamaria-Araujo, J.; Balk, J.; Mendel, R. R.; Bittner, F. *Plant Cell.* **2010**, *22*, 468-480. https://doi.org/10.1105/tpc.109.068478.
237. Dahl, J.-U.; Urban, A.; Bolte, A.; Sribhaya, P.; Donahue J. L.; Nimtz, M.; Larson, T. J.; Leimkühler, S. *J. Biol. Chem.* **2011**, *286*, 35801-35812. https://doi.org/10.1074/jbc.M111.282368.
238. Bevers, L. E.; Hagedoorn, P. L.; Santamaria-Araujo, J. A.; l Magalon, A.; Hagen, W. R. and Schwarz, G. *Biochemistry*. **2008**, *47*, 949-956. https://doi.org/10.1021/bi7020487.
239. Reschke, S.; Sigfridsson, K. G. V.; Kaufmann, P.; Leidel, N.; Horn, S.; Gast, K.; Schulzke, C.; Haumann, M.; Leimkühler, S. *J. Biol. Chem.* **2013**, *288*, 29736-29745. https://doi.org/10.1074/jbc.M113.497453.
240. Okamoto, K.; Kusano, T.; Nishino, T. *Curr. Pharm. Des.* **2013**, *19*, 2606-2614. https://doi.org/10.2174/1381612811319140010.

241. Yokoyama, K. *Biochemistry.* **2018**, *57*, 390-402. https://doi.org/10.1021/acs.biochem.7b00878.
242. Hover, B.; Loksztejn, A.; Ribeiro, A.; Yokoyama, K. *J. Am. Chem. Soc*. **2013**, 135, 7019–7032. https://doi.org/10.1021/ja401781t.
243. Mehta, A. P.; Abdelwahed, S. H.; Begley, T. P. *J. Am. Chem. Soc.* **2013**, *135*, 10883-10885. https://doi.org/10.1021/ja4041048.
244. Mehta, A. P.; Abdelwahed, S. H.; Begley, T. P. *Biochim. Biophys. Acta* **2015**, *1854*, 1073-1077. http://dx.doi.org/10.1016/j.bbapap.2015.04.008.
245. Mehta, A. P.; Hanes, J. W.; Abdelwahed, A. H.; Hilmey, D. G.; Hänzelmann, P.; Begley, T. P. *Biochemistry.* **2013**, *52*, 1134-1136. https://doi.org/10.1021/bi3016026.
246. Mehta, A. P.; Abdelwahed, S. H.; Xu, H.; Begley, T. P. *J. Am. Chem. Soc.* **2014**, *136*, 10609-10614. https://doi.org/10.1021/ja502663k.
247. Hover, B.M.; Tonthat, N. K.; Schumacher, M. A.; Yokoyama, K. *Proc. Natl. Acad. Sci. U. S. A.* **2015**, *112*, 6347-6352. https://doi.org/10.1073/pnas.1500697112.
248. Hover, B. M.; Lilla, E. A.; Yokoyama, K. *Biochemistry.* **2015**, *54*, 7229-7236. https://doi.org/10.1021/acs.biochem.5b00857.
249. Yokoyama, K. Leimkühler, S. *Biochim. Biophys. Acta.* **2015**, *1853*, 1335-1349. http://dx.doi.org/10.1016/j.bbamcr.2014.09.021.
250. Mehta, A. P.; Abdelwahed, S. H.; Mahanta, N.; Fedoseyenko, D.; Philmus, B.; Cooper, L. E.; Liu, Y.; Jhulki, I.; Ealick, S. E.; Begley, T. *J. Biol. Chem.* **2015**, *290*, 3980-3986. https://doi.org/10.1074/jbc.R114.623793.
251. Carmona-Martínez, V.; Ruiz-Alcaraz, A. J.; Vera, M.; Guirado, A.; Martínez-Esparza, M.; García-Peñarrubia, P. *Med. Res. Rev.* **2019**, *39*, 461-516. https://doi.org/10.1002/med.21529.
252. Stoicescu, D. F.; Rotaru, M. *Anti-Cancer Agents Med. Chem.* **2013**, *13*, 364-372. https://doi.org/10.2174/1871520611313020022.
253. Kazunin, M. S.; Voskoboynik, O. Y.; Shatalova, O. M.; Maloshtan, L. N.; Kovalenko, S. I. *Chem. Heterocycl. Compd.* **2019**, *55*, 408-415. https://doi.org/10.1007/s10593-019-02473-x.
254. Shi, G.; Shaw, G.; Liang, Y.-H.; Subburaman, P.; Li, Y.; Wu, Y.; Yan, H.; Ji, X. *Bioorg. Med. Chem.* **2012**, 47-57. http://dx.doi.org/10.1016/j.bmc.2011.11.032.
255. Low, P. S.; Henne, W. A.; Doorneweerd, D. D. *Acc. Chem. Res.* **2008**, *41*, 120-129. https://doi.org/10.1021/ar7000815.
256. Vlahov, I. R.; You, F.; Santhapuram, H. K. R.; Wang, Y.; Vaughn, J. F.; Hahn, S. J.; Kleindl, P. J.; Fan, M.; Leamon, C. P. *Bioorg. Med. Chem. Lett.* **2011**, *21*, 1202-1205. http://dx.doi.org/10.1016/j.bmcl.2010.12.085.
257. Cooper, I.; Fridkin, M.; Schechter, Y. *PLoS ONE.* **2016**, *11*, e0158352. https://doi.org/10.1371/journal.pone.0158352.
258. Marques, S.M.; Enyedy, É.A.; Supuran, C.T.; Krupenko, N.I.; Krupenko, S.A.; Santos, M.A. *Bioorg. Med. Chem.* **2010**, *18*, 5081-5089. https://doi.org/10.1016/j.bmc.2010.05.072.
259. Tulloch, L.B.; Martini, V.P.; Iulek, J.; Huggan, J.K.; Lee, J.H.; Gibson, C.L.; Smith, T.K.; Suckling, C.J.; Hunter, W.N. *J. Med. Chem.* **2010**, *53*, 221-229. https://doi.org/10.1021/jm901059x.
260. Cavazzuti, A.; Paglietti, G.; Hunter, W. N.; Gamarro, F.; Piras, S.; Loriga, M.; Allecca, S.; Corona, P.; McLuskey, K.; Tulloch, L.; Gibellini, F.; Ferrari, S.; Costi, M.

P. *Proc. Natl. Acad. Sci. U.S.A*. **2008**, *105*, 1448−1453. https://doi.org/10.1073/pnas.0704384105.

261. Corona, P.; Gibellini, F.; Cavalli, A.; Saxena, P.; Carta, A.; Loriga, M.; Luciani, R.; Paglietti, G.; Guerrieri, D.; Nerini, E.; Gupta, S.; Hanaert, V.; Michels, P. A. M.; Ferrari, S.; Costi, P. M. *J. Med. Chem.* **2012**, *55*, 8318-8329. https://doi.org/10.1021/jm300563f.

262. Ruiz-Alcaraz, A. J.; Carmona-Martinez, V.; Guirado, A.; Gálvez, J.; Martinez-Esparza, M.; Garcia-Peñarrubia, P. *Naunyn-Schmiedeberg's Arch. Pharmacol.* **2019**, *392*, 219-227. https://doi.org/10.1007/s00210-018-1587-0.

263. Jasheway, K.; Pruet, J.; Anslyn, E. V.; Robertus, J. D. *Toxins*. **2011**, *3*, 1233-1248. https://doi.org/10.3390/toxins3101233.

264. Suckling, C. J.; Gibson. C. L.; Huggan, J. K.; Morthala, R. R.; Clarke, B.; Kununthur, S.; Wadsworth, R. M.; Daff, S.; Papale, D. *Bioorg. Med. Chem. Lett.* **2008**, *18*, 1563-1566. https://doi.org/10.1016/j.bmcl.2008.01.079.

265. Zhang, L.; Zhang, Q.-Q.; Tang, F.; Zhang, J.; Wang, J.; Yao, Q. Z. *Jiegou Huaxue.* **2018**, *37*, 1371-1378. https://doi.org/10.14102/j.cnki.0254-5861.2011-1909.

266. Prins, L. H. A.; Petzer, J. P.; Malan, S. F. *Bioorg. Med. Chem.* **2009**, *17*, 7523-7530. http://dx.doi.org/10.1016/j.bmc.2009.09.019.

267. Dzierba, C. D.; Tebben, A. J.; Wilde, R. G.; Takvorian, A. G.; Rafalski, M.; Kasireddy-Polam, P.; Klaczkiewicz, J. D.; Pechulis, A. D.; Davis, A. L.; Sweet, M. P.; Woo, A. M.; Yang, Z.; Ebeltoft, S. M.; Molski, T. F.; Zhang, G.; Zaczek, R. C.; Trainor, G. L.; Combs, A. P.; Gilligan, P. J. *J. Med. Chem.* **2007**, *50*, 2269-2272. https://doi.org/10.1021/jm0611410.

268. Devi, E. R.; Sreenivasulu, R.; Rao, K. P.; Nadh, R. V.; Siressha, M. *Lett. Org. Chem.* **2020**, *17*, 54-60. https://doi.org/10.2174/1570178616666190528095548.

269. Lin, J.; Wang, X.; Wang, J.; Xu, X.; Chan, Y.; Li, Z. *J. China. Pharm. Univ.* **2018**, *49* 64-71. https://doi.org/10.11665/j.issn.1000-5048.20180109.

270. Minuesa, G.; Albanese, S. K.; Xie, W.; Kazansky, Y.; Worroll, D.; Chow, A.; Schurer, A.; Park, S.-M.; Rotsides, C. Z.; Taggart, J.; Rizzi, A.; Naden, L. N.; Chou, T.; Gourkanti, S.; Cappel, D.; Passarelli, M. C.; Fairchild, L.; Adura, C.; Glickman, J. F.; Schulman, J.; Famulare, C.; Patel, M.; Eibl, J. K.; Ross, G. M.; Bhattacharya, S.; Tan, D. S.; Leslie, C. S.; Beuming, T.; Patel, D. J.; Goldgur, Y.; Chodera, J. D.; Kharas, M. G. *Nature Commun.* **2019**, *10*, 1-15. http://dx.doi.org/10.1038/s41467-019-10523-3.

271. Liu, K. K.-C.; Bagrodia, S.; Bailey, S.; Cheng, H.; Chen, H.; Gao, L.; Greasley, S.; Hoffman, J. E.; Hu, Q.; Johnson, T. O.; Knighton, D.; Liu, Z.; Marx, M. A.; Nambu, M. D.; Ninkovic, S.; Pascual, B.; Rafidi, K.; Rodgers, C. M.-L.; Smith, G. L.; Sun, S.; Wang, H.; Yang, A.; Yuan, J.; Zou, A. *Bioorg. Med. Chem. Lett.* **2010**, *20*, 6096-6099. http://dx.doi.org/10.1016/j.bmcl.2010.08.045.

272. Ali, H. I.; Ashida, N.; Nagamatsu, T. *Bioorg. Med. Chem.* **2007**, *15*, 6336–6352. https://doi.org/10.1016/j.bmc.2007.06.058.

273. Casalvieri, K. A.; Matheson, C. J.; Backos, D. S.; Reigan, P. *Bioorg. Med. Chem.* **2020**, *28*, 115303. https://doi.org/10.1016/j.bmc.2019.115303.

274. Huang, X.; Xie, Z.; Liao, C. *Future Med. Chem.* **2020**, *12*, 869-871. https://doi.org/10.4155/fmc-2020-0055.

275. Steegmaier, M.; Hoffmann, M.; Baum, A.; Lénárt, P.; Petronczki, M.; Krššák, M.; Gürtler, U.; Garin-Chesa, P.; Lieb, S.; Quant, J.; Grauert, M.; Adolf, G. R.; Kraut,

N.; Peters, J.-M.; Rettig, W. J. *Curr. Biol.* **2007**, *17*, 316–322. https://doi.org/10.1016/j.cub.2006.12.037.
276. Zhang, Z.; Kwiatowski, N.; Zeng, H.; Lim, S. M.; Gray, N. S.; Zhang, W.; Yang, P. L. *Mol. Biosyst.* **2012**, *8*, 2523-2526. https://doi.org/10.1039/c2mb25099c.
277. Gohda, J.; Suzuki, K.; Liu, K.; Xie, X.; Takeuchi, H.; Inoue, J.; Kawaguchi, Y.; Ishida, T. *Sci. Rep.* **2018**, *8*, 3521. http://dx.doi.org/10.1038/s41598-018-21942-5.
278. Carlino, L.; Rastelli, G. *J. Med. Chem.* **2016**, *59*, 9305-9320. https://doi.org/10.1021/acs.jmedchem.6b00438.
279. Liu, S.; Yosief, H. O.; Dai, L.; Huang, H.; Dhawan, G.; Zhang, X.; Muthengi, A. M.; Roberts, J.; Buckley, D. L.; Perry, J. A. Wu, L.; Bradner, J. E.; Qi, J.; Zhang, W. *J. Med. Chem.* **2018**, *61*, 7785-7795. https://doi.org/10.1021/acs.jmedchem.8b00765.
280. Koblan, L. W.; Buckley, D. L.; Ott, C. J.; Fitzgerald, M. E.; Ember, S. W. J.; Zhu, J.-Y.; Liu, S.; Roberts, J. M.; Remillard, D.; Vittori, S.; Zhang, W.; Schonbrunn, E.; Bradner, J. E. *ChemMedChem.* **2016**, *11*, 2575-2581. https://doi.org/10.1002/cmdc.201600502.
281. Watts, E.; Heidenreich, D.; Tucker, E.; Raab, M.; Strebhardt, K.; Chesler, L.; Knapp, S.; Bellenie, B.; Hoelder, S. *J. Med. Chem.* **2019**, *62*, 2618-2637. https://doi.org/10.1021/acs.jmedchem.8b01947.
282. Remillard, D.; Buckley, D. L.; Seo, H.-S.; Ferguson, F. M.; Dhe-Paganon, S.; Bradner, J. E.; Gray, N. S. *ACS Med. Chem. Lett.* **2019**, *10*, 1443-1449. https://doi.org/10.1021/acsmedchemlett.9b00243.
283. Walters, I.; Austin, C.; Austin, R.; Bonnert, R.; Cage, P.; Christie, M.; Ebden, M.; Gardiner, S.; Grahames, C.; Hill, S.; Hunt, F.; Jewell, R.; Lewis, S.; Martin, I.; Nicholls, D.; Robinson, D. *Bioorg. Med. Chem. Lett.* **2008**, *18*, 798-803. https://doi.org/10.1016/j.bmcl.2007.11.039.
284. Padmanabhan, B. *Theor. Biol. Med. Modell.* **2013**, *10*, 46. https://doi.org/10.1186/1742-4682-10-46.
285. Barthel, A.; Trieschmann, L.; Ströhl, D.; Kluge, R.; Böhm, G.; Csuk, R. *Arch. Pharm. Chem. Life Sci.* **2009**, *342*, 445–452. https://doi.org/10.1002/ardp.200800196.
286. Koltun, D. O.; Parkhill, E. Q.; Vasilevich, N. I.; Glushkov, A. I.; Zilbershtein, T. M.; Ivanov, A. V.; Cole, A. G.; Henderson, I.; Zautke, N. A.; Brunn, S. A.; Mollova, N.; Leung, K.; Chisholm, J. W.; Zablocki, J. *Bioorg. Med. Chem. Lett.* **2009**, *19*, 2048-2052. http://dx.doi.org/10.1016/j.bmcl.2009.02.019.
287. Butzbach, K.; Epe, B. *Free Radical Biol. Med.* **2013**, *65*, 821-827. http://dx.doi.org/10.1016/j.freeradbiomed.2013.08.168.
288. Ghisoni, K.; Aguiar, A. S.; de Oliveira, P. A.; Matheus, F. C.; Gabach, L.; Perez, M.; Carlini, V.P.; Barbeito, L.; Mongeau, R.; Lanfumey, L.; Prediger, R.D.; Latini, A. *Brain Behav. Immun.* **2016**, *56*, 156–164, https://doi.org/10.1016/j.bbi.2016.02.019.
289. Scheffer, D. D. L.; Latini, A. *Biochim. Biophys. Acta, Mol. Basis Dis.* **2020**, *1866*, 165823. https://doi.org/10.1016/j.bbadis.2020.165823.
290. Cronin, S. J. F.; Seehus, C.; Weidinger, A.; Talbot, S.; Reissig, S.; Seifert, M.; Pierson, Y.; McNeill, E.; Longhi, M. S.; Turnes, B.L.; Kreslavsky, T.; Kogler, M.; Hoffmann, D.; Ticevic, M.; da Luz Scheffer, D.; Tortola, L.; Cikes, D.; Jais, A.; Rangachari, M.; Rao, S.; Paolino, M.; Novatchkova, M.; Aichinger, M.; Barrett, L.; Latremoliere, A.; Wirnsberger, G.; Lametschwandtner, G.; Busslinger, M.; Zicha, S.; Latini, A.; Robson, S.C.; Waisman, A.; Andrews, N.; Costigan, M.; Channon, K. M.;

Weiss, G.; Kozlov, A. V.; Tebbe, M.; Johnsson, K.; Woolf, C.J.; Penninger, J. M. *Nature* 2018, *563*, 564–568. https://doi.org/10.1038/s41586-018-0701-2 .

291. Latremoliere, A.; Latini, A.; Andrews, N.; Cronin, S. J.; Fujita, M.; Gorska, K.; Hovius, R.; Romero, C.; Chuaiphichai, S.; Painter, M.; Miracca, G.; Babaniyi, O.; Remor, A. P.; Duong, K.; Riva, P.; Barrett, L.B.; Ferreirós, N.; Naylor, A.; Penninger, J. M.; Tegeder, I.; Zhong, J.; Blagg, J.; Channon, K. M.; Johnsson, K.; Costigan, M.; Woolf, C. J. *Neuron*. **2015**, *86*, 1393–1406. https://doi.org/10.1016/j.neuron.2015.05.033.

292. Karimi Shervedani, R.; Yaghoobi, F.; Torabi, M.; Rahnemaye Rahsepar, F.; Samiei Foroushani, M. *Bioelectrochemistry.* **2018**, *122*, 149-157. https://doi.org/10.1016/j.bioelechem.2018.03.008.

293. Samiei Foroushani, M.; Niroumand, N.; Karimi Shervedani, R.; Yaghoobi, F.; Kefayat, A.; Torabi, M. *Bioelectrochemistry.* **2019**, *130*, 107347. https://doi.org/10.1016/j.bioelechem.2019.107347.

294. Azcona, P.; López-Corral, I.; Lassalle, V. *Colloids Surf., A.* **2017**, *537*, 185-196. https://doi.org/10.1016/j.colsurfa.2017.10.025.

295. Castillo, J. J.; Rindzevicius, T.; Rozo, C. E.; Boisen, A. *Nanomater. Nanotechnol.* **2015**, *5*, 29. https://doi.org/10.5772/61606.

296. Teixeira, R. A. R.; Lima, F. R. A.; Silva, P. C.; Costa, L. A. S.; Sant'Ana, A. C. *Spectrochim. Acta, Part A.* **2019**, *223*, 117305. https://doi.org/10.1016/j.saa.2019.117305.

297. Permyakova, E. S.; Antipina, L. Y.; Kiryukhantsev-Korneev, P. V.; Kovalskii, A. M.; Polčak, J.; Manakhov, A.; Gudz, K. Y.; Sorokin, P. B.; Shtansky, D. V. *Nanomaterials*. **2019**, *9*, 1658. https://doi.org/10.3390/nano9121658.

Author biographies

Sharon Rossiter studied her B.Sc. at King's College London and stayed there to complete her Ph.D. with Professor Keith Jones, on a Wellcome Prize Studentship studying synthesis of an anti-parasitic quinoline natural product. She continued in medicinal chemistry research with postdoctoral positions at the Gray Cancer Institute, Mount Vernon Hospital, Middlesex, followed by the Wolfson Institute for Biomedical Research, University College London, with Professor David L. Selwood and Sir Patrick Vallance. She then moved to the new School of Pharmacy at the University of Hertfordshire in 2005 to begin her independent academic career as a Senior Lecturer and, since 2015, Principal Lecturer in Medicinal and Pharmaceutical Chemistry. Her research interests are organic synthesis applied to collaborative research in drug discovery, at the interface of chemistry, biology and medicine.

Mehrnoosh Ostovar obtained her PhD in organic chemistry from UCL (2005-09), where she worked in the area of natural product synthesis under the supervision of Prof. Karl Hale and Prof. Charles Marson. Upon completion of her studies, she joined Prof. Varinder Aggarwal's group as a postdoctoral research associate in the School of Chemistry at University of Bristol. In this period, she worked on asymmetric aziridinations and also palladium-mediated annulation of vinyl aziridines with Michael acceptors to synthesize stereocontrolled substituted pyrrolidines and the application to a formal synthesis of (–)-α-Kainic Acid (2009-2012). In October 2012, Mehrnoosh started working as a posdoctoral research officer for Prof. Stephen Husbands in the Department of Pharmacy and Pharmacology at University of Bath. Her research focus was on discovery and development of new opioid ligands as relapse prevention agents for the treatment of opioid abuse and as analgesics with low abuse potential. Since 2018, she has been appointed as a visiting lecturer in chemistry at University of Hertfordshire where she also undertakes research activities in the area of medicinal chemistry.